Role of MukBEF in *Escherichia coli* chromosome organization

Anjana Badrinarayanan

Linacre College, Oxford

A thesis submitted to the Faculty of Biological Sciences for the degree of Doctor of Philosophy at the University of Oxford

Michaelmas 2011

The research presented in this thesis is my own original work except where otherwise stated and has not been submitted for any other degree

For amma and appa

Acknowledgements

This was probably the hardest part of the thesis to put in words. So many people have contributed to making this possible – I am indebted to them all (while I will attempt to acknowledge everyone, my sincere apologies for missing anyone out). I am well within the word limit of the thesis, so I could ramble on in this section – but I will attempt to be concise.

This has been a personal journey for me of discovering my love for science (microbiology in particular) and none of this would have been possible without my supervisor, Dave. I would like to thank Dave for giving me the opportunity to work with him. I am eternally indebted to him for his support, encouragement and inspiration. I will always be in admiration and awe for his contagious enthusiasm and love for science. Thank you Dave for making me the scientist I am – I couldn't have asked for better place to begin my scientific journey.

My sincere thanks to Rodrigo (the fox), who co-supervised me through the DPhil. Thank you Rod for your support, encouragement and ideas. I have learnt an immeasurable amount of science from you and I am eternally grateful for that. I will cherish the endless discussions we have had on the mysteries of MukBEF. Special thanks to my "koosi partner " Christian. Thanks Christian for the enthusiastic support you have given me through the DPhil and for being a great office neighbour. I am grateful for your stimulating scientific and philosophical insights.

I am very grateful to Mark Leake, our collaborator on the Stoichiometry project. Thanks Mark, for building the coolest microscope ever and for being a great collaborator and a source of ideas to tackle the realm of "*in vivo* biochemistry".

This journey would have been incomplete without the support and encouragement of the many members of the Sherratt family. Trying not to leave anyone out – A very special thanks to Ian for his support, helpful discussions and witty humour. A very warm thanks to Xindan for her help on numerous occasions (with techniques and strains) and for her support and helpful discussions. Special thanks to Rachel for keeping the lab ticking (you are truly superwoman!), Pawel, Heather for her wonderful discussions and thoughts on evolution, Estelle for being a great office and lab-bench neighbour, James for his encouragement and support and Dave Brown for being a great party buddy. Warm thanks to Lidia for introducing me to the world of *E. coli* and MukBEF. Thanks also to Penny and Alex for being great second floor buddies and to Jenny for making some lovely cakes. A special thanks to the two new additions to the MukBEF family – Sophie and Emilien. It has been a pleasure to get to know you guys and I hope you will be able to provide more insight into the functioning of this mysterious protein complex. Thanks to Vik for making the best pancakes ever and his hospitality in Boston.

A very special thanks to Nicole, my Linacre College advisor. You have been great support and source of inspiration for me – thank you! This acknowledgement would be incomplete without thanking my extended family in Oxford – Rodrigo, Nohelia, Christian and Nelly (and of course little Olivia) thank

you for being there through all the ups and downs. Thank you for your love, warmth and support. A special thanks to Christian and Nelly for introducing me to "*Le Petit Prince".* A very warm thank you to Manish and Susmita – I will always cherish our endless conversations over cups of chai.

I cannot express in words the gratitude I have for the support from my parents. Thank you amma for everything and more. The journey till now has been turbulent, but your steadfastness has pulled me through it all – thank you for always supporting me, for believing in me and for being the rock protecting us from the storm. Thanks appa for your love, support, protection and encouragement. You may not be around physically but you are always in my heart. To Sai, a very special thank you. Thanks for being there, for your love and encouragement and for being the best sister in the whole wide world. Finally, my sincerest thanks to Kris. I couldn't have come this far without your undying love and support. Thanks for being there through it all, for believing in me when I wasn't sure and for making this journey with me.

Abbreviations

International units of measurement for biology were used throughout. Other abbreviations are listed in the following table

Abbreviation	Full name/ Description
aa	amino-acid(s)
amp	ampicillin
approx. or (~)	approximately
AT	anhydrotetracyclin
ATP	adenosine 5'-triphosphate
bp	base pair
BSA	bovine serum albumin
B. subtilis	*Bacillus subtilis*
C. crescentus	*Caulobacter crescentus*
ChIP	Chromatin Immunoprecipitation
CFP	cyan fluorescent protein
Cm	Chloramphenicol
DAPI	4', 6-diamidino-2-phenylindole
DTT	dithiothreitol
E. coli	*Escherichia coli*
EDTA	ethylenediaminetetraacetic acid
FISH	fluorescent *in situ* hybridization
FROS	fluorescent repressor-operator binding system
Gm	Gentamycin
GFP	green fluorescent protein
hrs	hours
IPTG	isopropyl-β-D-thiogalactoside
kb	kilobase pairs
Kn	kanamycin
<L-R>	*<Left-Right>*
LB	Luria Broth
mbp	megabase pairs
min	minutes
ms	milliseconds
No.	number
nm	nanometers
OD	optical density
ori	origin
PBS	phosphate buffered saline
PBST	phosphate buffered saline (0.1% Tween)
PCR	polymerase chain reaction
SC	supercoiling
SDS	sodium dodecyl sulphate
st dev or SD	standard deviation
sec	second
SEM	standard error of mean
YFP	yellow fluorescent protein

Abstract

In *E. coli* cells, spatial chromosome organization reflects the genetic map, with the origin located at mid-cell and left and right replichores in either cell half. In contrast to the eukaryotic cell cycle, chromosome segregation occurs progressively as replication proceeds. The highly conserved SMC complex, MukBEF, plays a central role in chromosome organization and segregation, with null mutants having temperature sensitive growth and mispositioned chromosomal regions. However, despite much effort, their mechanism of action *in vivo* remains elusive.

The current work aimed to shed light on MukBEF function by developing tools to investigate its mode of action in live cells. Degron derivatives of MukBEF were developed as a rapid way of depleting cells of MukBEF to observe its effects on chromosome organization. “Real-time” Muk depletion/ repletion shows that MukBEF can establish and maintain position of chromosomal loci independent of the cell cycle. Origin relocation from cell-pole to mid-cell is a slow process, preceded by the formation of MukBEF foci at various locations on the chromosome. Hence, Muk-mediated shaping of the chromosome is a replication-independent phenomenon. In addition, while ATP binding is required for focus formation, ATP hydrolysis is required for MukBEF function in the cell. ATPase mutants are inviable *in vivo*, highlighting the importance of MukB ATPase activity.

In a complementary approach, the composition and dynamics of MukBEF foci were assessed *in vivo.* The stoichiometries of wild type and ATP-hydrolysis deficient (Walker B) MukBEF complexes in fluorescent foci were estimated using slimfield microscopy. These results suggest that MukBEF complexes are ATP bound in foci with a broad and heterogeneous distribution. Only 19% of total MukBEF molecules are present at a given time in foci. Furthermore, unlike wild type foci, which localize around the origin, Walker B foci colocalize with the terminus. One model proposed is that the terminus may represent the loading site for wild type complexes and that Walker B MukBEF may represent the loading complex, which can associate with the loading site, but requires ATP hydrolysis for movement to the origin.

This work provides insight into the role of MukBEF in spatial chromosome organization as well as the *in vivo* significance of MukB ATPase activity.

Table of Contents

CHAPTER 1

Introduction

1.1 *Escherichia coli* cell cycle

Central to the process of life is the faithful replication and segregation of genetic material into daughter cells. While previously thought to be “bags of enzymes”, it is now known that the bacterial cell is organized and metabolic processes are tightly regulated. *E. coli* has a 4.6mbp long, single circular chromosome. Its cell cycle can be divided into three periods: B period: time between birth and replication initiation; C period: time for DNA replication and D period: the time from replication termination to cell division. Slow growing *E. coli* cells have long generation times (more than 100 min) which provides enough time for replication to finish before division occurs; hence B, C and D periods are separate. However, at fast growth rate (when the C+D period is longer than the generation time), new rounds of replication initiate before completion of the previous one, resulting in overlapping replication cycles. This allows *E. coli* to have generation times of only 30 minutes.

Replication initiates only once per cell cycle by the binding of ATP bound replication initiator protein, DnaA, to *oriC.* The event of initiation is tightly regulated – while an early model suggested that critical *oriC* mass or cell volume is important for initiation, others have suggested that this may not be the case; the ratio of DnaA-ATP to DnaA-ADP may play an important role in controlling initiation, where only ATP bound DnaA is capable of initiating (Donachie 1968; Boye et al. 2000; Wang et al. 2011). Initiation is restricted to only once per cell cycle by various mechanisms, such as sequestration of newly replicated (hemi-methylated) origins by SeqA (Waldminghaus and Skarstad 2009), the stimulation of ATP hydrolysis of DnaA-ATP to DnaA-ADP (Kaguni 2006) and the titration of DnaA to *dnaA* boxes (such as *datA*) (Katayama et al.

2010). Replication proceeds bidirectionally and loci are segregated as they are replicated, with a cohesion time of 5-15 minutes in minimal media (Nielsen et al. 2006; Wang et al. 2006). The action of TopoIV is required to separate sister loci (Wang et al. 2008). Replication termination occurs in the broad terminus region opposite *oriC* with the aid of the *ter*-Tus system (Breier et al. 2005; reviewed in Higgins 2007). Chromosome dimers are resolved by site-specific recombination at the *dif* site (located in the terminus) by the XerCD resolvase system and the DNA translocase, FtsK (Aussel et al. 2002; Grainge et al. 2007).

The polymerization of FtsZ (homolog of tubulin) at mid-cell is required for cell division to occur; this is followed by the recruitment of other divisome proteins required for septum formation and constriction (reviewed in de Boer 2010). FtsZ ring formation is regulated by two systems: the MinCDE system that regulates FtsZ ring position and polymerization and the nucleoid-occlusion protein (SlmA) that prevents FtsZ ring formation on the nucleoid (Bernhardt and de Boer 2005).

Processes like DNA replication, transcription and cell division are highly regulated. The chromosome is also spatially organized in the cell, possibly contributing to the spatial organization and regulation of the above-described processes (reviewed in Wang and Levin 2009).

1.2 Chromosome organization and compaction

The length of the extended bacterial chromosome is ~1.59mm. How does the cell compact this DNA more than 1000 times into a structure that is capable of transcription, replication, repair etc within limited space? Factors implicated in chromosome compaction and organization include macromolecular crowding due to high concentration of proteins and RNA in the cytoplasm (Woldringh and

Nanninga 2006; Foley et al. 2010), the degree of supercoiling and the action of DNA binding proteins (these are discussed below):

1.2.1 *E. coli* chromosome organization at sequence level

Sequence level organization of the chromosome is linked to replication. Highly expressed genes are located close to *oriC*, probably due to overrepresentation of *oriC* proximal loci during replication (Blattner et al. 1997). Also, essential/ highly expressed genes tend to be transcribed in the direction of replication, possibly to avoid collisions between RNA polymerase and the replisome (Rocha et al. 2003). *E. coli* also has over-representation of G over C (GC skew) on the leading strand, probably due to difference in mutation rates of the leading and lagging strands due to replication (reviewed in Reyes-Lamothe et al. 2008b). This skew changes sign at *oriC* and *ter* (replichore boundaries). Indeed, some of these skewed sequences have been evolutionarily selected for specific function (Lobry and Louarn 2003). An example is KOPS (FtsK orienting polarized sequence), which are oriented to direct the action of the DNA translocase FtsK towards the *dif* site (Bigot et al. 2005; Hendrickson and Lawrence 2006). Another example is Chi sites, which serve as hotspots for homologous recombination (reviewed in Lobry and Louarn 2003; Reyes-Lamothe et al. 2008b).

1.2.2 Topological organization and DNA supercoiling

The majority of chromosome compaction in bacteria is achieved by unrestrained negative supercoiling (Higgins et al. 2010). Coiling of DNA upon itself can result in changes in the twist or writhe of the molecule, which can compact it. Writhe can be present in the form of plectonemic supercoils where

the DNA helix winds over itself in the same molecule. Alternatively, the action of proteins can generate constrained toroidal supercoils (Fig 1.1A). Maintaining negative supercoiling of the *E. coli* chromosome is essential as reduced supercoiling affects chromosome segregation and gene expression (Holmes and Cozzarelli 2000) and increased supercoiling causes the formation of structures that can block RNA transcription or DNA replication (Deng et al. 2005).

E. coli has four DNA topoisomerases that maintain supercoiling: Gyrase, TopoI, TopoIII and TopoIV. The only enzyme to introduce negative supercoiling is DNA Gyrase (Hardy and Cozzarelli 2005), which introduces negative supercoils by acting on relaxed or positive supercoiled substrates. This activity is counteracted by TopoI and TopoIV.

Processes that act on DNA can affect supercoiling of the chromosome. For example, DNA replication causes an increase in positive supercoils ahead of the fork (Fig 1.1B), which are acted upon by Gyrase. Alternatively, the replisome could rotate and allow diffusion of positive supercoils behind the fork resulting in the formation of precatenenes (which are good substrates for TopoIV activity). Finally, replication could also result in the circular DNA molecules being catenated. TopoIV has been implicated in the final decatenation as well (Espeli et al. 2003b).

In order to explain how global negative supercoiling could be maintained in case of processes like replication or events of double strand break, both of which should change DNA topology, it was proposed that the bacterial chromosome is organized into topologically isolated domains (Higgins et al. 1996). EM experiments on isolated nucleoids from *E. coli* suggested that they

had a central core with loops emanating from it (Fig 1.1C) (Stonington and Pettijohn 1971; Kavenoff and Bowen 1976). It was found that, *in vitro*, the supercoiled state of an isolated *E. coli* chromosome was not lost by introducing a single break; instead many breaks were required to completely relax the molecule (Sinden and Pettijohn 1981; Scheirer and Higgins 2001). While earlier studies suggested that the chromosome was organized into 4-40 topologically isolated domains, recent studies *in vivo* have suggested ~ 400 domains about 10kb each in size (Postow et al. 2004). This study directly measured the change in transcription levels of ~300 supercoil sensitive genes upon introduction of double strand breaks at various locations on the chromosome. Factors thought to limit domain size and act as domain barriers include DNA binding proteins (such as nucleoid associated proteins (NAPs)), topoisomerases, replication and transcription (Deng et al. 2005).

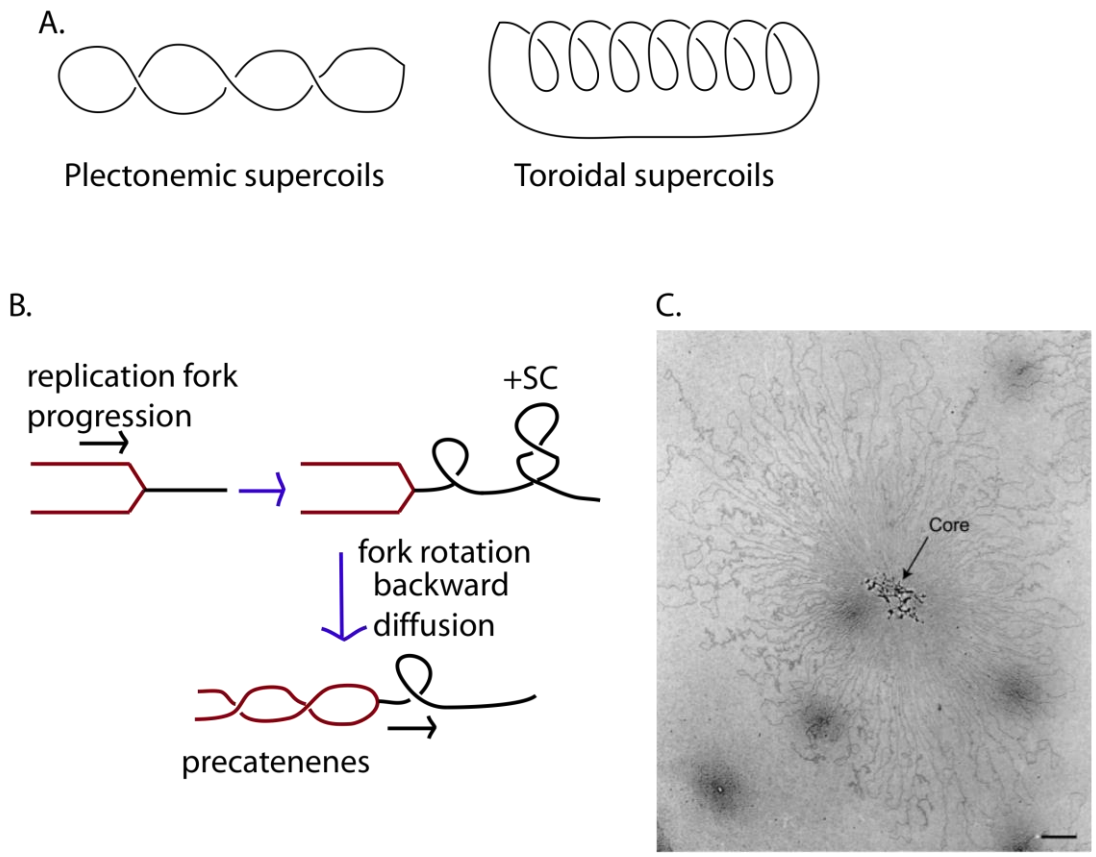

Fig 1.1: Topological organization and supercoiling of the *E. coli* chromosome

A. Maintaining negative supercoiling is essential for chromosome compaction and function. *In vitro,* negative supercoils are plectonemic in the absence of constraining factors such as proteins, while the action of proteins generates toroidal supercoiling (adapted from Reyes-Lamothe et al. 2008b).

B. During replication, positive supercoils accumulate ahead of the fork, which are acted upon by DNA gyrase. Alternatively, if the fork rotates, positive supercoils can diffuse behind the fork such that the newly replicated sisters become interwound, generating precatenenes. These are a good substrate for TopoIV activity. Thus it is thought that gyrase acts ahead of the fork while TopoIV releaves precatenenes behind the fork and facilitates segregation of replicated DNA (adapted from Reyes-Lamothe et al. 2008b; Wang et al. 2008). Red lines: Replicated DNA; Black lines: unreplicated DNA

C. Electron micrograph of an isolated chromosome from *E. coli.* The chromosome appeared to consist of a central core with loops of DNA emanating from it. Multiple nicks were required to completely relax the entire molecule (adapted from Toro and Shapiro 2010; original picture from Kavenoff and Bowen 1976). It is thought that the *E. coli* chromosome is comprised of ~40-400 topologically independent domains (Postow et al. 2004). Domain barrier elements include nucleoid-associated proteins as well as transcription and replication. Scale bar = 1µm

1.2.3 Spatial organization of the chromosome

Based on the above, it was proposed that the *E. coli* chromosome was organized into a rosette-like structure, with a central core and loops emanating from it. If this were true, then any region of the chromosome would have a random position in the cell (Breier and Cozzarelli 2004). However, studies localizing different regions of the chromosome (in various bacteria) found that this was not the case (Webb et al. 1997; Niki and Hiraga 1998; Teleman et al. 1998; Jensen and Shapiro 1999). By fluorescently marking different chromosomal regions using techniques of FISH and FROS, it was established that the genetic map was recapitulated inside the cell i.e. position of the DNA locus on the chromosomal map corresponded to its position in the cell. Viollier et al. 2004 inserted 112 transposons carrying *lac* arrays into various regions of the *C. crescentus* chromosome and found that the markers were linearly organized from *ori* to *ter* (Fig 1.2A). Replication started at *ori* and each marker segregated to the opposite cell half soon after its replication, so the linear order was recapitulated as replication occurred.

In contrast *C. crescentus* and *B. subtilis* (Fig 1.2B), the *E. coli* chromosome displays a translational symmetry (Wang et al. 2005b; Nielsen et al. 2006; Wang et al. 2006). In new-born/ non-replicating cells, *oriC* is positioned at mid-cell and the left and right replichores flank it (Fig 1.2C). The terminus region seems to span the entire nucleoid, with the *ter2* marker localizing to the left pole and *ter4* to the right pole. Chromosome segregation occurs asymmetrically with an <*L-ori-R*> organization of each replichore (Nielsen et al. 2006; Wang et al. 2006). This organization is maintained in *E. coli* with a linear chromosome (Cui et al. 2007) or in cells undergoing multifork replication (Wang et al. 2006;

Nielsen et al. 2007). Even in cells carrying a chromosome with two origins of replication (Wang et al. 2011), organization does not change. Similarly, when only an ectopic *oriC* is present, it remains at its original position showing that active *oriC* does not necessarily relocate to mid-cell (Wang et al. 2011). Thus, these studies show that the bacterial chromosome is highly organized. There is not only supercoiling that compacts the chromosome, but also spatial organization of chromosomal regions.

1.2.4 Macrodomain organization in *E. coli*

It has been proposed that the *E. coli* chromosome is organized into macrodomains – regions that behave independently as segregation units and have their own structural properties (Fig 1.2D). There are 4 macrodomains in *E. coli: Ori, Ter*, Right and Left (flanking *Ter*) as well as two non-structured regions flanking *Ori* (Niki et al. 2000; Valens et al. 2004). The integrity of these macrodomains has been shown to be required for normal cell viability (Lesterlin et al. 2005). Consistent with the idea that macrodomains may be structured by specific proteins, Mercier et al. 2008 identified MatP, a macrodomain organizing protein, which binds 23 *matS* sites spread across 800kb of the *ter* region and organizes it. MatP foci colocalize with *ter* and absence of MatP perturbs *ter* localization causing premature segregation of this region. It is interesting to note that in contrast to the above, others have shown that regions just 200kb apart can occupy separate positions in the cell and segregate independently (Viollier et al. 2004; Fekete and Chattoraj 2005). Hence the role of macrodomain organization of chromosomes remains unclear.

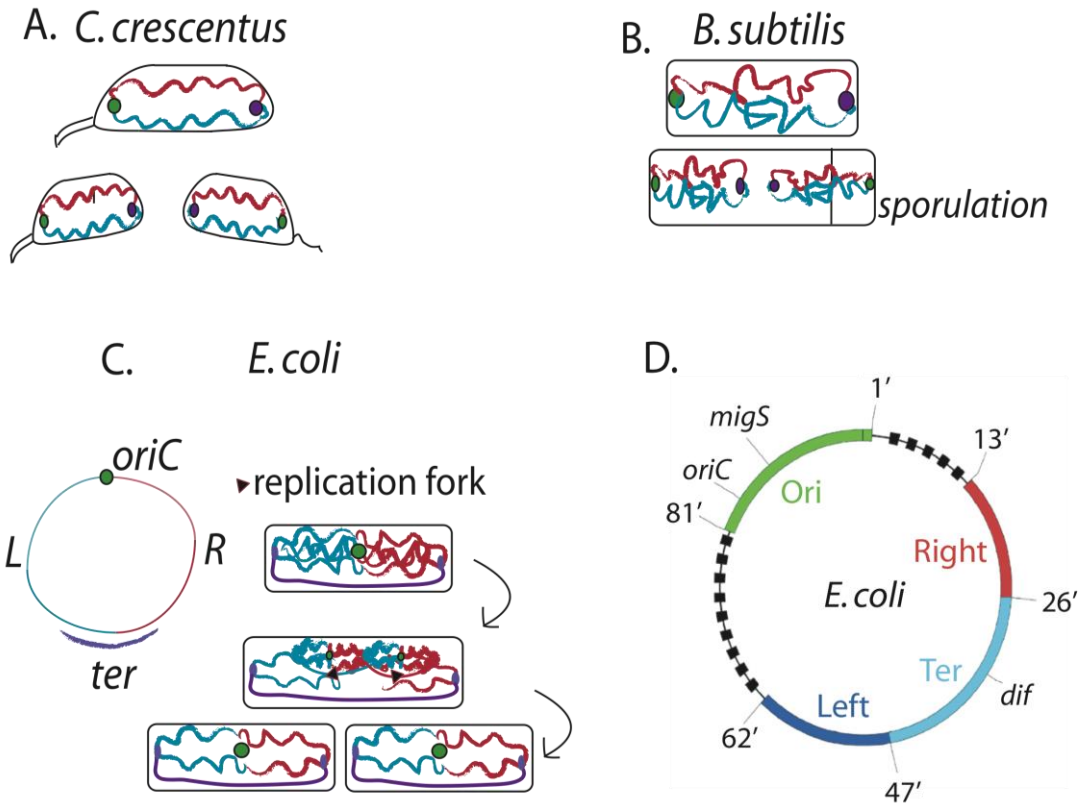

Fig 1.2: Spatial chromosome organization in bacteria

A. In *C. crescentus,* origins localize to the stalk pole (green spot) and terminus at the swarmer pole (purple spot). Replication arms of the chromosome have a linear organization along the cell's long axis. After replication, cells maintain mirror symmetry in chromosome organization (Viollier et al. 2004). (adapted from Toro and Shapiro 2010)

B. In *B. subtilis* chromosome organization is as in *C. crescentus,* with *ori* at one pole and *ter* at opposite. During sporulation, the daughter chromosome is anchored to the opposite pole via its origin and the rest of the chromosome is pumped into the forespore by the action of SpoIIIE (Wu and Errington 1994). (adapted from Reyes-Lamothe et al. 2008b)

C. As opposed to *B. subtilis* and *C. crescentus,* in newborn *E. coli*, origin (green) is localized to the middle of the cell and the left (blue) and right (red) replichores on either side. The *ter* region (about 400kb) spans the entire length of the nucleoid (most often seen at the left or right pole of the nucleoid) (purple line and dots). There is asymmetric segregation of replicated DNA and <*L*-*R*> organization is maintained in daughter cells (adapted from Wang et al. 2005b; Wang et al. 2006).

D. It is proposed that the *E. coli* chromosome is organized into 4 macrodomains (Ori, Ter, Right and Left). While regions within a macrodomain can interact, this is not possible between macrodomains. There are two non-structured regions flanking the Ori macrodomain. The role of macrodomain organization of the chromosome is unclear. (adapted from Valens et al. 2004)

1.2.5 Chromosome organization shaped by replication

An expectation of the asymmetric segregation model in *E. coli* would be that replisomes would move to quarter position after origin duplication (Wang et al. 2006). Indeed, Bates and Kleckner 2005 observed the appearance of two replisomes at quarter position in *E. coli* few minutes after replication initiation indicating that replisomes were not fixed at mid-cell (Lemon and Grossman 2001). By following fluorescently labelled replisome components in live *E. coli* cells, it was found that replisomes are mobile; they split within 5 min of *ori* duplication and track independently along DNA (Reyes-Lamothe et al. 2008a).

Furthermore, replication fork stalling changed the <*LRLR*> pattern to <*LRRL*> or <*RLLR*> depending on which arm the fork was blocked on (Liu et al. 2010a). Thus, it has been proposed that replication could shape spatial chromosome organization in *E. coli* by the sequential layering of newly replicated DNA around each origin (Reyes-Lamothe et al. 2008b; Liu et al. 2010a). Indeed, MukBEF may play a central role in coordinating the same, as chromosomal loci are mispositioned in *muk*$^{-}$ cells (Danilova et al. 2007; discussed later).

A recent study by Wiggins et al. 2010 proposed that the bacterial nucleoid is not an unstructured polymer, but rather a precisely organized nucleoid filament. They suggested that there are be two forces for organization: internal (intranucleoid interactions through proteins like MukB) or external (which act only on particular regions (like FtsK)). By measuring fluctuations in inter focal distances and individual locus positions in the chromosome it was concluded that intranucleoid interactions play a dominant role in chromosome organization. The authors propose that the *E.coli* chromosome resembles a mitotic chromosome.

1.2.6 Nucleoid-associated proteins

Two groups of proteins have been implicated in the process of chromosome condensation and organization: Nucleoid-associated proteins (NAPs) (reviewed in Dillon and Dorman 2010) and SMCs (discussed in detail later).

Common property of NAPs is to control transcription positively or negatively by binding DNA and changing its structure by bending, bridging or wrapping.

H-NS (histone-like nucleoid structuring protein) functions as homodimers, but can form higher order structures as well. H-NS forms DNA-protein-DNA bridges and stiffens it. It is thought that the bridging role compacts DNA, while the stiffening promotes gene silencing (because it coats the DNA and blocks access by RNA polymerase) (Grainger et al. 2006; Liu et al. 2010b). Another well-characterized NAP is HU (heat-unstable protein). HU binds DNA non-specifically, but has preference for binding bent or distorted DNA (Castaing et al. 1995). HU either stiffens DNA or promotes toroidal supercoiling and contributes to 30-40% of constrained negative supercoiling in *E. coli* (Guo and Adhya 2007; Higgins et al. 2010). Other NAPs include Fis, which bends DNA and regulates transcription (McLeod et al. 2002), IHF that also bends DNA and affects transcription and replication initiation and Dps (DNA protection during starvation protein) (reviewed in Higgins et al. 2010). It is important to note that deletion of one single NAP does not cause problems in transcription or nucleoid organization, indicating redundancy in their function (reviewed in Reyes-Lamothe et al. 2008b; Dillon and Dorman 2010).

1.3 Mechanism of chromosome segregation

Chromosome segregation can be defined as the process by which replicated DNA are partitioned into daughter cells. Indeed, chromosome organization and segregation are interdependent and cannot be entirely separated.

An early model for chromosome segregation was put forward by Jacob and Brenner 1963 who proposed that replicated DNA could be anchored to the membrane and passively segregated by cell growth. However, recent studies have shown that the timing of locus segregation after replication is too fast for the process to be completely passive or just driven by longitudinal cell growth (Fiebig et al. 2006; reviewed in Reyes-Lamothe et al. 2008b; Toro and Shapiro 2010). Abrupt and rapid segregation of replicated origins suggested that an active segregation mechanism was involved (Webb et al. 1998; Viollier et al. 2004). Consistent with this, the Par (partition) system was identified to play a role in chromosome and plasmid partition (reviewed in Gerdes et al. 2010); knocking out chromosomal Par systems has only a weak or conditional effect on chromosome segregation, whereas it significantly impairs plasmid inheritance (Dubarry et al. 2006). Par systems have three components: a centromere-like par site (*parS)*, a DNA binding protein that attaches to *parS* and an ATPase that promotes the movement of DNA bound to protein by oscillation or polymerization (Ebersbach et al. 2006; Salje and Lowe 2008). The ParAB system has been implicated in chromosome segregation for many bacteria (Lewis and Errington 1997; Fogel and Waldor 2006), along with the action origin anchoring proteins (TipN, PopZ in *C. crescentus* and RacA in *B. subtilis*) (Ben-Yehuda et al. 2003; Toro et al. 2008). Recent studies also link ParB to SMC (discussed later) (Gruber and Errington 2009; Sullivan et al. 2009).

Although there are no *parAB* homologs in *E. coli,* Yamaichi and Niki 2004 identified a 25bp *parS*-like sequence (*migS*) close to the origin. However, its mechanism of action is unclear, as deletion of *migS* does not lead to significant impairment of chromosome segregation (Yamaichi and Niki 2004; Fekete and Chattoraj 2005).

Another model for segregation is the "Extrusion-capture" model, where it is thought that a stationary replication machinery (located at cell centre) generates the force required to separate replicated sisters to opposite cell halves (Lemon and Grossman 2001). However, recent studies have shown that replicated loci remain cohesed for at least 5-15 minutes before segregation (Nielsen et al. 2006; Wang et al. 2006). Additionally, replisomes in *E. coli* are highly dynamic and independently move as if tracking along the DNA; hence, they do not act as factories and could not provide the necessary force required for segregation to occur (Reyes-Lamothe et al. 2008a).

Apart from replication, transcription (Dworkin and Losick 2002), transertion (Woldringh and Nanninga 2006) or MreB (the actin-like cytoskeleton element) action (reviewed in Gitai et al. 2005) have also been implicated in chromosome segregation. However, recent studies have shown that neither is required for effective chromosome segregation (Karczmarek et al. 2007; Wang and Sherratt 2010). Faithful segregation of replicated chromosomes also requires the action of the translocase FtsK and TopoIV. While some studies have suggested that the FtsK mediated action of TopoIV is restricted to the end of the cell cycle for decatenation of replicated chromosomes (Espeli et al. 2003a), a recent study has demonstrated the requirement for TopoIV activity throughout the cell cycle (Wang et al. 2008). FtsK also activates XerCD mediated chromosome dimer

resolution at the *dif* site (Aussel et al. 2002; Lesterlin et al. 2004). The mechanism of chromosome segregation in bacteria remains unclear. It has been suggested that the force for segregation could be provided by entropy (Jun and Mulder 2006). The entropy model would be a good way of explaining chromosome segregation and why no single process has been identified as essential for this process to occur (Jun and Wright 2010). Cells without Par systems or SMC proteins are still able to segregate their chromosomes, albeit not as happily as wild type.

1.4 SMCs and their role in chromosome organization and segregation

SMC (structural maintenance of chromosome) proteins are an ancient and ubiquitous class of proteins found in all domains of life (Cobbe and Heck 2004; Cavalier-Smith 2010) (Fig 1.3). Most bacteria have a single SMC complex comprising of a homodimer of SMC interacting with two accessory subunits, ScpA (kleisin) and ScpB. *E. coli* and its relatives carry a distant homolog of SMC: MukBEF (MukB – SMC, MukF – kleisin). Eukaryotes, on the other hand, have specialized SMC complexes: the cohesin complex (required for sister chromatid cohesion), the condensin complex (for chromosome organization/ segregation) and the SMC5/6 complex (involved in DNA repair) (reviewed in Nasmyth and Haering 2005; Nasmyth and Haering 2009). Each complex is made up of heterodimers of SMC proteins (SMC1/3 in cohesin, SMC2/4 in condensin and SMC5/6 in the repair complex) that interact with accessory subunits (one of them being kleisin) to form a functional holocomplex.

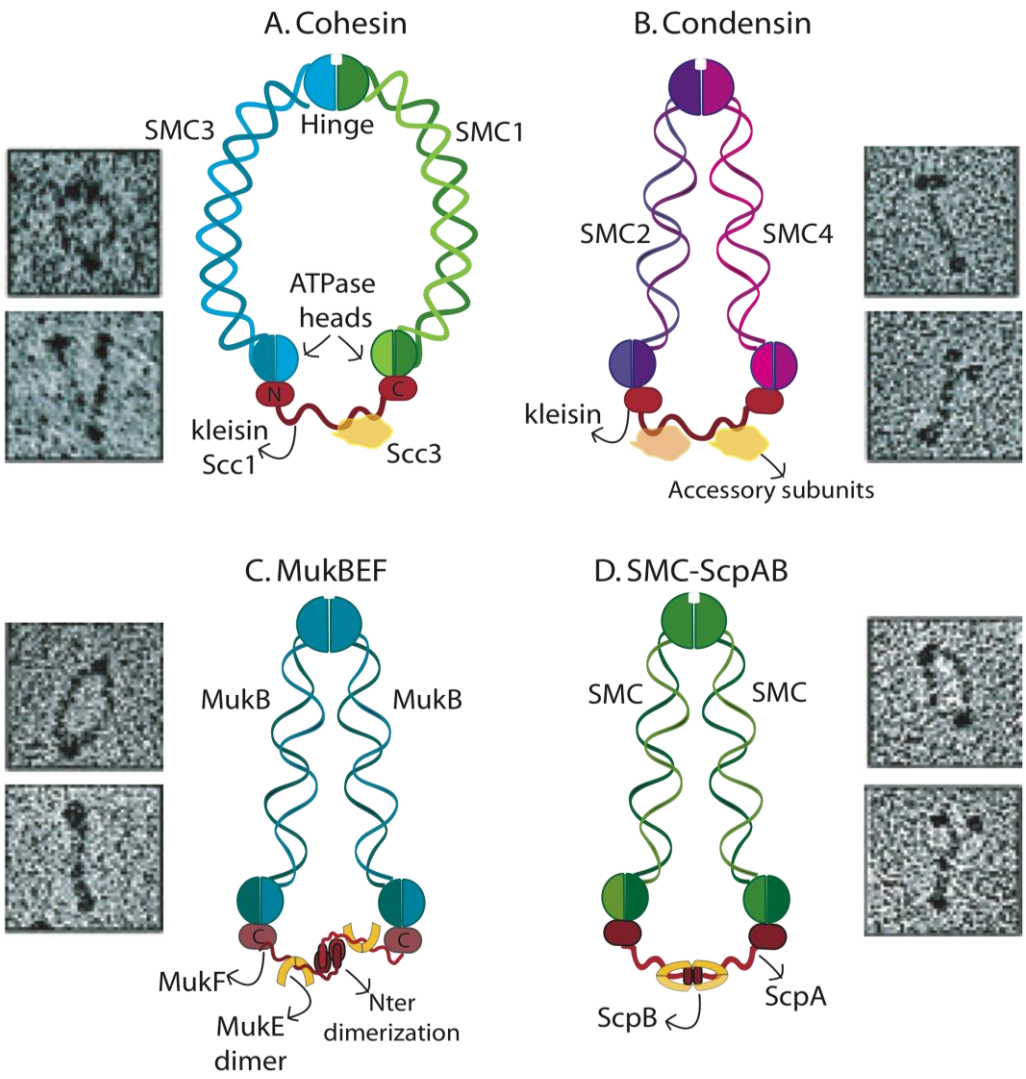

F

ig 1.3: SMC complexes in prokaryotes and eukaryotes

A. Yeast cohesin is comprised of two SMC subunits (SMC1/3), a kleisin subunit (Scc1) and an accessory subunit (Scc3). Dimerization occurs via the hinge and SMC heads have ATPase activity. The interaction interface of kleisin and SMC1 has been characterized (Haering et al. 2004). It is proposed that cohesin forms a ring around DNA. EM images shown on left (adapted from Nasmyth and Haering 2005)

B. Condensin has similar structure to cohesin. However, EM suggests that while two arms in the cohesin dimer are apart, they are tightly interwound in condensin (adapted from Nasmyth and Haering 2005).

C, D. *E. coli* has a distant relative of SMC, MukB, with two accessory subunits, MukF (kleisin) and MukE. MukF forms a domain swapped dimer at its N terminus and its C-ter interacts with MukB. One MukE dimer interacts with a MukF monomer (Woo et al. 2009). Most bacteria have an SMC homolog that interacts with ScpA (kleisin) and ScpB. It is thought that SMC-ScpAB form complexes similar to MukBEF (adapted from Hirano 2006; Cuylen and Haering 2011). EM images adapted from Nasmyth and Haering 2005

1.4.1 Discovery of SMC proteins

SMC proteins in eukaryotes were found to be required for maintenance of chromosome structure in *Xenopus* egg extracts (Hirano and Mitchison 1994; Hirano et al. 1997). Purified chromosomes from the eggs had, apart from histones, TopoII and the SMCs XCAP-C and E (the condensin complex) (Hirano et al. 1997). Cohesin was identified as an SMC complex required for proper segregation of chromosomes via screens looking for mutants that caused loss of sister-chromatid cohesion or chromosome loss (Guacci et al. 1997; Michaelis et al. 1997; Toth et al. 1999).

The prokaryotic SMC protein, MukB, was identified much earlier, but it was realised only later that it was an SMC protein. MukB was discovered in a screen to find *E. coli* mutants with chromosome segregation defects (Hiraga et al. 1989; Hiraga et al. 1991). Genes thus found were named “mukaku” which means anucleate in Japanese. One of the candidates identified was MukB, a 177kDa protein, whose mutation caused the cells to become temperature sensitive and produce anucleate cells. While mutated MukB grew well at low temperatures with 5% anucleate cells, viability of the strain dropped and anucleate cell production increased with increasing temperature (up to 10-20% at 42°C). At high temperatures, in rich media, *mukB*$^{-}$ cells were filamentous. Deletion of two accessory subunits (present in the same operon) *mukF* and *mukE* had the same phenotype as *mukB,* while deletion of *smtA,* a gene upstream of *mukF*, had no detectable phenotype. Hence, the *mukB* operon consists of 4 genes (*smtA-mukF-mukE-mukB*) expressed under the *smtA* promoter (Niki et al. 1992; Yamanaka et al. 1995; Yamanaka et al. 1996).

Recently, presence of MukB-like homologs in bacteria carrying an SMC complex has been reported (reviewed in Gruber 2011; Petrushenko et al. 2011). Although there is little sequence homology, the predicted secondary structure is similar to MukB. A marked difference between MksB (Muk-like B) and MukB is that the coiled-coil is shorter for the former. MksB deletion in *P. aerogenosa* leads to production of only 1% anucleate cells. Interestingly, SMC deletion in *P. aerogenosa* does not lead to a drastic phenotype either. Several other bacteria (*D. radiodurans*, *S. pneumoniae* and *S. aureus*) have no phenotype upon SMC deletion as well (Bouthier de la Tour et al. 2009; Yu et al. 2010; Minnen et al. 2011). Thus it is likely that some bacteria could also have multiple SMC-like complexes with overlapping functions, but this needs to be confirmed with better assays.

1.4.2 Structure of the SMC complex

SMC proteins belong to the ABC transporter family and carry a highly conserved WalkerA motif in the N terminus and a WalkerB motif and ABC signature motif in the C terminus (all involved in ATPase activity). EM studies with purified SMC showed that they formed V-shaped dimers (Melby et al. 1998 (*B. subtilis* and *E. coli* SMC); Anderson et al., 2002 (Condensin and Cohesin)). Furthermore biochemical studies showed that SMCs formed intra-molecular dimers via the hinge, with anti-parallel coiled-coils thus allowing the N and C terminus of the heads to be juxtaposed on each end (Fig 1.4A/B) (Hirano et al. 2001; Haering et al. 2002).

Structural studies on *Pyrococcus* Rad50 heads as well as *Thermotoga* and *Pyrococcus* SMC heads (Hopfner et al. 2000; Löwe et al. 2001; Lammens et al. 2004) suggest that in the absence of ATP, the two heads of the dimer are apart.

When ATP binds, the Walker A motif (lysine-serine residues in particular) and the serine and glycine of the signature motif of the opposite head participate, bringing the two heads together. The Walker B motif provides two essential residues to the ATPase cycle: aspartate and glutamate. While aspartate is thought to be required for stably binding ATP to the heads, the glutamate may act as the catalytic base (Orelle et al. 2003). In this manner, each SMC dimer can bind two ATP molecules stabilized by interaction with the signature motifs of the opposite head (Arumugam et al. 2003; Weitzer et al. 2003) (Fig 1.4C). Recent structural studies with Rad50-Mre11 complexes suggest that ATP binding to the heads induces changes in the interaction of Mre11 with the complex as well as the coiled-coil region of Rad50, allowing it to take up a clamp-like structure. This may modulate the complex's DNA binding and nuclease activity (Lammens et al. 2011; Lim et al. 2011).

Thermotoga SMC hinge appears to have a doughnut shape interface between each monomer with a small gap/ hole in the central region (Haering et al. 2002). MukB hinge, however, seems to lack this central hole, instead the interface appears to be long and continuous (Ku et al. 2010; Li et al. 2010a). MukB also lacks a DNA binding surface on the hinge, as has been suggested for *B. subtilis* (Hirano and Hirano 2006).

Due to the unique structure of the SMC hinge, it is thought to participate in DNA interaction, possibly allowing DNA to enter into the SMC complex's ring-like structure (Gruber et al. 2006; Hirano and Hirano 2006; reviewed in Ocampo-Hafalla and Uhlmann 2011). Indeed, biochemical head-hinge interaction has been also reported for the cohesin complex (Mc Intyre et al. 2007). *In vitro,* DNA binding to the hinge stimulates head ATPase activity in *Bs*SMC (Hirano

and Hirano 2006). It remains to be seen whether this is the case for MukB as well.

Woo et al. 2009 (reviewed in Rybenkov 2009) determined the complete structure of the MukBEF holocomplex (from *H. ducreyi)* using a simplified version of MukBEF: MukB heads, MukE (full length) and MukF (middle and C ter regions). MukF forms a domain swapped dimer via its N terminus (Fennell-Fezzie et al. 2005). Its C-ter WHD is responsible for interaction with MukB, while the middle region provides a binding interface for one MukE dimer (Woo et al. 2009; Gloyd et al. 2011). Based on the crystal structures of the complex, it has been proposed that MukB, MukE and MukF exist in a 2:2:1 ratio respectively upon ATP binding (closed complex) and take up an open 2:4:2 conformation when ATP is hydrolysed (open complex) (Fig 1.4D). The asymmetric 2:2:1 complex is generated due to the detachment of one MukEF complex (2:1) from the MukEF heterohexamer (Shin et al. 2009). Indeed, biochemical studies have proposed that the MukBEF 2:2:1 complex is more stable than the 2:4:2 complex (Petrushenko et al. 2006b). It is interesting to note that bacterial SMCs have DNA binding regions in their head domain (Lim and Oh 2009), a feature not seen in eukaryotic SMCs. Although mutating these abrogates DNA binding *in vitro*, its physiological significance remains to be determined (Woo et al. 2009).

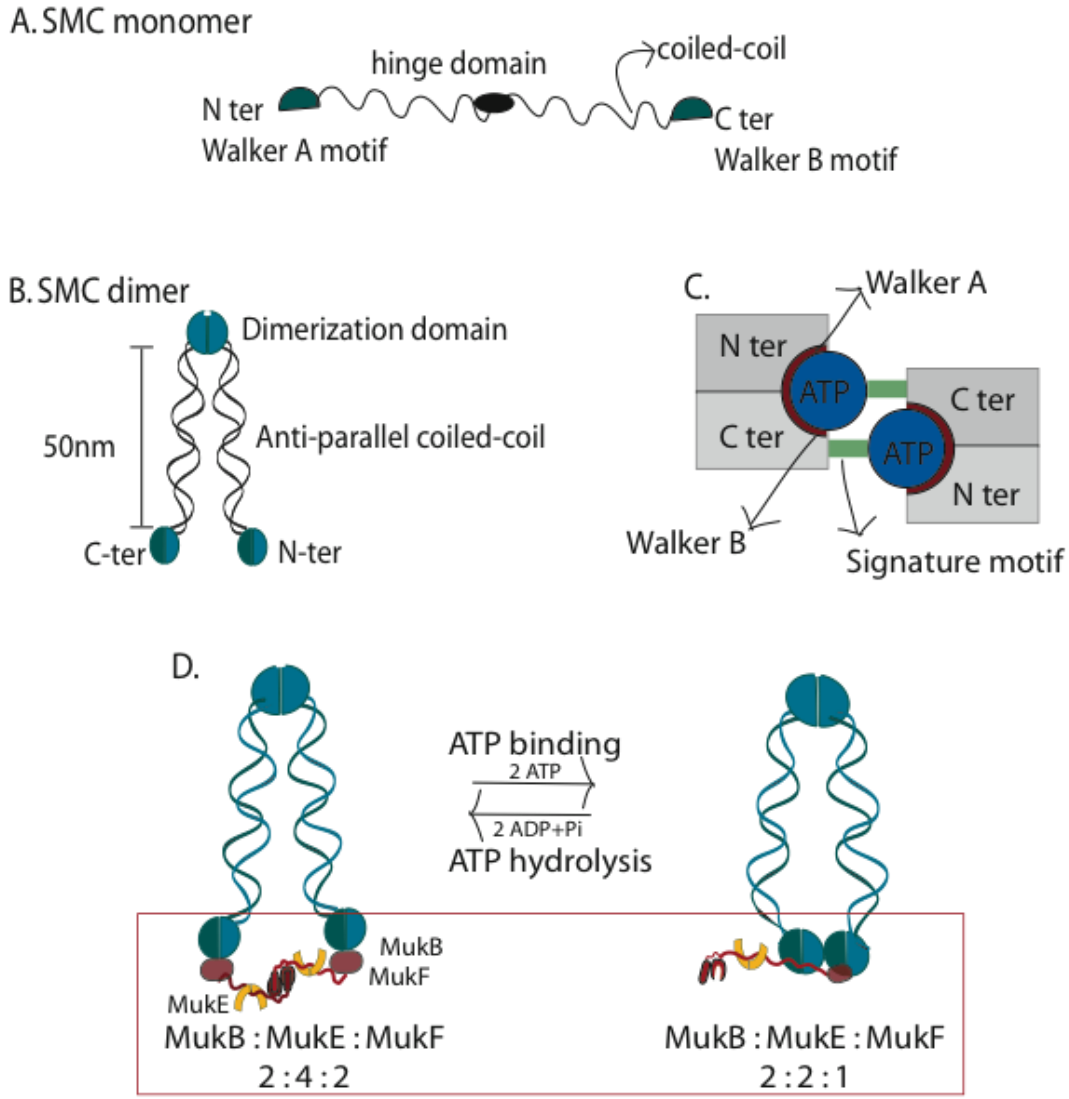

Fig 1.4: Structure of the SMC complex

A. SMC monomer comprises of a central hinge domain, N-ter Walker A motif capable of ATP-binding and C-ter Walker B motif for ATP hydrolysis, both separated by 100nm of coiled-coil. B. A monomer can fold on itself, forming anti-parallel coiled-coils (50nm in length) thus juxtaposing the N and C ter. Each monomer can form a dimer via its hinge domain (from Nasmyth and Haering 2005). C. ATP binding brings SMC heads together. Each SMC can bind one ATP via its Walker A motif, this is stabilized by interaction of the signature motif from the opposite monomer. An SMC dimer binds 2 ATP molecules. Upon ATP hydrolysis, the two heads would move apart (adapted from Arumugam et al. 2003). D. Based on crystal structures of MukB heads in complex with MukEF, Woo et al. 2009 proposed that the MukBEF complex has a 2:4:2 (MukB:E:F) ratio (open complex) in the absence of ATP. The binding of ATP brings the MukB heads together and displaces one MukEF complex resulting in a 2:2:1 (MukB:E:F) closed complex (adapted from Woo et al. 2009)

1.4.3 Insight into SMC mechanism of action *in vitro*

Early experiments with condensin complexes from *Xenopus* proposed that condensin induced positive supercoils into plasmids in an ATP dependent manner (in the presence of TopoI), by toroidal wrapping of DNA around SMC heads (Kimura and Hirano 1997) (Fig 1.5A). The compensatory negative supercoils generated would be removed by TopoI, giving the DNA overall positive supercoiling. Furthermore, the incubation of nicked circular DNA with 13S condensin and TopoII resulted in positive knotting of DNA (Kimura et al. 1999). This activity required ATP and the condensin holocomplex. *E. coli* MukB and *S. cerevisiae* SMC2/4 also generated positive knotting in the presence of TopoII. However, unlike 13S condensin, *S. cerevisiae* condensin did not change net supercoiling (Stray and Lindsley 2003; Stray et al. 2005) while MukB action resulted in negative supercoiling (Petrushenko et al. 2006a) in the absence of accessory subunits or ATP (Stray et al. 2005; Petrushenko et al. 2006a). In addition, SMC2/4 and MukB readily multimerized on DNA. Contrary to *Xenopus* condensin, addition of MukEF to the reaction disrupted MukB action on DNA (Petrushenko et al. 2006b). The DNA reshaping activities described above required excess of protein in the reaction. Despite the discrepancies in the action of condensin, generation of positive knots (in the presence of TopoII) in nicked plasmid substrate seems to be a conserved feature of these complexes (Fig 1.5B) (reviewed in Carter and Sjogren 2011).

Single molecule experiments showed that MukB could compact DNA against force (Chen et al. 2008; Cui et al. 2008). While ATP was required for the initial nucleation step, it was not required for the contraction process (Cui et al. 2008). Contrary to this, Chen et al. showed that the contraction process required the

presence of hydrolysable ATP and accessory proteins (similar to *Xenopus* condensin I (Strick et al. 2004)).

A recent study has proposed that MukB can bridge two DNA molecules, independent of its DNA reshaping activity (Petrushenko et al. 2010) (Fig 1.5C). While preassembled MukBEF complexes (with a ratio of 2:4:2) were found to inhibit bridging, the addition of MukEF after MukB stabilized the bridges. It is thought that the ratio of MukB:E:F is 2:2:1 or less in this case. Unlike DNA binding activity, ATP enhanced the bridging action of MukB. EM and biochemical studies have also proposed that MukBEF could assemble into macromolecular structures (Matoba et al. 2005; Woo et al. 2009).

Although *in vitro* experiments provide insight into the mechanism of action of SMC proteins, the *in vivo* significance of all of these activities remains to be established.

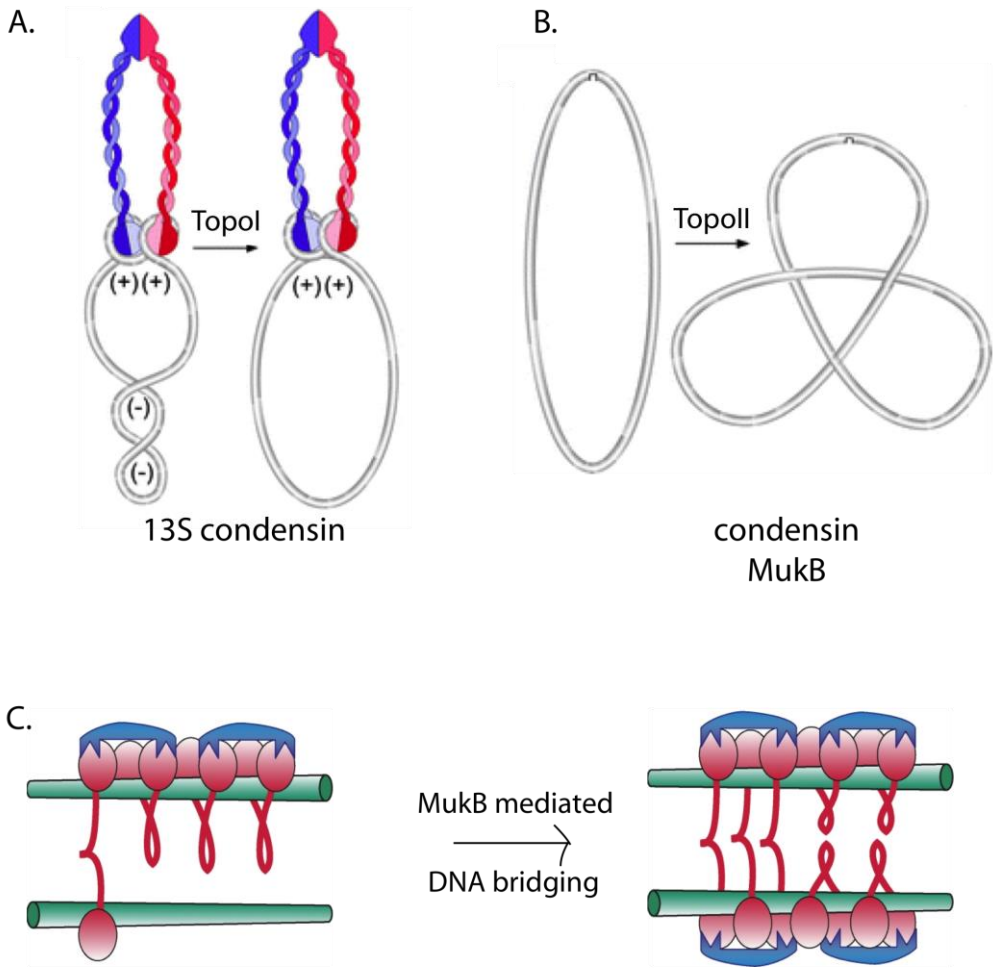

Fig 1.5: Effect of condensin/ MukB on DNA *in vitro*

A. *In vitro,* 13S condensin (+TopoI) induced positive supercoiling in a closed plasmid substrate. One hypothesis was that condensin does so by toroidal wrapping of DNA. The compensatory negative supercoils generated would be removed by TopoI (Kimura and Hirano 1997). However, in a similar reaction, SMC2/4 did not affect net supercoiling, while MukB induced negative supercoiling (adapted from Nasmyth and Haering 2005).

B. 13S condensin, SMC2/4 and MukB promote the generation of right-handed knots into nicked circular DNA in the presence of TopoII (adapted from Nasmyth and Haering 2005).

C. Single molecule studies have suggested that MukB can bridge two DNA molecules *in vitro*. This activity is thought to be independent of its DNA reshaping activity. MukEF was found to modulate the bridging activity (MukB in red, MukEF in blue) (adapted from Petrushenko et al. 2010).

1.4.4 Significance of SMC ATPase activity

Purified SMC proteins have weak ATPase activity *in vitro.* While for condensin this is between 5-20 ATP/min/dimer (reviewed in Cuylen and Haering 2011), it is even slower for MukB, 0.8-4 ATP/min/dimer (Chen et al. 2008; Woo et al. 2009). *Bs*SMC ATPase activity is stimulated in the presence of DNA while ScpA and ScpB suppress this stimulation (Hirano and Hirano 2002; Hirano and Hirano 2004). In contrast, DNA has little effect on MukB ATPase activity but MukEF stimulates it ~7 fold (Chen et al. 2008; Woo et al. 2009). Similar to MukBEF, it has been shown that Scc1 stimulates ATPase activity of SMC1/SMC3, while presence of DNA has no effect (Arumugam et al. 2006). Mutations in the Walker A/ Walker B motifs of *Bs*SMC heads showed, that while ATP binding/ hydroysis is not required for complex formation (Hirano and Hirano 2004; Mascarenhas et al. 2005), ATP binding to SMC1 is required for Scc1 association with SMC1/3 in cohesin (Arumugam et al. 2003; Weitzer et al. 2003). ATPase mutants are inviable *in vivo*, highlighting the significance of this property (Arumugam et al. 2003; Weitzer et al. 2003; Mascarenhas et al. 2005; Woo et al. 2009). *In vitro,* two views have emerged for condensin and cohesin ATPase significance:

*Bs*SMC Walker B mutants that were disengagement deficient (E to Q) stably associated with doubled-stranded DNA (Hirano and Hirano 2004). Wild type SMC, on the other hand, associated transiently with dsDNA. This association was enhanced in the presence of ScpA, dependent on order of addition. It was proposed that ATP dependent SMC head engagement was required for stable association with DNA. Interestingly, mutations in the basic residues of the hinge (which abrogated its interaction with DNA) affected dsDNA stimulated ATPase

activity of the SMC heads (Hirano and Hirano 2006). It was thus proposed that initial DNA interaction of the hinge triggers ATP hydrolysis at the SMC heads and allows stable hinge association with DNA. ATP binding reengages the heads intra/ inter-molecularly (Hirano and Hirano 2006; reviewed in Hirano 2006).

In contrast to the above, yeast cohesin Walker B (E to Q) mutants are thought to be unstable on DNA (Arumugam et al. 2003; Weitzer et al. 2003). A recent study by Hu et al. 2011 found that the Walker B mutant localized to the same region (centromeres) as the Scc2/4 loading complex. However, they did not relocate to pericentric regions (where wild type cohesin is present). Thus, ATP binding was essential for complex formation, while hydrolysis was essential for stable localization and function. Although ATP dependent SMC action may differ for condensin/ cohesin, their activity seems to be physiologically significant.

1.4.5 Understanding the function of the bacterial SMC complex *in vivo*

Fluorescent fusions of *Bs*SMC/ MukB form foci on the nucleoid (den Blaauwen et al. 2001; Ohsumi et al. 2001; Danilova et al. 2007). Furthermore, Danilova et al. 2007 found that MukB foci colocalized with the origin region with an average ratio of 1.4:1 MukB:*ori1* (Fig 1.6). Time-lapse imaging showed that MukB foci seemed to duplicate and move to ¼ or ¾ position along with or just before segregation of replicated origins. Based on this it was proposed that MukBEF organizes newly replicated DNA around the origin region. However, ChIP studies failed to pick up specific sequence association (Danilova et al. 2007).

Bacterial SMC mutants have disorganized and poorly segregated chromosomes (as judged by position of chromosomal markers) (Jensen and

Shapiro 1999; Weitao et al. 2000; Danilova et al. 2007). Danilova et al., 2007 proposed that origin position is not random in *muk*$^{-}$ cells; the chromosome instead adopts a new spatial organization. While in wild type cells the origin is at mid-cell with left and right replichores on either side, in *muk*$^{-}$ cells the origin localizes to the cell pole with a linear organization of the rest of the chromosome (Fig 1.6). This is reminiscent of the spatial chromosome organization *C. crescentus* or chr1 of *V. cholerae* (Viollier et al. 2004; Fogel and Waldor 2005). Furthermore, deletion of the ParAB system in *Vibrio* results in chr1 having an *E. coli* type chromosome organization (Fogel and Waldor 2006) suggesting that without origin constraint due to partitioning, an *E. coli*-type spatial organization may be the default situation in other bacteria.

SMC is recruited to the origin in *B. subtilis* as well (Sullivan et al. 2009; Gruber et al. 2009). Formation of SMC foci, in this case, depends on binding of Spo0J (ParB) to *parS* sites (independent of ParA). In cells lacking Spo0J, only weak SMC foci are seen. This could be due to SMC association with regions of high transcription (from ChIP) (Gruber et al. 2009). It was hence suggested that SMC organizes the origin regions and thus promotes effective chromosome segregation. A similar mechanism of SMC recruitment was seen in *S. pneumoniae* (Minnen et al. 2011). Interestingly, there is no Soj homolog in this species, suggesting the ParB-SMC interaction may be evolutionarily more conserved. A similar mechanism cannot be proposed for MukBEF, as *E. coli* has no ParB homolog. However, MukBEF foci also localize around the origin region (Danilova et al., 2007).

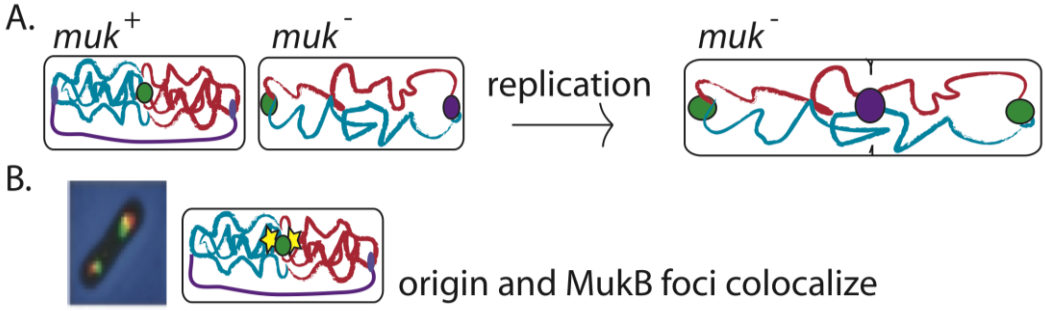

Fig 1.6: MukBEF is required for wild type positioning of the origin region

A. Deletion of MukB led to loss of wild type spatial organization of the chromosome (as judged by the position of chromosomal markers) with origins at cell pole (green) instead of mid-cell. Also, <*L* (blue)-*R* (red)> organization was lost and the chromosome has been proposed to adopt a linear organization from *ori* to *ter* (similar to *C. crescentus*). In replicating cells, origins localize to opposite poles instead of cell quarters (adapted from Danilova et al. 2007).

B. In wild type cells, MukB foci colocalize with *ori* (MukB focus is yellow and origin in green). The ratio of MukB focus to origin was 1.4:1 i.e. between one to two MukB foci per origin (adapted from Danilova et al. 2007).

1.4.6 Synthethic lethality/ suppression of the Muk- phenotype

A suppressor of *muk*¯ temperature sensitivity and anucleate cell production maps to a mutation in *topA*, the gene for TopoI, which would result in an increase negative supercoiling. Consistently, *muk* mutants are hypersensitive to gyrase inhibition (Weitao et al. 1999; Sawitzke and Austin 2000; Lindow et al. 2002 in *B. subtilis*). It was hence proposed that MukB organizes and segregates the chromosome by directly affecting the level of negative supercoiling, possibly by constraining DNA and promoting topoisomerase activity (reviewed in Holmes and Cozzarelli 2000)**.**

Furthermore, overexpression of TopoIV could rescue an *smc*¯ phenotype in *B. subtilis* (Tadesse et al. 2005). Recent studies have also reported direct interaction between MukB and ParC (subunit of TopoIV), which stimulated decatenation and relaxation activity of TopoIV *in vitro*. ParC mutants defective in MukB interaction had a partial *par* phenotype, while a MukB hinge mutant that disrupted its interaction with ParC was *muk*¯ *in vivo* (Hayama and Marians 2010; Hirano 2010; Li et al. 2010b). Loss of TopoIV activity prevents segregation of sister loci (Wang et al. 2008). Thus, it is possible that MukBEF promotes chromosome organization, providing TopoIV with optimal substrate for decatenation and chromosome segregation (Gruber 2011).

Translocase activity in the C terminus of FtsK was also found to be essential *muk*¯ cells (Yu et al. 1998; Sivanathan et al. 2009). One reason for this could be due to increased dimer formation in *muk*¯ cells. Indeed, *recA* and *muk* are synthetic lethal (Hiraga 2000; Kouzminova et al. 2004) suggesting an increase in DNA damage in *muk*¯ cells that needs to be resolved by homologous

recombination. Alternatively FtsK translocation may be required to sort the disorganized *muk*$^{-}$ chromosome efficiently prior to cell division.

HU was also found to be synthetic lethal with Muk, however, the reason for this is unclear (Jaffe et al. 1997). Other suppressors of the Muk- phenotype include *smbB* (which causes truncation of RnaseE) and genes that cause condensation of nucleoids in the presence of camphor (which decondenses the nucleoid) (Hiraga 2000).

seqA deletion rescues *muk*$^{-}$ cells (Hiraga 2000; Weitao et al. 2000). Interestingly, *seqA*$^{-}$ cells have hypercompact nucleoids while *muk*$^{-}$ cells have decondensed nucleoids. MukFEB and SeqA are thought to have coevolved with the methyltransferase Dam. A bioinformatics study found 18 putative proteins conserved in genomes that carried *dam* that could have potential DNA structuring ability (Brezellec et al. 2006). One of the candidates identified from this was the organizer of the *ter* macrodomain, MatP (Mercier et al. 2008). Also, bacteria that do not have the *mukBEF-seqA-dam* entourage have the SMC and ParAB system, and alternative chromosome organization.

1.4.7 Insight from eukaryotic SMCs

1.4.7.1 Condensin

Although eukaryotic SMCs are more specialized than their prokaryotic counterparts, they may share conserved mechanisms of action. Early experiments identified condensin to be essential for mitotic chromosome assembly and maintaining chromosome structure (Hirano and Mitchison 1994; Hirano et al. 1997); condensin and TopoII maintained chromosome structure even in the absence of histones (Maeshima and Laemmli 2003). Furthermore, in the absence of condensin, “chromosome anchoring proteins” (such as non-

histone proteins and TopoII) were mislocalized (Hudson et al. 2003; reviewed in Hudson et al. 2009). The absence of condensin did not cause decondensation; it was predominantly required for chromosome shape maintenance.

ChIP studies on yeast condensin showed that it is was enriched at centromeric regions (Wang et al. 2005a; D'Ambrosio et al. 2008b). Furthermore, condensin and the cohesin loader (Scc2/4) colocalized at tRNA genes as well as highly transcribed genes; interestingly, condesin could bind highly transcribed genes even in the absence of transcription (D'Ambrosio et al., 2008b). It is interesting to note that sequence dependent loading as well as association with regions of high transcription has been shown for prokaryotic SMCs as well (Gruber and Errington 2009; Sullivan et al. 2009; Minnen et al. 2011). Thus, this might be a conserved mechanism for SMC loading on DNA.

In anaphase, condensin absence leads to lagging and poor segregation of chromosomes (Oliveira et al. 2005; Gerlich et al. 2006; reviewed in Hudson et al. 2009). It has been proposed that condensin promotes recoiling of chromosome arms, which could also aid in removing residual cohesin from the arms (Renshaw et al. 2010; Cuylen and Haering 2011). Another reason for poor segregation could be due to reduced decatenation activity of TopoII. Indeed, MukB and TopoIV have been shown to physically and functionally interact *in vitro* (Hayama and Marians 2010; Li et al. 2010b). D'Ambrosio et al. 2008a found that in the absence of condensin, foreign TopoII could effectively achieve decatenation, suggesting that condensin mediated TopoII action was required for proper chromosome segregation. Indeed, the lack of rigid structure/ organization of the chromosomes could itself result in segregation defects, a

proposed model for bacterial SMC function (reviewed in Thanbichler and Shapiro 2006; Danilova et al. 2007).

1.4.7.2 Cohesin

Cohesin is also required for the effective segregation of sisters. Cohesin is loaded onto the chromosomes by the recruitment complex Scc2/4 (Ciosk et al. 2000). Sister chromatid cohesion is established during replication and persists until anaphase. Cleavage of Scc1 by the protease, Separase, occurs at the metaphase-to-anaphase transition and allows the segregation of the mitotic chromosomes to opposite poles (Uhlmann et al. 1999; Hornig and Uhlmann 2004). ChIP studies showed that cohesin was enriched at the centromeres and recruited to the same sites as condensin (by Scc2/4); while in *Drosophila,* it seemed to remain associated with its loading site, cohesin relocated to sites of convergent transcription along the chromosome arms in yeast (Lengronne et al. 2004; Schmidt et al. 2009; reviewed in Hudson et al. 2009). The relocation of cohesin has been attributed to translocation of the complex by RNA polymerase action (Lengronne et al. 2004; Schmidt et al. 2009; reviewed in Ocampo-Hafalla and Uhlmann 2009). Indeed, blocking transcription of a particular gene prevents the detection of cohesin downstream of the gene. The colocalization of cohesin with transcriptional insulators as well as its effect on expression of genes near its binding site has suggested that cohesin may also regulate gene expression (reviewed in Nasmyth and Haering 2009; Pauli et al. 2010). Cohesin has also been implicated in double strand break repair (Sjogren and Nasmyth 2001; reviewed in Nasmyth and Haering 2009).

1.4.8 The SMC complex may form a ring

Cleaving the coiled-coil of SMC3 causes the release of cohesin from chromosomes suggesting that cohesin may form a ring around DNA (Gruber et al. 2003). Furthermore, opening of cohesin's hinge was essential for its association with DNA, but not its dissociation (Gruber et al. 2006). Indeed, chemical crosslinking of SMC1/3 and Scc1 created a covalently closed ring that cohesed sister minichromosomes even after protein denaturation. Only linearization allowed cohesin to slide off DNA (Haering et al. 2008) suggesting that cohesin topologically entraps DNA within rings (Fig 1.7A).

AFM and EM studies have suggested that ring formation might be specific only to cohesin as condensin arms seem to be closely associated (Anderson et al. 2002; Yoshimura et al. 2002). In addition, proteolytic cleavage of the SMC2 coiled-coil did not release condensin from the chromosome (Hudson et al. 2008). However, cleavage of the coiled-coil in this case was at different positions and may not have opened the ring (Cuylen and Haering 2011). Indeed, a recent study has shown that condensin also forms a ring around DNA in a manner similar to cohesin (Cuylen et al. 2011). Opening of the ring caused telomeric regions to segregate poorly, suggesting that linking of chromosomal regions by condensin was necessary for organization of the chromosome and effective segregation (Cuylen et al. 2011). Ring formation has also been proposed for *Bs*SMC (Volkov et al. 2003).

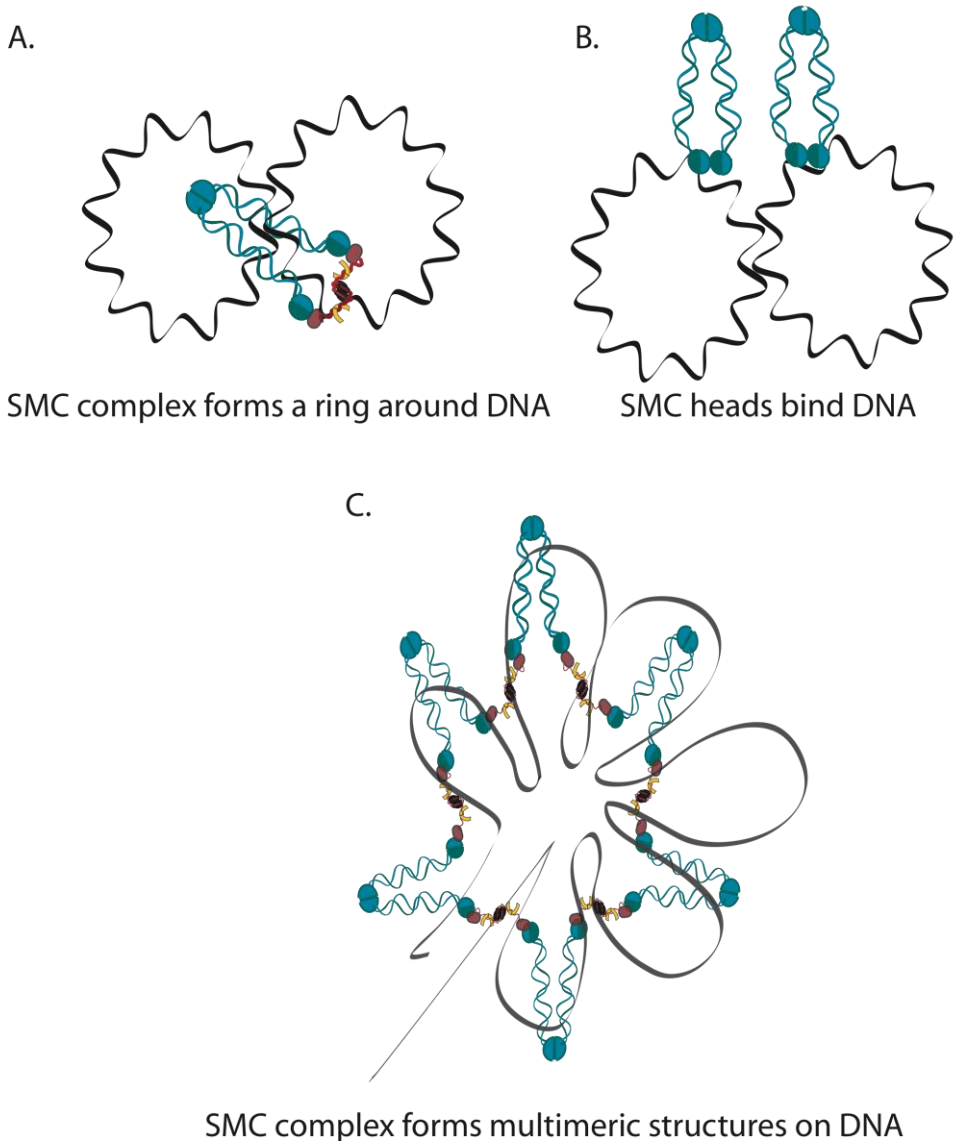

Fig 1.7: Proposed modes of action for SMC complexes

A. It has been shown that cohesin and condensin form rings around DNA and can topologically entrap minichromosomes (Haering et al. 2008; Cuylen et al. 2011). Furthermore, FRET experiments suggest that cohesin may act as single rings (Mc Intyre et al. 2007).

B. MukB heads have DNA binding activity *in vitro*. It has been proposed that the heads can bring regions of DNA together by bridging them (Petrushenko et al. 2010; Woo et al. 2009). However, these experiments were done with excess of protein (or in the absence of accessory subunits); their *in vivo* significance is unclear

C. EM and biochemical studies have also suggested the formation of multimeric complexes that could hold loops of DNA within them – this remains to be tested inside the cells. (adapted from Cuylen and Haering 2011).

1.4.9 A unified mechanism of action for SMC complexes

The mechanism of action of bacterial SMCs *in vivo* remains unclear (reviewed in Graumann and Knust 2009). Recent advances have begun to shed light into their mechanism of association with DNA and their probable roles in chromosome organization and segregation. The fundamental principles for loading on chromosomes seem to be a conserved feature amongst condensins and bacterial SMCs (for MukBEF this remains to be established). While it is suggested that condensin topologically entraps DNA by ring formation, crystal structures and EM have also suggested multimers of SMC acting on the chromosome (Fig 1.7C). There is also *in vitro* evidence of MukB heads interacting with DNA directly (Fig 1.7B). It must be remembered though, that most *in vitro* assays utilize excess protein and may be carried out in non-physiological conditions and without accessory proteins. Thus, it is important to test the *in vivo* significance of proposed *in vitro* mechanisms of action. In light of emerging crystal structures as well as development of better tools and assays, it is now possible to obtain mechanistic insight into the function of SMCs in chromosome organization and segregation *in vivo*.

CHAPTER 2

Role of MukBEF in spatial organization of the *E. coli* chromosome

2.1 Objectives

The bacterial chromosome is compacted into a cell that is ~1000 times smaller than its length and faithfully replicated, segregated and transcribed within a confined space. *In vitro* and *in vivo* work has revealed that the chromosome is not only compacted, but also spatially organized with chromosomal regions occupying specific positions in the cell (reviewed in Toro and Shapiro 2010). In newborn *E. coli*, the origin is located at mid-cell and the left and right replichores occupy either cell halves. During replication, origins migrate to cell quarters and rest of the chromosome segregates asymmetrically generating a highly reproducible <*L-ori-R*> pattern (Wang et al. 2005b; Wang et al. 2006). It has been proposed that this pattern could be a consequence of layering of newly replicated DNA around the origins (Reyes-Lamothe et al. 2008b; Liu et al. 2010a), removing the need for any positional markers in the cell. Indeed, the highly conserved SMC complex, MukBEF may play an important role in this process as in its absence, the <*L-ori-R*> position of chromosomal regions is lost (Danilova et al. 2007). The aim of the current work was to develop a set of tools to address questions about the role of MukBEF in the spatial organization of the *E. coli* chromosome.

Is MukBEF required for (Fig 2.1):

a. Global chromosome organization
b. Segregation of newly replicated DNA
c. Positioning of replicated origins and organization of newly replicated DNA around the origin

In particular I wished to study the following questions:

a. Is MukBEF required at particular stages of the cell cycle or is it needed all the time?
b. Can MukBEF maintain <*L-ori-R*> organization independent of replication?
c. Is MukBEF focus formation dependent on ongoing replication and required for function?

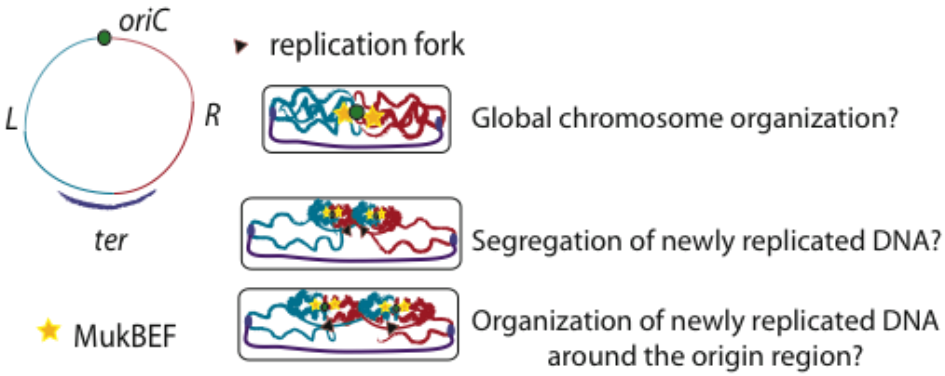

Fig 2.1: Hypothetical roles of MukBEF in *E. coli* chromosome organization and segregation. See text for details.

2.2 A “real-time” approach to studying MukBEF function *in vivo*

Much of the *in vivo* role of MukBEF has been assessed using deletions of the genes. Deletions of *muk* grow slowly at low temperatures, are filamentous in rich media and are prone to pick up suppressor mutations (Sawitzke and Austin 2000). It is also likely that the cells have had enough time to adjust to a *muk*$^{-}$ condition. A better way to study the MukBEF complex *in vivo* would be to turn on and off its function in the cell within minutes and assess the effects on chromosome organisation and segregation. A powerful tool to do so is targeted protein degradation such as the TEV cleavage system (Kapust and Waugh 2000). TEV sites introduced into the desired protein are cleaved by TEV protease causing loss of protein function in “real-time”. However, attempts to construct a functional TEV cleavable MukF in either of four different sites failed (data not shown).

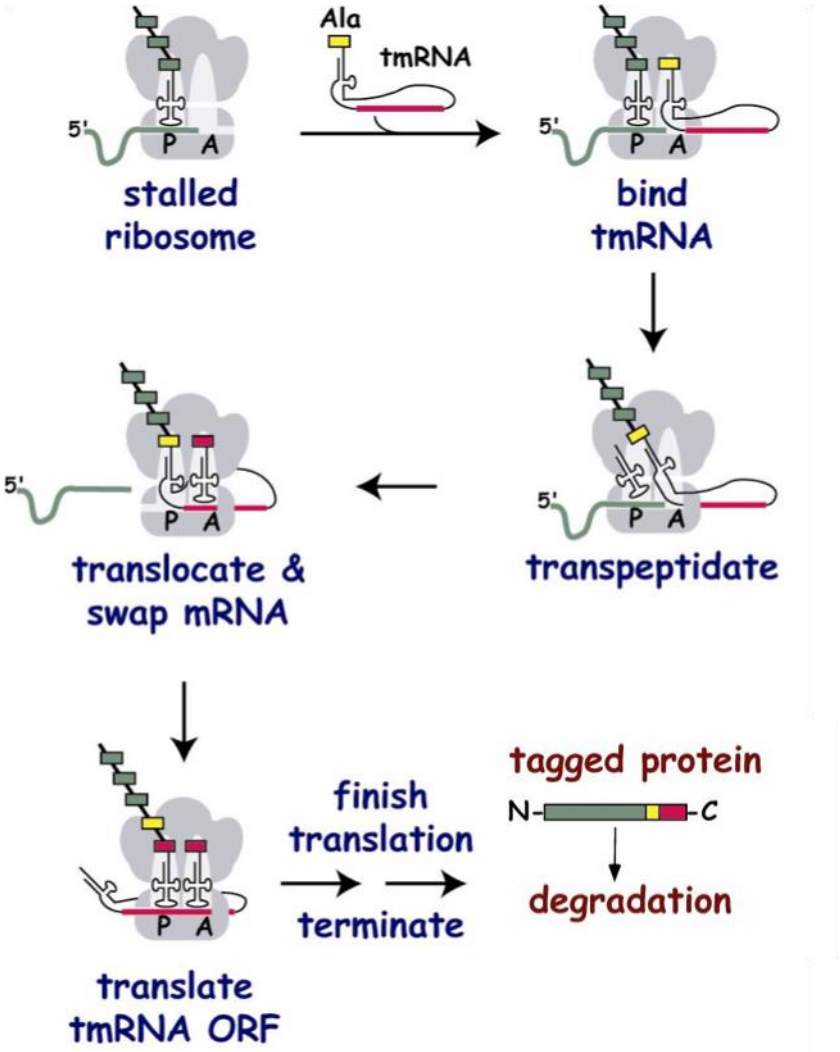

Moore SD, Sauer RT. 2007.
Annu. Rev. Biochem. 76:101–24

Fig 2.1.1: tmRNA mediated degron-tagging and rescue of stalled ribosome. tmRNA comprises of an mRNA domain with an ORF of 10 amino acids and a stop codon and an Alanyl-tRNA domain. When a ribosome is stalled, the RNA chaperon SmpB mediates tmRNA binding to the stalled site. The alanyl-tmRNA then adds an alanine to the polypeptide chain (yellow). The mRNA is swapped and the tmRNA ORF (AANDENYALAA) is translated (red). The tagged protein is now targeted for degradation and the ribosome is recycled for new rounds of protein synthesis. The degradation of degron-tagged proteins can be aided by SspB, which transports the protein to the protease for degradation. Adapted from Moore and Sauer 2007.

2.2.1 The depletion system

Another method of inducible protein degradation in *E. coli* makes use of the endogenous ClpXP system (McGinness et al. 2006; Griffith and Grossman 2008). ClpXP is a protease that selectively recognizes proteins carrying an *ssrA*-tag. In physiological conditions, when protein synthesis comes to a premature halt or termination does not occur properly, one mechanism to disassemble the stalled ribosome and degrade the defective polypeptide is to use the trans-translation system (Fig 2.1.1). This system consists of the highly conserved ClpXP proteases, tmRNA and SmpB (an RNA chaperon). tmRNA or transfer mRNA is a small, stable RNA that is made up of (a). An mRNA domain with an open reading frame of 10 amino acids and a stop codon (b). An alanyl tRNA domain (reviewed in Moore and Sauer 2007). When a ribosome is stalled, tmRNA, with the aid of SmpB, is recruited to the site. The mRNA domain of the tmRNA provides a short open reading frame and the polypeptide is extended by AANDENYALAA. Proteins tagged in such a manner are called ssrA-tagged proteins. ClpX specifically recognizes the last three amino acids (LAA) of the tag (McGinness et al. 2006) and the protease degrades the polypeptide. While ClpXP can directly interact with an ssrA-tagged protein and degrade it, the chaperon SspB, which delivers the substrate to ClpXP, aids the reaction. The binding site of SspB lies upstream of the ClpXP binding site (ANDENY). Mutating the ClpX binding site of the tag makes the degradation process dependent on SspB. Exploiting this property, McGinness et al. 2006 engineered tags that make degradation by ClpXP solely dependent on SspB. By fusing them onto the C-ter of a protein, McGinness et al. could now specifically ablate the protein by controlled expression of SspB. The DAS+4-tag, which consists of

mutations in the C-terminus of the tag and the addition of 4 amino acids between the SspB and ClpX binding sites (AANDENYSENYADAS), showed the highest difference in degradation ±SspB, with almost no degradation in the absence of SspB.

Degron tagging was used to study effects of Muk depletion on chromosome organization and segregation (Fig 2.2A). The system has been previously used in the lab to study replisome components (Reyes-Lamothe et al. 2010). ssrA tags preceded by a single repeat of the c-Myc tag were introduced on the C terminus of *mukB* or *mukE* at the gene locus, expressed under their endogenous promoter (*Psmta)*. The only copy of *sspB* was under an arabinose inducible promoter (McGinness et al. 2006) on the chromosome.

For further experiments, MukE-ssrA tagged construct was used (MukE-degron henceforth). This strain was functional and similar to wild type in growth and cell morphology when SspB was repressed. Expression of SspB from the chromosome (by arabinose induction) led to a partial Muk- phenotype – cells were filamentous but there was still residual growth at non-permissive temperature (as judged by growth of small colonies on plates). However, expression of SspB from a pBAD24 plasmid caused temperature sensitive growth, suggesting incomplete MukE degradation previously, probably due to insufficient SspB. Over expression of SspB alone had no effect on the cells.

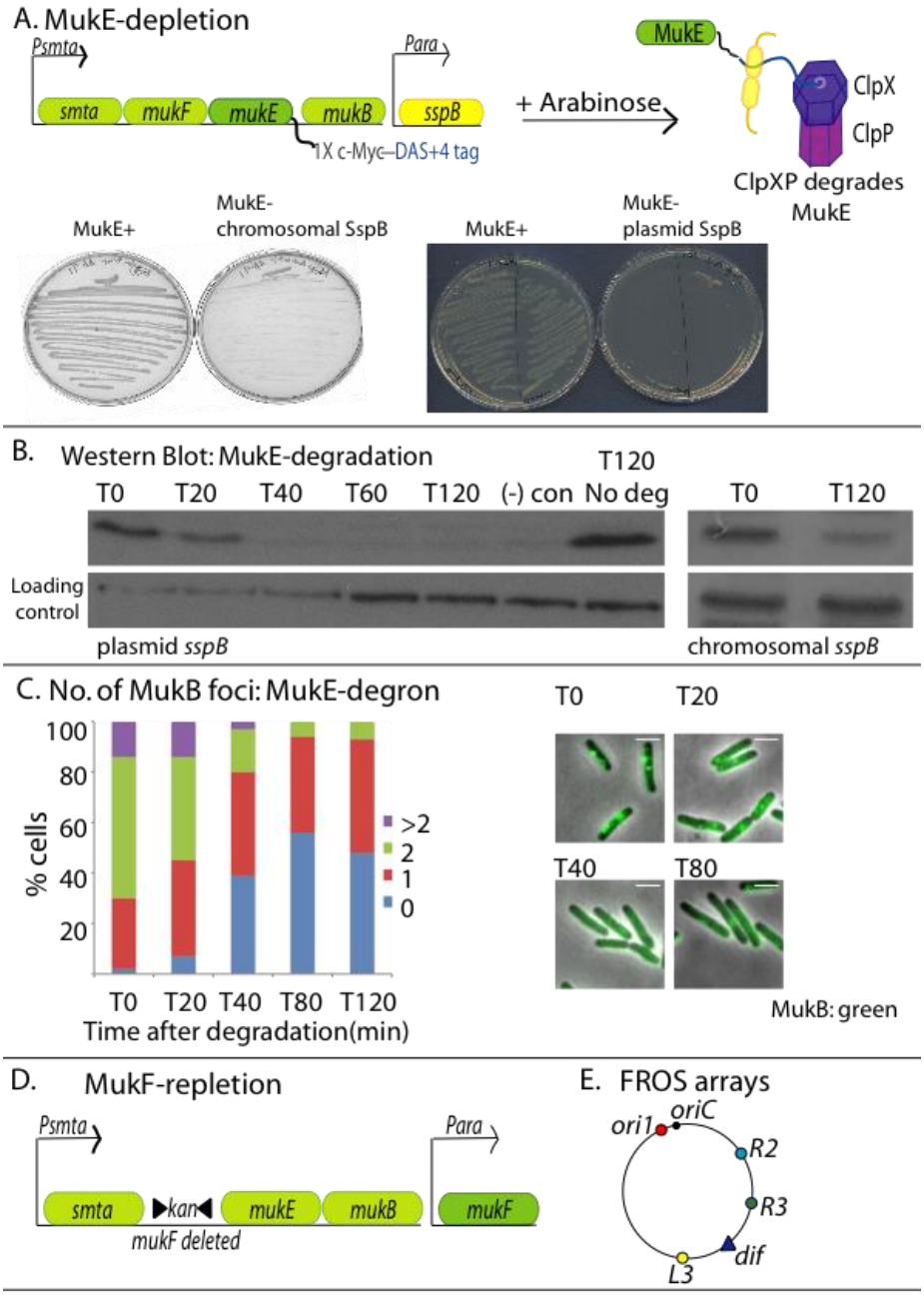

Fig 2.2: Depletion/ Repletion

A. Depletion system: Arabinose induced SspB takes Degron-tagged MukE (1xc-Myc-DAS+4tag) to ClpXP for degradation. SSpB expression from chromosomal arabinose inducible copy causes loss of growth at 37°C. Residual growth (small colonies) could be due to incomplete degradation as SspB expressed from plasmid causes complete loss of growth on plates at 37°C.

B. Degradation observed by Western Blot. Samples before (T0) and 20, 40, 60, 120 min after induction of SspB (from plasmid or chromosome). Non-specific interaction of antibody with sample is used as loading control (bottom panel; can be seen in negative control as well).

C. Loss of MukB foci followed 20, 40, 80 and 120 min after MukE degradation. % cells with 0, 1, 2 or > 2 foci is plotted. n≥200. Scale bar = 2µm

D. Repletion system: Chromosomal *mukF* is deleted. MukF under arabinose control is introduced at an ectopic location. Induction complements *mukF*¯ cells.

E. Position of loci followed by FROS: *ori1, R2, L3* and *R3*.

Western Blots (cells grown in rich media) with plasmid expressed SspB showed that 60% of MukE had been degraded within 20 min of induction while most protein disappeared by 40 min. The weak band seen in the Western can be attributed to the non-specific band seen in the control without c-Myc (Fig 2.2B). Western Blots with chromosomally expressed SspB showed 70% degradation at the end of 2hrs (Fig 2.2B). The remaining 30% MukE could account for the residual growth on plates.

In vivo, depletion of MukE caused an increase in cell length from 3.5±0.6μm to 4.6±0.7μm as well as an increase in percentage of anucleate cells from 2% to 10% (comparable to *muk*$^{-}$ cells). Loss of MukBEF foci was assayed in a strain carrying MukE-degron and *mukB-mYPet*. Cells were followed over a period of 2 hrs after SspB induction with snapshots taken at 20, 40, 80 and 120 min (Fig 2.2C). Before degradation 98% cells had MukB foci with 28% having one focus, 56% having two foci and 14% with two or more foci. 20 min after degradation, the percentage of cells with one focus increased to 38% and after 80 min, only 44% cells had one or two weak foci and 56% of cells had no MukB focus. These numbers did not vary much at the end of 2hrs (Fig 2.2C). Thus this system could be a rapid way of becoming *muk*$^{-}$ to study the transient effects of its phenotype within a single generation (generation time for AB1157 in minimal media is ~110 min).

2.2.2 The repletion system

Complementary to the above would be a system where cells can be made *muk*$^{+}$ from *muk*$^{-}$ to observe the events of MukBEF focus formation and its effects on the chromosome. For this, a strain deleted for endogenous *mukF* and carrying an ectopic copy of *mukF* under an arabinose inducible promoter (*Para-mukF)*

was used (Fig 2.2D). While this can also be used for depletion, enough time needs to be provided to substantially reduce pre-existing protein levels, which could extend to several generations of growth. The system has been characterized in the lab as a tool for *mukF* depletion to study the requirement of FtsK C-ter in *muk*$^{-}$ cells (Sivanathan et al. 2009). Cells were temperature sensitive in the absence of arabinose. Upon arabinose addition, cells became MukF^{+} with growth similar to wild type at 37°C. In order to validate the system *in vivo,* MukB-GFP was used to observe focus formation after MukF reintroduction. Before induction, 80% of cells had no MukB foci and fluorescence occupied the entire cell. 20% of cells had one weak MukB focus. Within 5 min of induction, multiple MukB foci formed on the nucleoid (Fig 2.9). Thus, using depletion/ repletion system, one can go from Muk^{+} to Muk^{-} and vice versa within a single generation and observe its effects on chromosome organization and segregation.

2.3 MukBEF is required for effective chromosome segregation

The effect MukE degradation on the position of chromosomal loci (*ori1, R2, L3* and *R3)* was observed in replicating cells. Cells were grown in minimal media-glycerol and arabinose was added to induce degradation. Snapshots were taken before (T0) and 2hrs after SspB induction (T120). The results of cells with a single copy of each locus are discussed later. For cells with two segregated loci (considered replicated) of *ori1, R2, L3* or *R3*, the mean position (and st dev) of the pair of loci in each cell was plotted as % of cell length (see materials and methods).

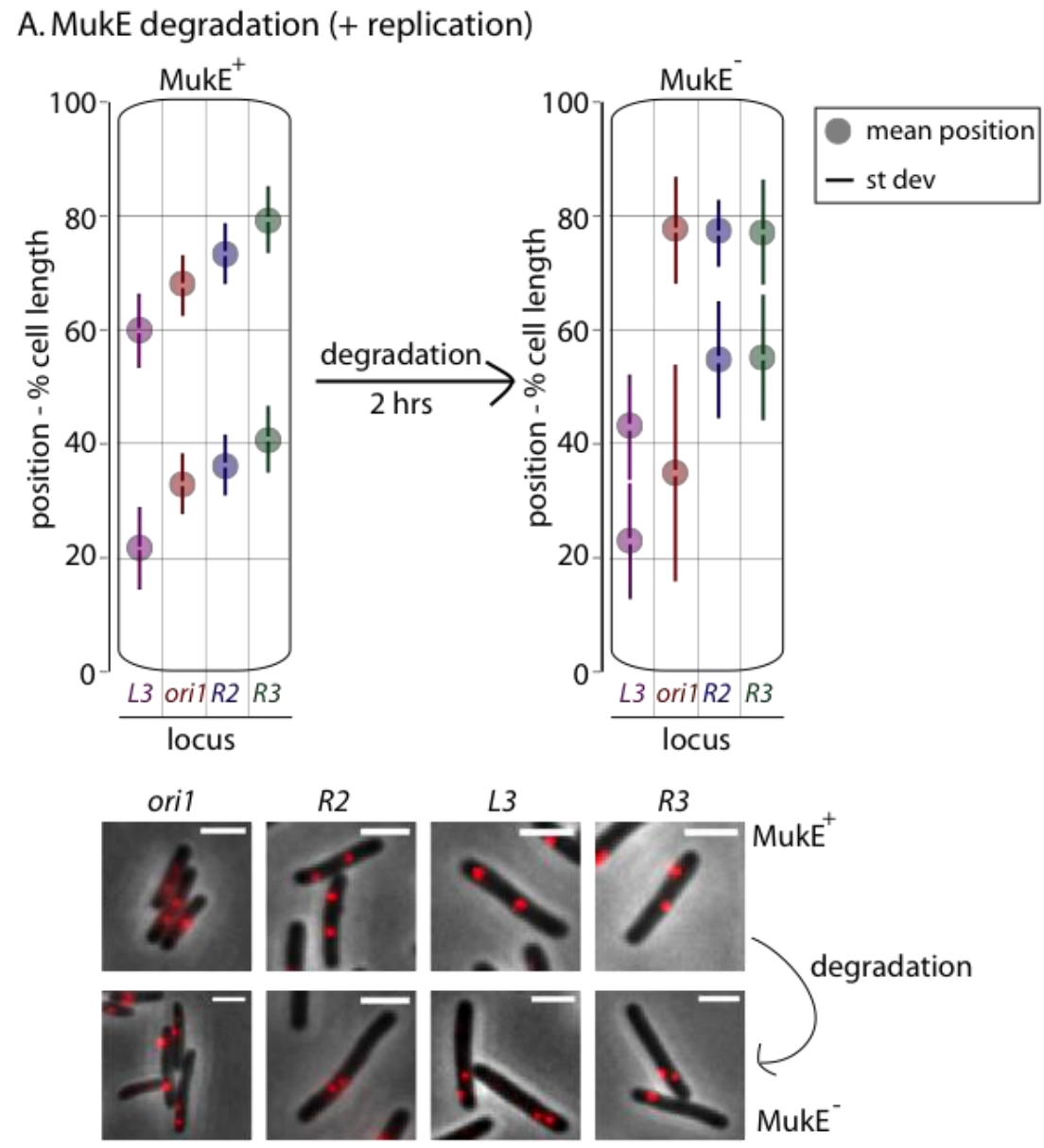

Fig 2.3: MukE degradation affects position of loci in replicating cells

A. Position of replicated (hence two copies of each locus) *ori1* (red), *R2* (blue), *L3* (purple) or *R3* (green) (X-axis) is estimated as % of cell length before and after MukE degradation; mean position (circle) and standard deviation (vertical lines) is plotted. n≥300. Scale bar = 2μm

B. Distance between two replicated loci is measures as Sister chromatid distance (SCD) expressed as % of cell length. Change in SCD before and after degradation is shown in the box.

Before degradation, the mean position of replicated *ori1* loci was 68±5% and 33±5% of cell length. Hence, sisters seemed to be positioned at cell quarters (¼ or ¾) of each cell with little deviation (Fig 2.3A; red circles). This is similar to wild type (Wang et al. 2005b). After 2hrs of degradation, loci seemed to have a broader distribution across cell length (Fig 2.3A; red circles). The mean position of each *ori1* was now 78±8% and 35±18% of cell length, suggesting more polar than quarter positioned replicated origins. Indeed, although the mean values are not very different from that observed before MukE degradation, the increase in standard deviation is indicative of the spread in *ori1* position due to MukE degradation; while *ori1* was at opposite cell poles in some cells, others had poorly segregated sisters located in the same cell half. Sister chromatid distance (the distance between two replicated loci, expressed as % of cell length) increased from 35% to 46% (Fig 2.3B). Instead of seeing only polar replicated origins (as reported by Danilova et al., 2007 in *muk*$^{-}$ cells), the rapid degradation of MukE permits the observation of intermediate steps that might result in the *muk*$^{-}$ phenotype.

MukE degradation had a more pronounced segregation defect on other loci. In contrast to *ori1,* sister chromatid distance reduced from 35% to 24% for *R2, L3* and *R3* (Fig 2.3B). The mean position was also no longer wild type upon degradation (Fig 2.3A). Before degradation, sister *R2* loci (blue circles) had an mean position of 73±5% and 36±6% (% cell length); after degradation this changed to 77±6% and 55±10%. Similarly *L3* (purple circles) loci position changed from 59±6% and 21±7% to 45±7% and 23±10% respectively; *R3* position (green circles) went from 40±7% and 79±8% to 57±12% and 77±8% (of cell length) respectively.

The decrease in SCD as well as change in localization of replicated *R2, L3* and *R3* loci suggests defective segregation upon MukE degradation.

Across all markers visualized, the number of cells with one or two loci changed as functional MukBEF was removed from the cell. Before degradation, there were 1.6 *ori1* foci per cell on average, while after degradation this reduced to 1.2 foci per cell. Similar reductions were seen for *R2* (from 1.4 to 1.2), *R3* (from 1.3 to 1.1) and *L3* (1.3 to 1.1). Wild type cells have an average cohesion time of ~15 minutes between replicated sister loci (Wang et al. 2008; Joshi et al. 2011). This is dependent on TopoIV activity; overexpression of the enzyme can decrease cohesion time and its inactivation causes loss of separation of loci after replication (Wang et al. 2008). Based on the above, it is possible that MukBEF inactivation increases cohesion time. *In vitro,* MukBEF directly interacts with TopoIV and enhances its activity (Hayama and Marians 2010; Li et al. 2010b). It is hence possible that absence of MukBEF in the cell affects TopoIV function, resulting in increased cohesion time. Alternatively, TopoIV activity could be reduced due to other topological changes caused directly by MukBEF absence on the chromosome. In either case, it would be important to test whether cell cycle parameters are unchanged during MukE degradation to ascertain whether these values reflect change in cohesion. Indeed, Danilova et al., found that the length of the C period did not change in *muk*$^{-}$ cells. Hence, it is likely that the above experiments could provide *in vivo* evidence of MukBEF's effect on cohesion time. Previous reports have suggested that MukBEF does not play a role in modulating cohesion (Danilova et al. 2007; Adachi et al. 2008). However, these experiments were done in slow growing *muk*$^{-}$ cells,

which may have compensated for the lack of MukBEF and the effect may be hidden.

The above results suggest that MukBEF is required for effective segregation of newly replicated DNA. While replicated origins succeed in segregating to opposite cell halves, they are mislocalized. A greater segregation defect is seen on loci other than the origin, suggesting a role for MukBEF in organizing newly replicated DNA around the origin, hence facilitating chromosome segregation. These data are consistent with the observations made by (Danilova et al. 2007) in *mukB*$^{-}$ cells. However, in the study, *L3* and *R3* could not be imaged in live cells (the arrays were unstable). Indeed, the cells do not reconstitute a complete *muk*$^{-}$ phenotype, possibly due to two reasons: (a). There is some residual MukE remaining (~ 30%). (b). These cells have been *muk*$^{-}$ for only one generation; the previously observed *muk*$^{-}$ phenotype could be a consequence of the absence of MukBEF for several generations. Thus the immediate phenotype of *muk*$^{-}$ could be mislocalization of chromosomal regions, before the "*Caulobacter*-like reorganization" suggested previously (Danilova et al. 2007).

2.4 MukE depletion leads to loss of spatial chromosome organization independent of replication

It has been proposed that spatial organization of the *E. coli* chromosome (<*L-ori-R*>) is generated by MukBEF dependent layering of newly replicated DNA either side of the origin, which would locate the origins at cell quarters and thus, around mid-cell in newborn cells (Danilova et al. 2007; Reyes-Lamothe et al. 2008b; Liu et al. 2010a). Can MukBEF loss lead to loss of spatial chromosome

organization independent of replication and can it regenerate chromosome organization in the absence of replication? Using the depletion/ repletion systems with *dnaC* or *dnaA* mutants to block replication, position of *ori1, L3* or *R3* was studied in cells having a single copy of its chromosome. The position of these markers was measured as % of nucleoid length and divided into three categories: nucleoid middle (40-60% of nucleoid), nucleoid quarter (60-80% of nucleoid) and nucleoid edge (80-100% of nucleoid) (see materials and methods). Since *L3/ R3* usually localized at opposite poles, interfocal distance between single *L3* and *R3* markers (% nucleoid length) was measured as well.

The effect of MukE degradation was first characterized in an asynchronous population. Similar to observations made with cells having two copies of *ori1*, cells with a single *ori1* marker also displayed aberrant localization in replicating cells (Fig 2.4A +replication). Before degradation, *ori1* was localized to mid-nucleoid in 76±2% cells. 21% cells had *ori1* at quarter and only 3% were at nucleoid edge. This is similar to wild type. 2hrs after degradation, only 14±5% cells had *ori1* at mid-nucleoid, 61±1% at nucleoid quarter and 25±6% at nucleoid edge. The mean *ori1* position in cells before degradation was 56% of nucleoid length (around mid-nucleoid) while after degradation this shifted to 68% of nucleoid length (closer to nucleoid edge). Cells that were muk^{-} had a more pronounced phenotype with 50% of cells having *ori1* at nucleoid edge, 37% with origin at nucleoid quarter position and 13% at nucleoid middle (Fig 2.4A *muk*$^{-}$). The difference between the two could be due to residual MukE present in the cell (as discussed previously). Indeed, a more pronounced phenotype could also be due to being *muk*$^{-}$ for many generations (as opposed to ~1 generation during MukE degradation).

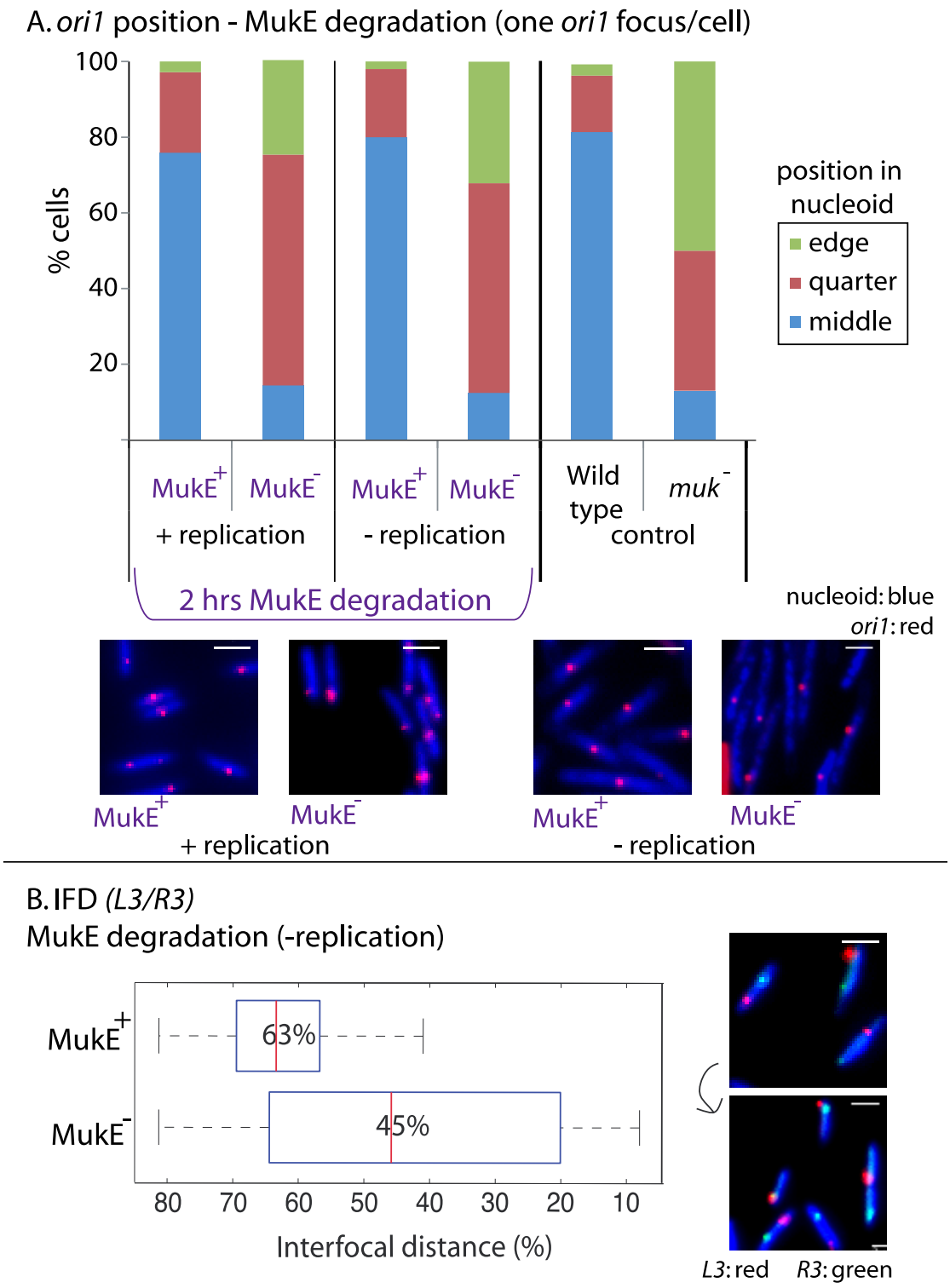

Fig 2.4: MukE degradation affects *ori1* and *L3/R3* localization independent of replication

A. *ori1* position estimated as % of nucleoid length; divided into 3 categories: middle (40-60%), quarter (60-80%) or edge (80-100%) of nucleoid. % cells with *ori1* in each category is plotted before and after degradation (± replication). Control (wild type and *muk*$^{-}$) *ori1* position is also plotted. n≥300. Scale bar = 2μm

B. Plot of Interfocal Distance (as % of nucleoid length) between *L3/R3* before and after degradation in non-replicating cells. Red line represents median IFD, blue box: inter-quartile range, whiskers: minimum and maximum. Median values are represented inside the box. n≥200. Scale bar = 2μm

The effect of MukE degradation could also be seen in cells with a single copy of *L3/R3* (data not shown). Before degradation, *L3* and *R3* localized to opposite ends of the nucleoid. The two markers were present in the same cell half in 17% of the cells. The average (median in this case) interfocal distance was 63.1% of nucleoid length. After 2hrs of degradation, the two markers had a broader distribution. 54% of *L3/R3* were now present in the same cell half. The average interfocal distance reduced to 40.4% of nucleoid length. These results could not be compared with *muk*$^{-}$ cells, as the two arrays are unstable in this strain. Thus functional MukBEF is required for wild type position of chromosomal regions in replicating cells.

The effect of MukE degradation was tested in non-replicating cells using a *dnaC2ts* mutant. After 2hrs of growth at non-permissive temperature, cells were elongated and 85% cells had a single nucleoid with a single copy of *ori1*. 15% of cells had two *ori1* probably due to incomplete replication/ division or escape from the block. Samples also had some anucleate cells, which probably are a result of division at polar, nucleoid-free regions in elongated cells. *dnaC2ts* cells are elongated (at non permissive temperature), but cells with MukE-degron were longer than wild type possibly due to a combined effect of multiple mutants in the same strain, none of which affected chromosome organization or segregation in the presence of MukE.

Before degradation most non-replicating cells had a single *ori1* at mid-nucleoid (80±1%), 18% cells had *ori1* at nucleoid quarter and 2±1% at nucleoid edge. The mean position of *ori1* was 54% of nucleoid length (mid-nucleoid) (Fig 2.4A - replication). After 2hrs of degradation, only 12±5% cells had *ori1* at mid-nucleoid, 55±1% at nucleoid quarter and 33±6% at nucleoid edge. The average

position of *ori1* shifted to 74% of nucleoid length (nucleoid edge). This is similar to observations in replicating cells, indicating that MukBEF is required to maintain origin position independent of replication.

In replication-blocked cells, single *L3*/*R3* loci localized to opposite nucleoid edges with a median interfocal distance of 63.5% (min 41%, max 85%) (Fig 2.4B MukE^{+}). *L3*/*R3* either colocalized or were present in the same cell half in 12% of cells. After 2hrs of MukE degradation, *L3/R3* localization became random, along various regions of the chromosome (Fig 2.4B MukE^{-}). The median IFD decreased to 45% of nucleoid length (min 4%, max 81%) with 54% of cells having *L3/R3* present in the same nucleoid half. These data indicate that MukE degradation in the absence of replication affects not only origin position, but also markers close to *ter*. Hence MukBEF may be required to maintain spatial chromosome organization independent of cell cycle. In order to validate these results, it would be good to test other chromosomal markers (± replication). Indeed, change in position of markers far apart on the chromosome suggests that the effect may be global.

2.5 MukE degradation leads to change in DAPI staining of nucleoids in non-replicating cells

Previous studies have suggested that *muk*$^{-}$ nucleoids appear diffuse (Hiraga et al. 1991; Niki et al. 1992). However, this is not clearly visible when cells are grown at permissive temperature in minimal media. During the depletion experiments, DAPI staining of nucleoids in non-replicating cells changed upon MukE degradation. It is possible that the effect is more visible in long cells (as the nucleoid has more space to expand) and hence not obvious in small cells. Before degradation, cells had a compact nucleoid located in the centre of the

cell (Fig 2.5A red profiles). As an example, 4 profiles are shown. DAPI staining was homogenous and the mean length of the nucleoid was 2.6±0.6μm. After 2 hrs of degradation, nucleoids appeared to be elongated, although they did not occupy the total length of the cell (Fig 2.5A blue profiles). The staining was not smooth and had ridge-like structures, with regions of bright and weak staining. The nucleoid did not appear diffuse; it seemed to have expanded in length (4.5±0.9μm), revealing smaller regions of compaction (indicated by the rough DAPI staining). This change was not due to cell elongation, arabinose or overexpression of SspB.

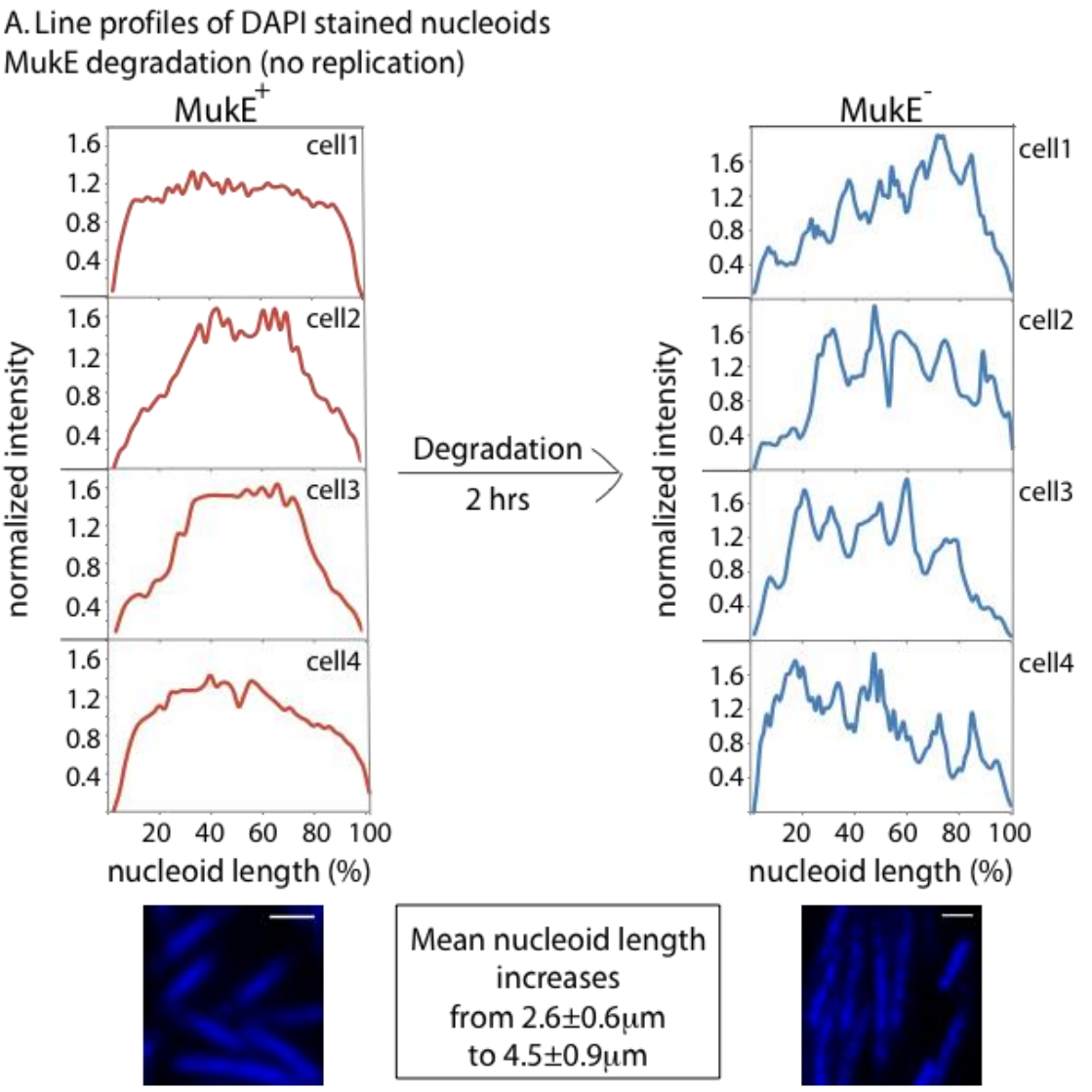

Fig 2.5: MukE degradation changes DAPI profiles of nucleoids in non-replicating cells

A. Line profiles of 4 representative DAPI stained nucleoids (stacked above each other) normalized to nucleoid length, before (red) and after (blue) 2hrs of MukE degradation. Change in mean nucleoid length (± st dev) is represented in the box. n≥100. Scale bar = 2μm

2.6 MukBEF can reposition *ori1* and *L3/R3* in the absence of replication

The above results suggest that MukBEF is required to maintain spatial chromosome organization independent of replication. Thus the sequential layering model driven by replication may not account for the *ori1* position seen in *E. coli.* Can MukBEF also reposition *ori1* and other regions in the absence of replication? In order to test this, the MukF repletion system with markers for *ori1* or *L3/R3* was utilized. Replication was blocked using *dnaC2ts* in the strain with *ori1*. For *L3/R3* the *dnaA46* mutant was used. Unlike the MukE-degron system with *dnaC2ts* (where cells were very abnormally elongated), the MukF-repletion system with *ori1* and *dnaC2ts* did not have abnormal cell elongation. Hence, this was used for time-lapse as well (discussed later). Analysis of snapshot images was done as described for the depletion experiments (-replication).

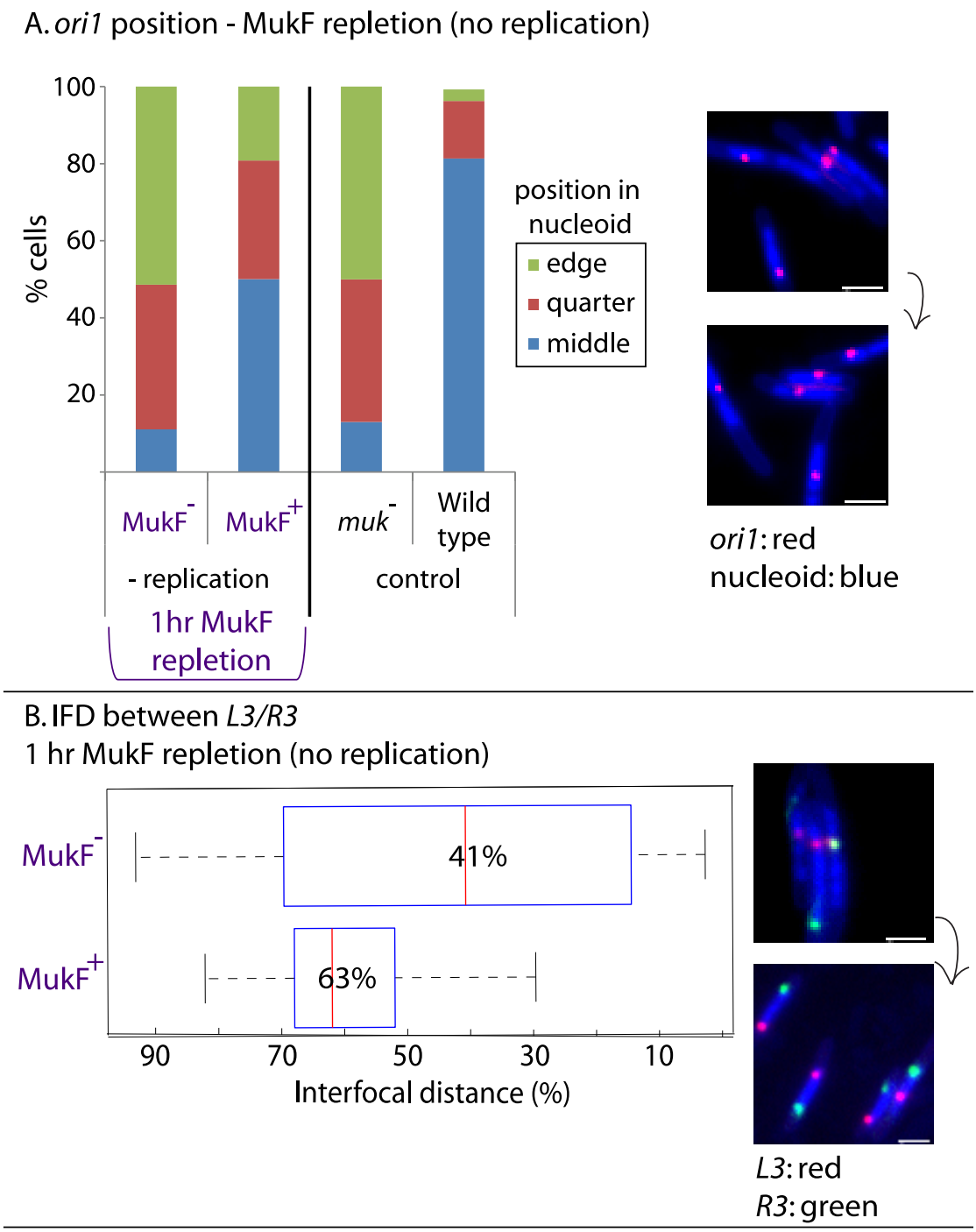

Fig 2.6: MukF repletion can reposition *ori1* and *L3/R3* in the absence of replication

A. *ori1* position was estimated as in Fig 2.4A. Result of MukF repletion in non-replicating cells is plotted. Control (wild type and *muk*¯) *ori1* position is also plotted. n≥300. Scale bar = 2µm

B. Plot of Interfocal Distance (as % of nucleoid length) between *L3/R3* before and after repletion in non-replicating cells. n≥300. Scale bar = 2µm

Before addition of arabinose, only 11±2% cells had *ori1* at mid-nucleoid (Fig 2.6A MukF^{-}), 38±1% at nucleoid quarter and 51% cells had *ori1* at nucleoid edge, with the mean origin position at 79% of nucleoid length (close to nucleoid edge). These values are comparable to *muk*$^{-}$ cells (Fig 2.6A *muk*$^{-}$). After 1hr or 2hrs of repletion, localization of *ori1* returned close to wild type (Fig 2.6A MukF^{+}). 50±5% of cells had *ori1* at mid-nucleoid, 31±4% at nucleoid quarter and only 19±1% at nucleoid edge, with the mean position at 62% of nucleoid length (nucleoid quarter to middle). Thus active MukBEF can reposition *ori1* independent of replication.

To test whether this effect could be seen in origin independent regions, interfocal distance between *L3/R3* was observed in non-replicating cells. Before arabinose addition, interfocal distance distribution of *L3/R3* was similar to that seen when MukE was degraded from the cell (Fig 2.6B MukF^{-}). Median IFD was 40.8% (minimum 2.8%, maximum 93.4%) of nucleoid length. After 1hr of repletion, *L3/R3* position returned close to wild type, similar to that seen before MukE degradation (Fig 2.6B MukF^{+}). The median IFD increased to 63.2% of nucleoid length (minimum 30%, maximum 84%). Only 24% of cells had *L3/R3* either colocalized or present in the same cell half (before repletion this number was 60%). The above results indicate that MukF repletion can reposition origin independent regions in the absence of replication.

2.7 MukF repletion leads to change in DAPI staining of nucleoids in non-replicating cells

Similar to change in nucleoid length upon MukE degradation (in non-replicating cells), nucleoid length reduced from 3.3±0.7μm to 2.6±0.5μm when MukF was repleted. Although DAPI staining did not show rough structures in the absence of MukF, difference in nucleoid morphology could still be observed. Nucleoids produced smooth staining (similar to wild type) only after MukF repletion (Fig 2.7A blue/red profiles). Nucleoid length reduced from 4.7±0.9μm to 3.2±0.6μm upon repletion in *dnaA46ts* cells. The difference between nucleoid morphology upon MukE degradation and that before MukF repletion could be due to: a. The phenotype obtained with MukE degradation was within one generation of growth and could be an immediate consequence of MukBEF loss. In the repletion experiment, cells were grown in as *muk*$^{-}$ for several generations and could have compensated for the absence of MukBEF. b. Replication blocked MukE-degron cells were longer than those of replication blocked MukF-repletion cells. Increase in cell length could provide more space for nucleoids to expand in the absence of MukBEF. Visualizing nucleoids in highly elongated *muk*$^{-}$ cells could test this.

The above data suggest that MukBEF can generate and maintain spatial chromosome organization independent of replication. One possibility is that local action of MukBEF around the origin results in the positioning of *ori1* and as a consequence, *L3/R3.* Alternatively, MukBEF could globally structure the chromosome resulting in the <*L-ori-R*> organization. Indeed, change in nucleoid morphology suggests that MukBEF may act more directly in global condensation/ structuring of the nucleoid.

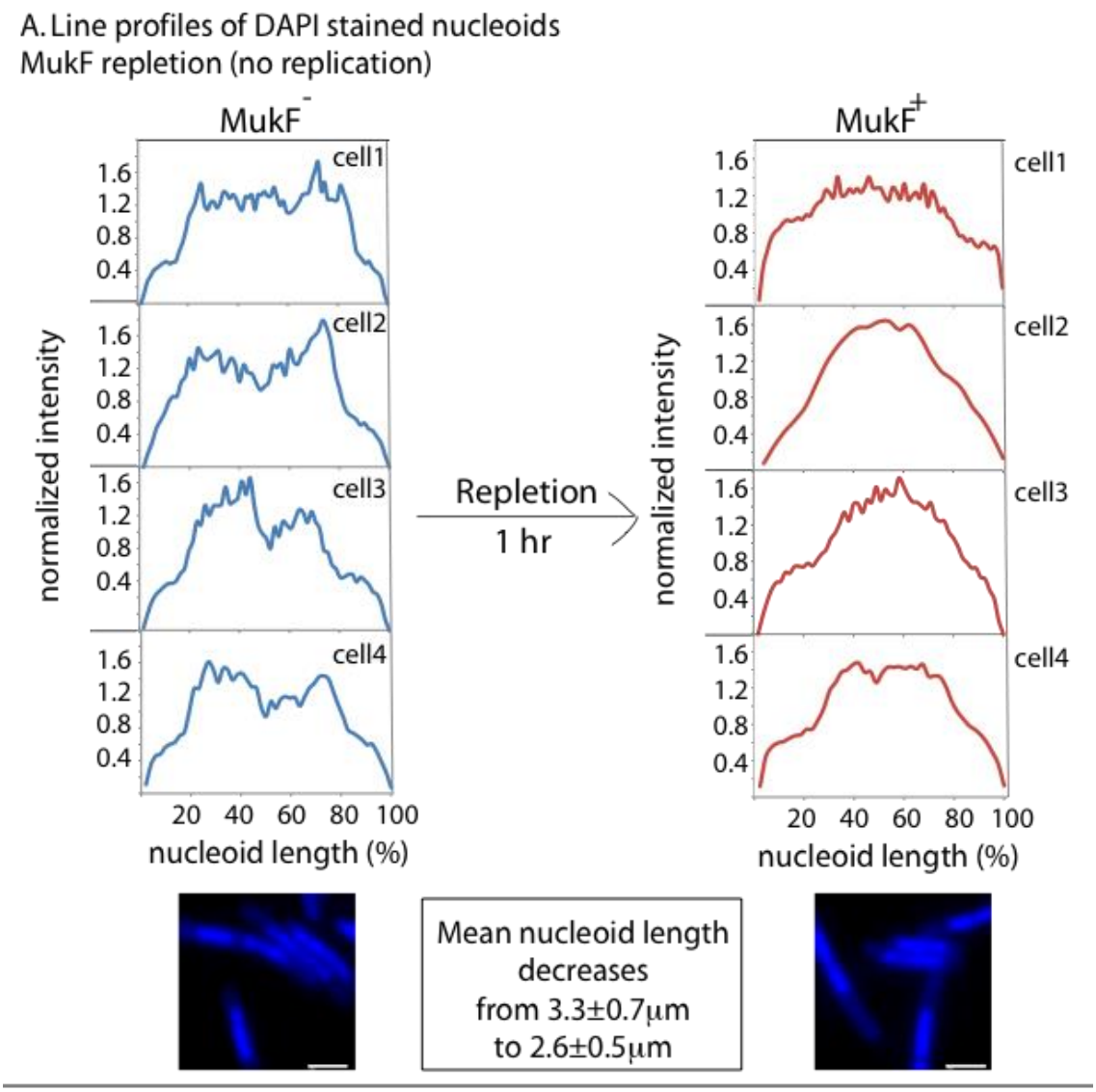

Fig 2.7: MukF repletion changes DAPI profiles of nucleoids in non-replicating cells

A. Line profiles of 4 DAPI stained nucleoids (stacked above each other) normalized to nucleoid length, before (blue) and after (red) MukF repletion. Change in mean nucleoid length (±st dev) is represented in the box. n≥100. Scale bar = 2µm

2.8 *ori1* relocation in the absence of replication is slow

Is MukBEF mediated relocation of *ori1* from nucleoid edge to mid-nucleoid a one step event, or a gradual process in the absence of replication? In order to understand the mechanism of *ori1* relocation, time-course/ time-lapse studies with the MukF-repletion system were done in non-replicating cells.

For the time-course samples were collected before addition of arabinose (T0) and 20 (T20), 40 (T40) and 60 (T60) min after repletion. As seen in the graph (Fig 2.8A), *ori1* position changed gradually upon MukF repletion. As seen previously, at T0 51% of cells had *ori1* at nucleoid edge, 38% cells at nucleoid quarter and only 11% at mid-nucleoid. 20 min after repletion, origin position begun to change – 25±4% cells had *ori1* at mid-nucleoid, 35±5% cells at nucleoid quarter and 40±1% at nucleoid edge. The percentage of mid-nucleoid *ori1* increased at T40 to 34±2%. By 60 min, 50% of cells had *ori1* at mid-nucleoid, 31% at nucleoid quarter and 19% at nucleoid edge. These results suggest that repositioning of *ori1* by MukBEF may be a slow process. Indeed, the data could be interpreted as edge positioned origins becoming quarter positioned; while quarter positioned origins move to mid-nucleoid.

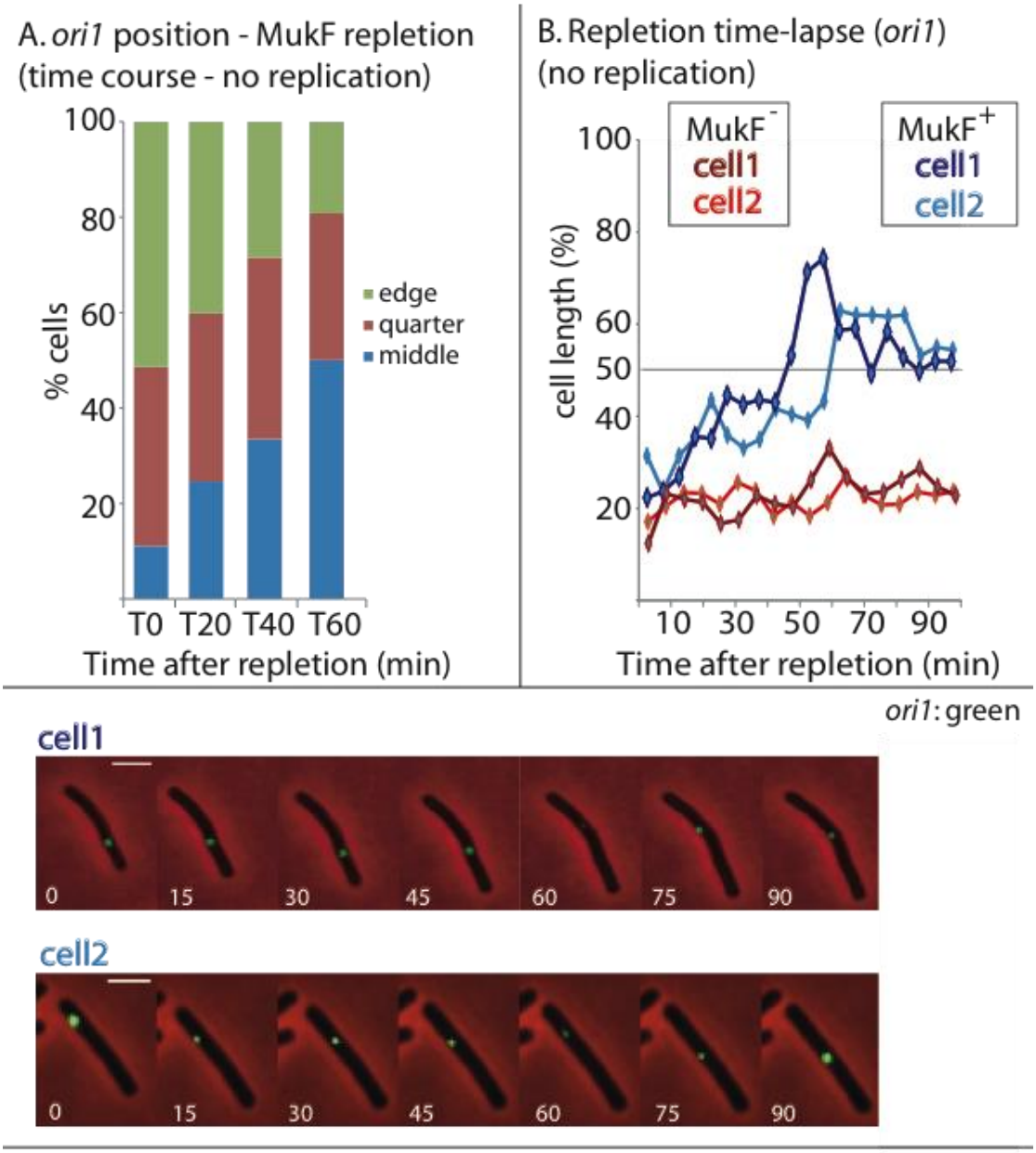

Fig 2.8: *ori1* repositioning is slow during MukF repletion in non-replicating cells

A. Time-course of MukF-repletion. Snapshots taken before (T0) and 20 (T20), 40 (T40) and 60 (T60) min after repletion. *ori1* position is estimated and plotted as Fig 2.4A (n≥300 for each time-point). Scale bar = 2μm

B. Time-lapse of *ori1* position during repletion (blue) or in MukF^{-} cells (orange). Images taken every 5min. Numbers in montages represent frame time. Two cells (for each category) are shown as representative (n≥17). Scale bar = 2μm

Time-lapse experiments also suggested gradual movement of *ori1* to mid-cell (Fig 2.8B blue cell1, 2); two cells shown as representative. There were a few cells where the origin travelled from one cell pole to the opposite before returning to mid-cell. In all cases, the origins moved dynamically across the long and short axis of the cell with a mean displacement of 0.37% of cell length per minute (along the long axis). It has been previously reported that chromosome regions are dynamic, but their movement is confined in a small region of the cell (Reyes-Lamothe et al. 2008a). These movements suggest an active mechanism of origin repositioning by MukBEF. This dynamic movement was dependent on MukF expression, as *mukF*$^{-}$ cells did not have such behaviour (Fig 2.8B orange cell1, 2); two cells shown as representative. The origin in these cells moved within a confined area and was not seen to travel across the length of the cell. Moreover, during the 90min of imaging, origins remain localized to cell pole or quarter. There were few events of dynamic origin movement, but this was usually when the position shifted from mid-cell to quarter or edge. Hence the reorganization of the chromosome by MukBEF in the absence of replication seems to be an active process, involving the dynamic relocalization of chromosomal regions (*ori1* in this case). The process of reorganization is not immediate. One possibility is that MukBEF may be changing the structure of the chromosome by layering or folding regions together, finally resulting in a wild type organization with the origin positioned at mid-cell. Indeed, it would be good to do time-lapses at shorter intervals to observe the dynamic nature of the reorganization process.

2.9 MukBEF focus formation is independent of ongoing replication

Fluorescent fusions of MukBEF form foci that localize around the origin region (Ohsumi et al. 2001; Danilova et al. 2007). It is thought that these foci may represent the centres of activity of the complex. The above results suggest that MukBEF can actively reposition regions of the chromosome independent of replication. Does this process require focus formation?

The MukF-repletion system (with *ori1* and *dnaC2ts)* and MukB-GFP was used for time course and time-lapse experiments to observe MukB foci dynamics.

I could not measure protein expression levels during the time course of MukF induction, as antibodies against MukF were non-functional. Hence, the exact time point when normal protein levels are established in the cell is unclear. However, as an indirect indication of the above, MukBEF focus formation was followed in steady state cells. MukF expression was blocked at specific time points after induction by the addition of rifampicin and all cells were imaged 60 min after induction of repletion. While foci begun to form 1 min after repletion induction, 15 min of MukF expression was sufficient to generate wild tupe focus number and intensity.

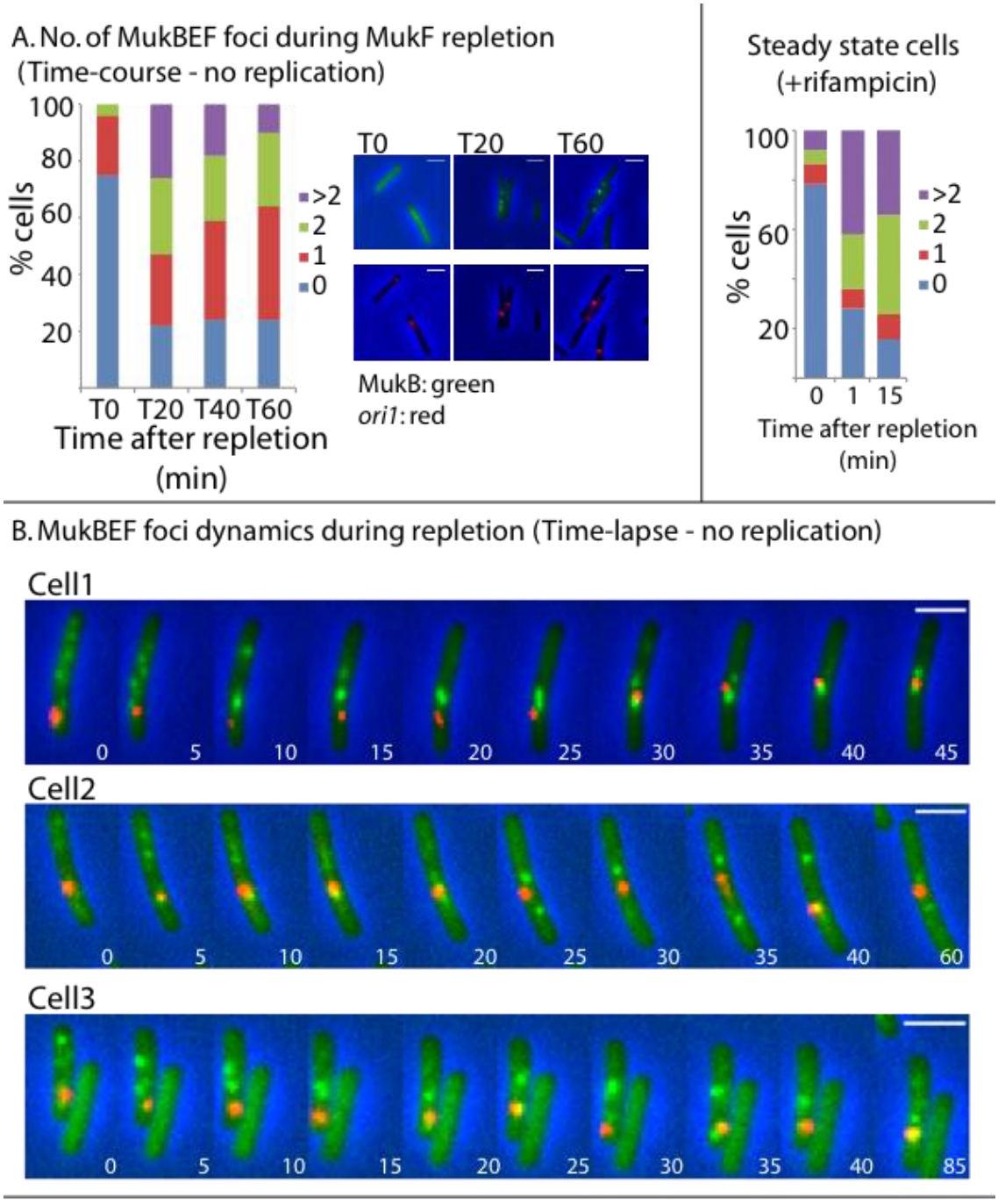

Fig 2.9: MukBEF foci dynamics during MukF repletion in non-replicating cells

A. Appearance of MukBEF foci is followed before (T0) and 20, 40 and 60 min after MukF repletion. % cells with 0, 1, 2 or > 2 foci per cell is plotted. n≥200. As a control, MukBEF focus formation is followed in steady state cells. MukF expression is blocked after 1, 15 and 60 minutes of induction by the addition of rifampicin. All cells are imaged 60 min after repletion induction. Focus formation was observed one minute after induction. 15 min of induction was sufficient to generate wild type focus number and intensity in steady state cells.

B. Montage of MukBEF foci during MukF repletion time-lapse. Three cells are shown as an example. Numbers represent time (in min) after repletion. Images were taken every 5 minutes. o*ri1* – red*;* MukB – green. Scale bar = 2µm

In time-course experiments, before MukF repletion, 75% cells had no MukB foci and fluorescence was seen throughout the cell (Fig 2.9A (T0)). 21% cells had one weak MukB focus and 4% cells had two weak foci. The presence of weak foci could be due to leaky expression of MukF, as *mukF*$^{-}$ cells do not form MukB foci. The weak foci sometimes localized with the origin, but in most cases they did not (Fig 2.10A). In cells with a single weak focus, the median distance of the focus from *ori1* was 600nm. Thus, *ori1* and MukBEF did not colocalize. In cells with two weak foci (only 4% of the population), one focus tended to localize around the origin (median distance of 270nm) while the other one had a median distance of 1.5μm from *ori1.* 20min after repletion, multiple MukBEF foci (per origin) were detected (Fig 2.9A (T20)). While 22% of cells had no MukBEF focus, 25% cells had one focus, 27% cells had two MukBEF foci and 26% cells had more than two foci (up to 5 foci in some cases). Indeed not all foci colocalized with the origin or were found near it. In cells with a single focus, the median distance between MukBEF and *ori1* was 480nm. Indeed, in cells with multiple MukBEF foci, one tended to localize around the origin, with a median distance of 270nm (Fig 2.10A). At T40, the number of cells with more than two MukBEF foci decreased to 18%. 35% cells had one focus, while 23% cells had two foci (24% with no foci). The median distance of MukBEF from *ori1* decreased to 280nm in cells with a single MukBEF focus, indicating increased colocalization between the two (Fig 2.10A). In cells with multiple MukBEF foci, their distance/ distribution from the origin was similar to T20. T40 also had the highest colocalization values for MukBEF and *ori1*, as at T60, this distance increased to 380nm (in cells with a single MukBEF focus). This is similar to wild type (330nm). The percentage of cells with no MukBEF foci remained at 24%.

However, now most cells had one or two MukBEF foci – 40% and 26% respectively. Only 10% cells had more than two foci. It is interesting to note that in cells with multiple MukBEF foci (≥2), the position of foci were similar over the course of repletion. While one tended to localize around the origin (around 280nm), the second focus was at a distance of 1.4μm from *ori1*. The third focus was ~2.5μm away from the origin. Thus, these data suggest that MukBEF foci tend to be positioned at specific locations along the chromosome. One possibility is that this is sequence driven. Nucleation of MukBEF at one site (which is likely not to be the origin. Data suggests that this might be the terminus – See chapter 3) could aid in the recruitment of more foci along the chromosome. Another possibility is that a ParAB type oscillatory system positions MukBEF foci at specific positions on the chromosome (these possibilities are reviewed in the discussion).

A. Distance of MukBEF focus from *ori1* (no replication)

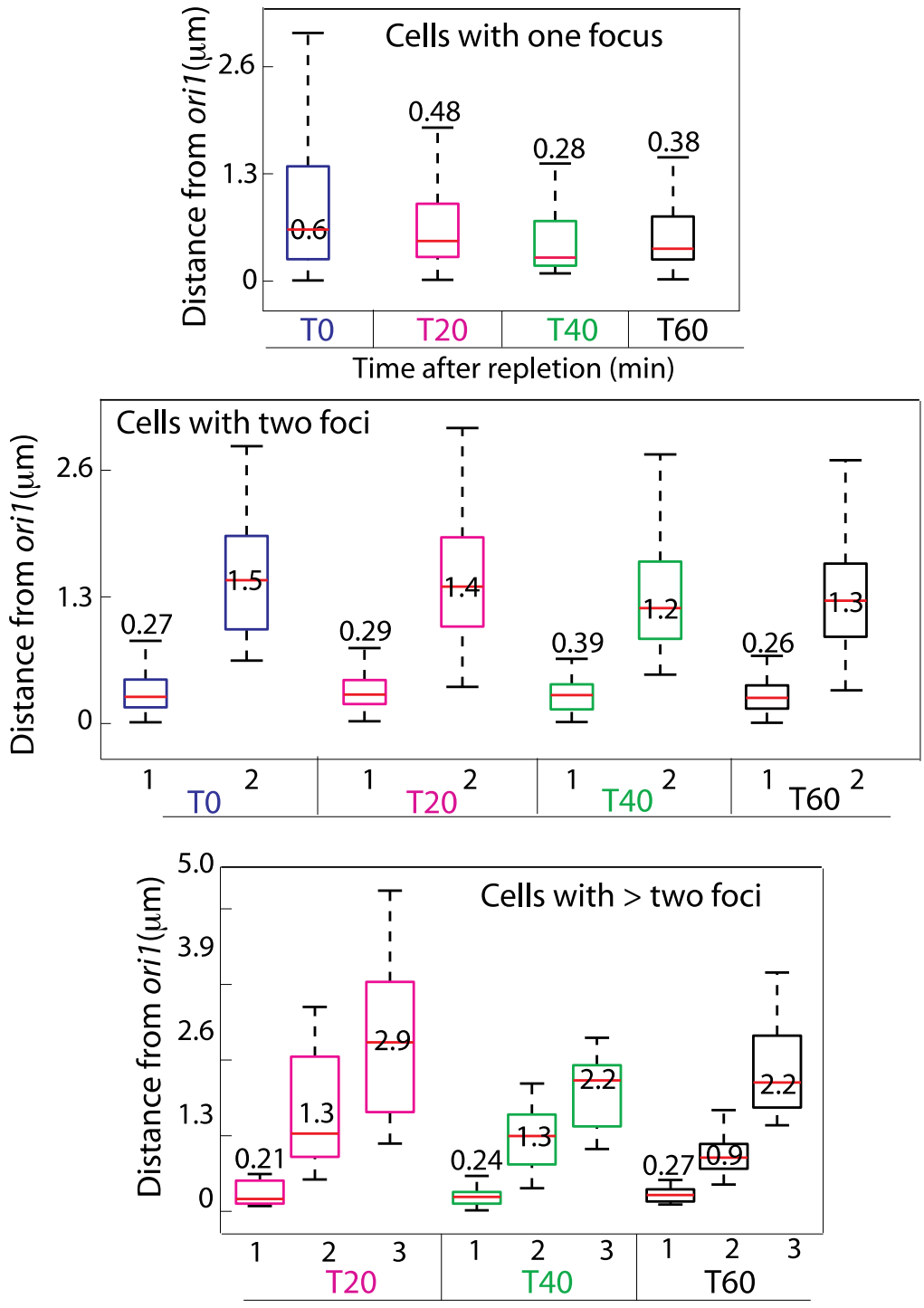

Fig 2.10: Colocalization of MukBEF focus with *ori1* during MukF repletion in non-replicating cells

A. Distance of MukBEF focus from *ori1* during repletion time-course (before (T0) and 20 (T20), 40 (T40) and 60 (T60) min after repletion). Cells are categorized into those with 1, 2 or >2 foci of MukBEF. Distance of first (1; nearest to origin), second (2) and third MukB focus from *ori1* is plotted. Median position is shown inside the box. All cells have a single origin. n≥200

MukBEF foci could not be followed for the same duration as *ori1* in time-lapse (Fig 2.9B). Also, due to the “messy” nature of the data, it was harder to track them over time. As an example 3 cells are shown. During the time-lapse, MukB foci begun to appear at the start of imaging or within 5min of repletion indicating that MukBEF foci formed before *ori1* repositioning. However, only few weak foci were seen during the time-course at T0. Early appearance of foci in time-lapse could be due to the time taken between induction on slide and imaging.

The foci were dynamic. As seen in the time-course, cells in the first few frames (up to 15 min) had multiple MukB foci (up to 4 or 5) that seemed to fuse together or split apart during the course of the experiment. By the end of the movie (when origins were close to mid-cell) these appear to combine into one or two foci around the origin. Hence, these results suggest that association of MukBEF with the origin may not be absolute; MukBEF foci seem to associate with multiple regions on the chromosome before repositioning themselves around the origin region.

2.10 Summary

In summary, the depletion/ repletion experiments provide insight into the role of MukBEF in spatial organization of the *E. coli* chromosome. Functional MukBEF is required to generate and maintain wild type *ori1* position (and *L3/R3* localization) independent of replication (Fig 2.11). Degradation of MukE in the absence of replication leads to the loss of chromosome organization (as judged by change in localization of *ori1* and *L3/ R3* and change in nucleoid morphology) while repletion of MukF leads to reorganisation of the chromosome. The process of origin relocation is gradual and dynamic, as *ori1* does not reposition to mid-cell soon after MukF repletion. The formation of MukBEF foci occurs before *ori1* repositioning. MukBEF foci appear at various locations on the chromosome as MukF is repleted, and dynamic foci seem to fuse together as the origin relocates to mid-cell. All foci do not colocalize with the origin and co-association increases as the relocation process in almost complete (when there are between 1 and 2 MukB foci per origin). Thus, MukBEF plays a dynamic role in spatial chromosome organization, with its activity begin required throughout the cell cycle.

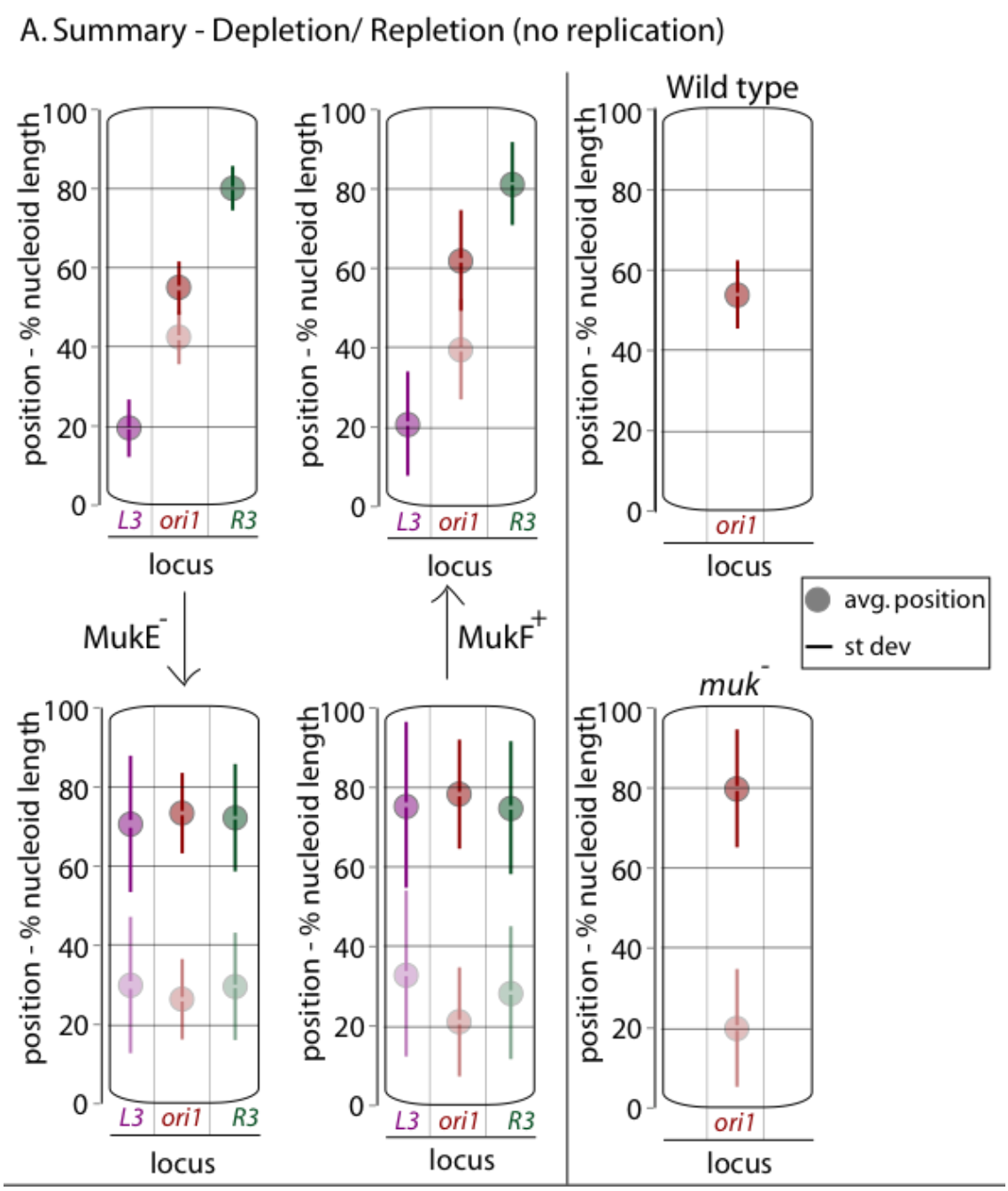

Fig 2.11: Summary of Muk Depletion/ Repletion in non-replicating cells

A. Mean position of single *ori1* (red), *L3* (purple) or *R3* (green) is represented as % of nucleoid length (X-axis) before and after MukE degradation/ MukF repletion. These experiments do not allow the differentiation between old or new cell poles. Hence the change in position of *ori1, L3* or *R3* is represented in both nucleoid halves (bright and transperant markers). Thus *L3-R3* could be positioned in the same nucleoid half or in opposite nucleoid halves; detailed representation of these data are in Fig 2.4 and 2.6. Position of single *ori1* locus in wild type and *muk*$^{-}$ cells is also shown. Circle: Mean position; vertical lines: st dev

2.11 Discussion

2.11.1 The degron system as a tool to study MukBEF function *in vivo*

Classical ways of understanding the function of a particular protein in the cell usually involve deleting its gene or overexpressing it. However, this strategy cannot be employed for essential proteins. Moreover, strains carrying deletion of genes such as *mukBEF* are prone to pick up suppressors (Sawitzke and Austin 2000). Thus, one needs to be careful to show that the observed phenotype is a direct consequence of being *muk*$^{-}$ and not due to compensatory mechanisms adopted by the cells over many generations of growth. In order to study the role of MukBEF in chromosome organization and segregation, degron-tagged Muk (McGinness et al. 2006) was used, which allows its rapid degradation within minutes; thus transient effects of being *muk*$^{-}$ can be followed. Complimentary to the above, the repletion system was used to rapidly reintroduce MukF in cells.

In wild type *E. coli,* a single origin is positioned at mid-cell, with left and right replichores on either side. Replicated origins move to quarter position and the rest of the chromosome segregates asymmetrically (Wang et al. 2005b; Wang et al. 2006b). It has been proposed that the chromosome is spatially organized by sequential layering of newly replicated DNA around each origin. Indeed, MukBEF is thought to be involved in this process (Danilova et al. 2007; Reyes-Lamothe et al. 2008b). The aim of this study was to understand the role of MukBEF in spatial organization of the *E. coli* chromosome.

2.11.2 MukBEF maintains spatial chromosome organization independent of replication

Degradation of MukE led to the loss of wild type *ori1* position independent of replication. Although comparable to *muk*$^{-}$ cells (Danilova et al. 2007), the phenotype is not completely *muk*$^{-}$ as only 33% cells have *ori* at nucleoid edge (as opposed to 50% in *muk*$^{-}$ cells). Why is the phenotype incomplete? Furthermore, why do origins relocate to nucleoid edge (it is unlikely that something anchors the origin to cell pole as cells are highly elongated and the nucleoid does not cover the entire length of the cell)? A few possibilities are:

a. Residual MukE (about 30%) due to incomplete degradation could contribute towards some chromosome organization. However, even with plasmid-expressed SspB, this does not vary much, suggesting that lower (%) of wild type Muk can generate a *muk*$^{-}$ phenotype.

b. Nucleoids are elongated upon degradation. Hence, it is possible that origins are polar, but they appear to be at quarter position. However, in repletion experiments (where nucleoids are slightly elongated before MukF repletion) origins are polar prior to MukF reintroduction.

c. Could degradation lead to random *ori* positioning in the absence of replication. If positioning is random, then on average, *ori* should localize in the middle, quarter or pole equally (i.e. 20% at mid-nucleoid, 40% quarter and 40% at edge). Current data suggests that this may be the case. Hence, it is likely that absence of MukBEF leads to random positioning of chromosomal regions; the previously reported phenotype could be a consequence of being *muk*$^{-}$ for several generations.

2.11.3 MukBEF reorganizes the chromosome independent of replication

Complementary to the above, reintroduction of MukF in *mukF*$^{-}$ cells led to wild type localization of *ori1* and *L3/R3* independent of replication. Thus functional MukBEF alone can generate <*Left-ori-Right*> organization. These data support the idea that the origin is not tethered to mid-cell or cell quarters. Could this form of organization be a consequence of cells having MukBEF? It is interesting to note that bacteria that have ParAB systems, have origins anchored at the cell pole and carry the SMC-ScpAB complex. Bacteria that have MukBEF seem not to have ParAB and have origins localized to mid-cell (reviewed in Reyes-Lamothe et al. 2008b; Toro and Shapiro 2010). In addition, deletion of ParAB of chr1 in *V. cholerae* leads to an *E. coli*-like chromosome organization for chr1 (Fogel and Waldor 2006). Based on this, it has been previously suggested that origin centric chromosome organization could be the default pattern and that origin anchoring to the poles in bacteria like *C. crescentus* leads to the <*ori*-out *ter*-in> organization (Danilova et al. 2007). The current data suggest that <*Left-ori-Right*> organization in *E. coli* is a direct consequence of MukBEF, rather than being generated due to replication and chromosome segregation.

Furthermore, confinement by macromolecular crowding (Foley et al. 2010) or DNA-DNA interactions (Wiggins et al. 2010) alone does not seem be responsible for wild type organization or compaction of the chromosome, as removal of MukBEF from the cell seemed to change nucleoid morphology. Instead of becoming diffuse or decondensed, the nucleoids became elongated and had rough DAPI staining (regions of bright and weak staining). However, this effect was visible only when MukE was rapidly degraded in long cells. While *mukF*$^{-}$ cells also had elongated nucleoids, DAPI staining was closer to

wild type. One possibility is that these cells compensate for the absence of MukBEF over few generations. Alternatively, it is possible that increased cell length provides more space for nucleoid elongation. It will be key to understand the mechanism for the change in nucleoid morphology.

It is tempting to propose that the bacterial chromosome has multiple layers of organization, similar to its eukaryotic counterparts (reviewed in Maeshima and Eltsov 2008). One possibility is that topological domains held together by nucleoid-associated proteins generate the first level of organization. These could be coordinated by MukBEF complexes that may act by bringing regions of the chromosome together. A recent study showed that condensin forms rings around DNA (Cuylen et al. 2011). Ring formation could enable condensin to embrace distance regions of the chromosome. Furthermore, *in vitro,* condensin/ MukBEF can bridge regions of the same DNA molecule (Strick et al. 2004; Petrushenko et al. 2006a). Although *in vivo* significance of the above remains to be established, it is possible that MukBEF also forms rings *in vivo*, entrapping/ bridging distant chromosomal regions within them.

Alternatively, it is possible that MukBEF action is concentrated locally around the origin region. The organization of the rest of the chromosome may be a consequence of origin positioning by MukBEF. Based on the change in position of origin independent regions (*L3/R3*) as well as change in nucleoid length/ morphology, I favour a model where MukBEF complexes may act in global chromosome organization.

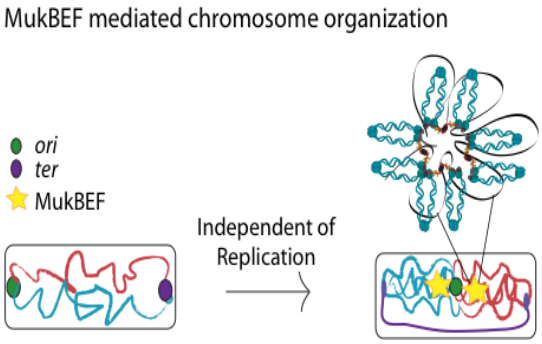

Fig 2.12: MukBEF can generate and maintain spatial chromosome organization independent of replication. One possibility is that MukBEF complexes form rings around distant regions of the chromosome and bring them together in foci.

2.11.4 Multiple MukBEF foci reorganize the chromosome dynamically

Consistent with the idea that MukBEF complexes may function in foci, reorganization of the chromosome was preceded by focus formation. Thus, MukBEF can associate with and act on the chromosome independent of replication. Interestingly, multiple MukBEF foci formed at various locations on the chromosome soon after MukF repletion. Even initial, weak foci were not origin associated. Time-lapse experiments suggested that the foci were dynamic and seemed to fuse together and move along the nucleoid over time. Indeed, even the origin was not relocated in a single step, but moved dynamically with a mean displacement of 0.37±0.1% of cell length/min through the long axis (±SEM). An interpretation of this data would be that MukBEF complexes associate with various regions on the chromosome and bring them together actively, finally localizing around the origin (Fig 2.12).

2.11.5 MukBEF foci may load at regions other than the origin

What could be the loading mechanism for MukBEF and how could it associate with multiple regions on the chromosome? A favourable model to explain MukBEF loading on DNA would be sequence driven. It has been shown that while condensin remains associated with its loading site, cohesin slides along

the chromosome arms (D'Ambrosio et al. 2008b; reviewed in Ocampo-Hafalla and Uhlmann 2011). In addition, recent work on cohesin (Onn and Koshland 2011) suggests that cohesin loading at one region of DNA facilitates loading of several other complexes around it. Thus, it is possible that MukBEF adopts a similar mechanism to associate with several regions of the chromosome after loading. Organization of chromosomal regions by these complexes could bring distant MukBEFs together into one or two foci that are positioned around the origin. It is also possible that MukBEF recognises certain properties of chromosomal regions, such as topological states, rather than specific sequences. ChIP studies on MukBEF have been inconclusive so far, as no single association site has been found (Danilova et al. 2007; Waldaminghaus et al. unpublished).

Although not shown for SMCs before, another model proposed is that MukBEF is positioned on the chromosome as a consequence of an oscillatory system. A similar mechanism has been described for the positioning and partition of the P1 *Par* system (Vecchiarelli et al. 2010). It has been proposed that the ATP dependent oscillation of ParA over the nucleoid positions ParB bound to plasmid at mid-cell or quarter-cell positions. The oscillation of protein sets up a gradient in the cell and foci tend to be located at the local minimum concentration. Imaging of MukBEF at fast timescales has suggested that the background fluorescence (not in foci) is dynamic, reminiscent of an oscillatory behaviour (data not shown). This could be a mechanism by which MukBEF positions itself at cell middle or quarter and capture origins to it, localize them at mid-cell or quarter position. However, it remains to be confirmed that the movement is oscillatory and not random.

2.11.6 MukBEF: the active organizer or segregator of the chromosome?

SMC/ Muk deletions have defects in chromosome segregation. MukBEF could also play an active role in chromosome segregation, as time-lapse suggest that MukBEF foci can duplicate and segregate before origins (Danilova et al. 2007). However, it is equally possible that segregation defects in *muk*$^{-}$ cells are a consequence of poor chromosome organization (Danilova et al. 2007). Indeed, Renshaw et al. 2010 have proposed that condensin mediated chromosome stiffening promotes effective segregation probably by aiding the removal of residual cohesion from chromosome (similar mechanism has been proposed for bacterial SMCs (Holmes and Cozarrelli 2000)). Hence, in cells depleted for condensin, segregation defects are more pronounced in chromosome ends (reviewed in Hudson et al. 2009; Renshaw et al. 2010; Cuylen et al. 2011). Similarly, upon MukE degradation, segregation defects were more obvious in regions farther from the origin; possibly suggesting that MukBEF mediated chromosome organization could contribute to the effective segregation. Another possibility is that the structuring of the chromosome by MukBEF provides a good substrate for TopoIV activity (a process that could affect chromosome segregation). It has been shown that TopoII activity is impaired in the absence of condensin (D'Ambrosio et al. 2008a) and MukB can stimulate TopoIV activity *in vitro* (Hayama and Marians 2010; Li et al. 2010b). Preliminary data from degradation experiments suggest that absence of MukBEF leads to increase in cohesion time (increased cohesion time indicates loss of TopoIV activity).

In conclusion, <*Left-ori-Right*> organization in *E. coli* can be generated and maintained by MukBEF independent of replication. Thus, the activity of "chromosome organization" may be a conserved feature of all condensins.

While it is thought that condensin is required to structure mitotic chromosomes (reviewed in Hudson et al. 2009), MukBEF action seems to be required throughout the cell cycle. Interestingly, it has been proposed that the *E. coli* chromosome is akin to a mitotic chromosome in structure (Wiggins et al. 2010). Current data also suggest that the loading site of MukBEF may be other than the origin (discussed in Chapter 3).

CHAPTER 3

Towards an understanding of the active MukBEF complex

3.1 Objectives

While *in vitro* studies give insight into the possible mechanism of action of MukBEF, in some cases reactions utilize excess MukB or do not test the effects of MukE or MukF. Thus, the *in vivo* significance of key MukB properties, such as ATPase activity or DNA binding ability remains to be established. *In vivo*, fluorescent derivatives of MukB form foci on the nucleoid, with 1-2 foci localizing around each origin (den Blaauwen et al. 2001; Ohsumi et al. 2001; Danilova et al. 2007). Are these foci centres of activity of the MukBEF complex? While a stable complex of MukBEF containing only two MukB molecules is often thought as the active form, higher order structures with several MukBEF molecules have also been suggested (Matoba et al. 2005; Woo et al. 2009). Furthermore, previous studies estimated by Western blots 200-600, 340 and 170 molecules per cell for MukB, MukE and MukF respectively (Petrushenko et al. 2006a; Petrushenko et al. 2006b). It is however unclear, what type of cells were analyzed and how many of the estimated MukBEF copies are active at a given time in the cell/ present in a focus. The objective of this work was the following:

a. Characterize the properties of MukBEF foci; estimate the stoichiometry MukBEF complexes in foci in relation to total protein in the cell and assess focus dynamics.
b. Understand the *in vivo* significance of ATPase activity in MukBEF focus formation and function.

3.2 Characterization of fluorescent fusions of MukBEF

mukFEB genes are present in an operon under control of the *smtA* promoter along with the *smtA* gene, a putative methyl transferase with no apparent function (Yamanaka et al. 1996) (Fig 3.1A). In order to study the stoichiometry and dynamics of Muk proteins *in vivo, mukBEF* genes were replaced with alleles coding for fluorescently tagged Muk proteins in the chromosome, expressed under their endogenous promoter. For single colour experiments, proteins were fused with mYPet, an YPet derivative carrying the A206K mutation to prevent dimerization. While *mukE* and *mukB* were fused at the C-terminus, MukF-mYPet was an N-terminal fusion. The strains were similar to wild type in terms of growth (Table 3.1) and no cell filamentation or increase in anucleate cells was observed (in rich/ minimal media). Western blots confirmed that fusion proteins were being expressed (Table 3.1).

	Generation time (min)	
	LB (37°C)	M9-gly (30°C)
Wild type	33±3	134±4
MukB-mYpet	34±2	132±5
MukE-mYpet	34±2	134±3
MukF-mYpet	36±2	134±3

Table 3.1: Characterization of fluorescent fusions of MukBEF

In vivo, MukBEF fusions formed foci. As measured by eye MukB, E and F colocalized in foci in all cells carrying two-colour fusions of MukB, MukE or MukF (Fig 3.1A). The average (median in this case) distance between MukB and E foci was 103nm; between MukB and F foci, 125nm; MukE and F foci, 117nm (Fig 3.1B). The maximum distance between the foci was no more than 300nm (increased distance could be due to computational error). Although

*Bs*SMC has been shown to colocalize with ScpA and ScpB, this has not been seen for MukBEF as yet (but they are expected to colocalize). Indeed, active MukF and MukE were required for MukBEF focus formation.

The mean number of MukBEF foci per cell was 2.06 (Fig 3.1C) with 53% cells having 2 MukBEF foci. Only 2% cells had no MukBEF foci (these were not anucleate). The mean ratio of MukBEF foci:*ori1* was 1.39:1, similar to that observed by Danilova et al. 2007. As reported previously, foci localized around the origin (Fig 3.9B), with median distance of 330nm of the nearest MukBEF focus from the origin.

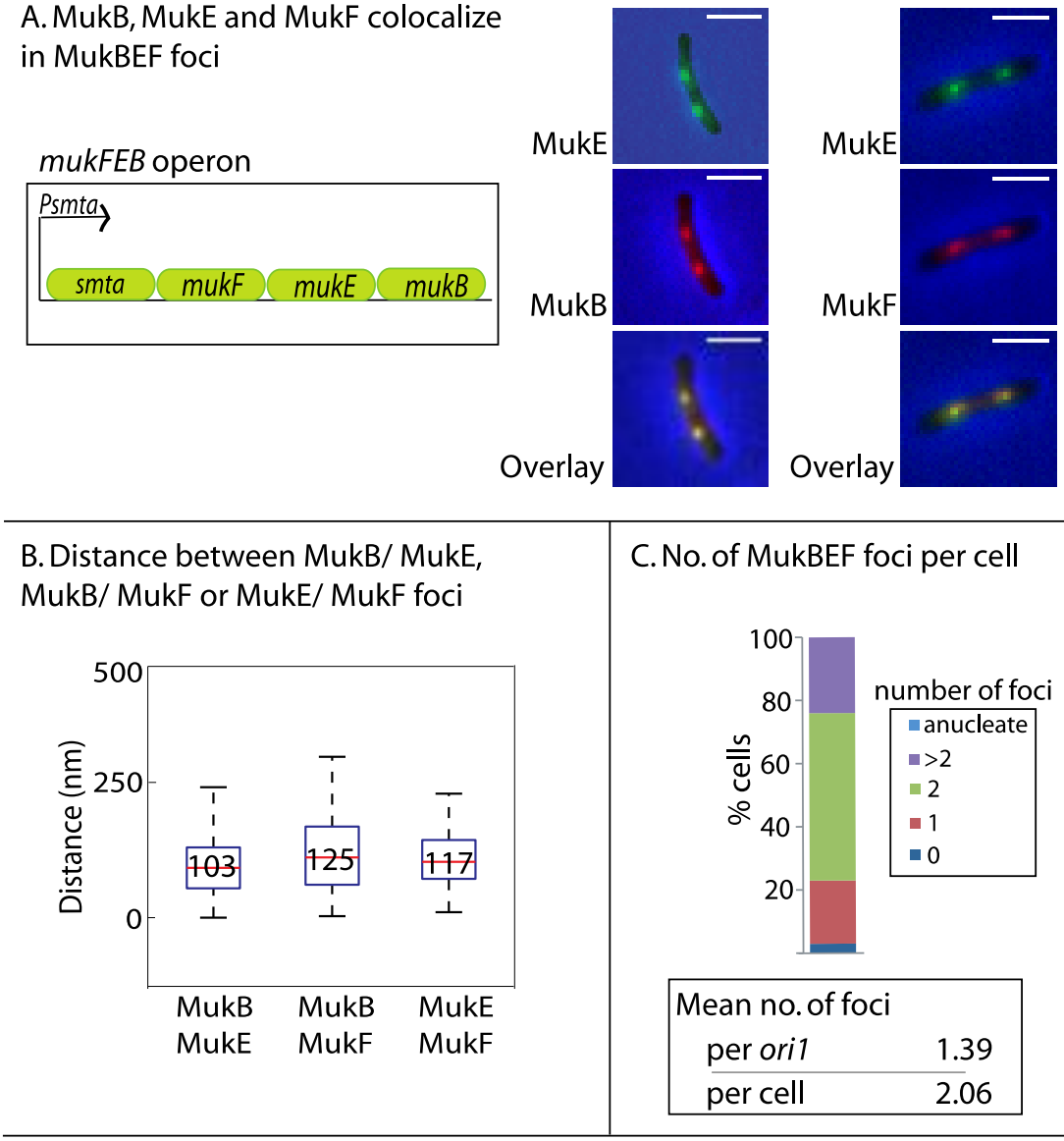

Fig 3.1: Fluorescent fusions of MukBEF form foci

A. Fluorescent fusions of MukB, MukE and MukF were constructed at the gene locus (in the *mukFEB* operon) expressed under their endogenous promoter. MukB, MukE and MukF colocalized in foci. Scale bar = 2µm

B. Distance between MukB and MukE, MukB and MukF or MukE and MukF foci was measured. Median distance (in nm) is indicated inside the box. n>500

C. No. of MukBEF foci per cell was estimated. % cells with 0, 1, 2 or >2 MukBEF foci per cell is plotted. Mean no. of foci per origin or per cell is indicated in the box. n>500

3.3 Slimfield microscopy to estimate number of MukBEF molecules in foci

The slimfield technique has been established in our lab previously by (Reyes-Lamothe et al. 2010) as a powerful way of determining *in vivo* stoichiometry of fluorescently tagged proteins. The technique was used to determine the architecture of an active replisome. “Slimfield” is created by under-filling the back-aperture of the objective with a collimated laser beam; the Gaussian excitation field generated at the sample is adjusted such that it encompasses a single *E. coli* cell – the intensity of such a field is about 100 times that of wide-field fluorescence (Plank et al. 2009; Reyes-Lamothe et al. 2010)(Fig 3.2A). Using this setup combined with fast capture rate of ~3ms, one can quantitatively detect single fluorescent molecules in live cells. Fast capture rate also permits visualization of transient interactions of fast diffusing proteins, which might otherwise appear blurred. Importantly, the high laser excitation did not seem to affect replication or flagellar rotation in bacteria, thus slimfield illumination may not generate observable photodamage in cells when used for short periods of time.

The system was used to estimate the stoichiometry of MukBEF complexes in foci (in collaboration with Dr. Mark Leake; data analysis was done by him).

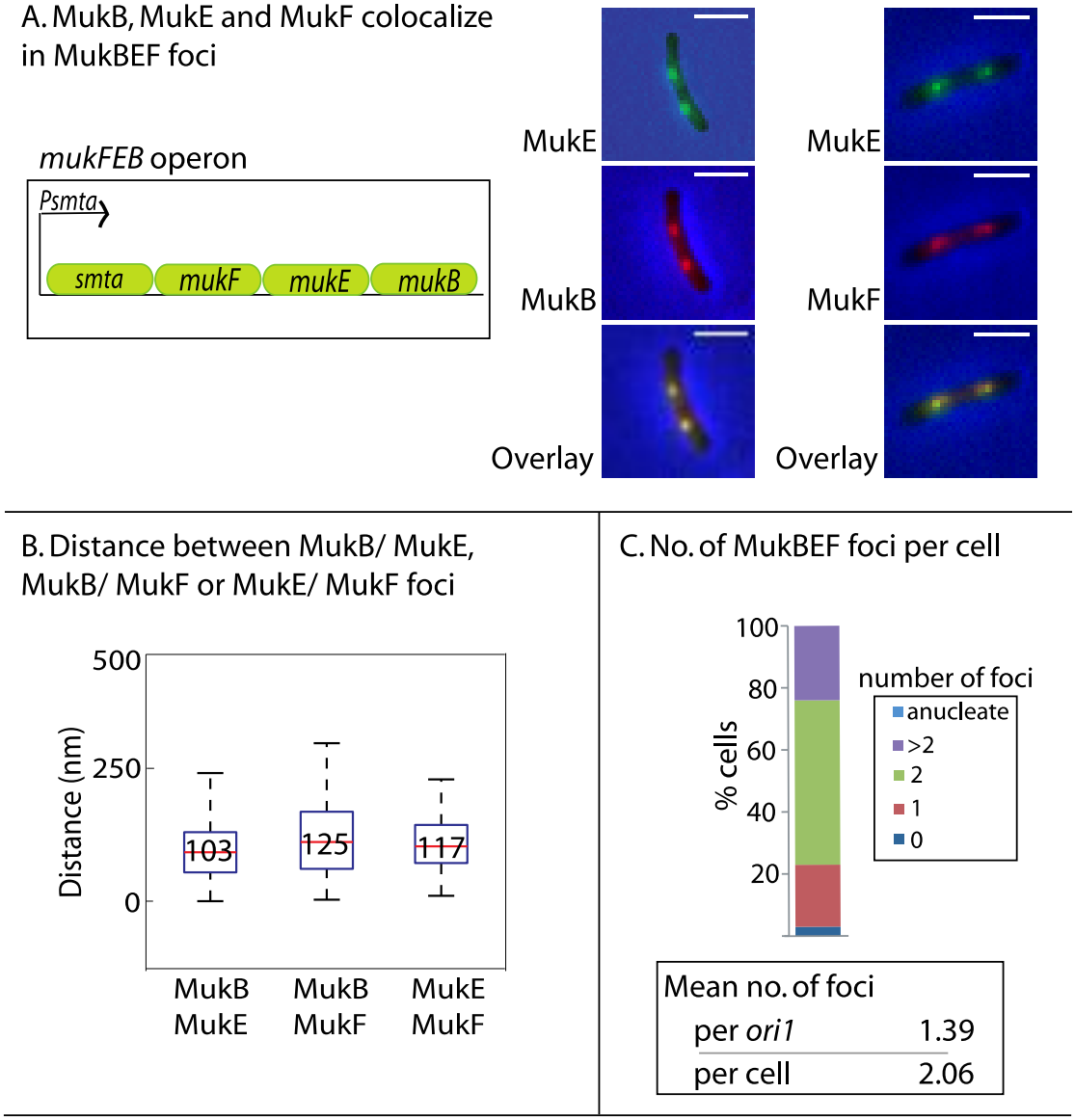

Fig 3.2: Slimfield imaging of MukBEF

A. Schematic of slimfield: Laser under-fills the back-aperture of the objective lens generating a high intensity Gaussian field large enough to image a single *E. coli* cell (adapted from Reyes-Lamothe et al., 2010). Examples of fluorescence images of MukB-mYPet and MukE-mYPet (frame averaged over 90ms) are shown. Foci or Regions of Interest (ROIs) are marked as circles.

B. Sample photobleaching traces (acquired at 3ms per frame) for low stoichiometry (left) and high stoichiometry (right) MukE-mYPet foci. The smallest step size should correspond to the intensity of a single mYPet molecule.

In order to estimate stoichiometry, images were captured every 3ms for about 300 frames (till total photobleaching had occurred). By drawing regions of interest (ROIs) around frame-averaged foci (Fig 3.2A), the shape, size and intensity of fluorescence in the spot were automatically measured and a step-like intensity trace was generated as photobleaching occurred (Fig 3.2B). In general, the smallest step size should correspond to the intensity of a single molecule. Step-size, in most cases, corresponded well with the value for a single molecule of purified mYPet *in vitro* ~1.1-1.2 kcounts. In order to achieve reliability, individual traces from all cells were collated and step-size was estimated using an average power spectrum. The step size thus obtained was in agreement with the *in vitro* single molecule mYPet value as well as estimates from studies with the *E. coli* replisome (Reyes-Lamothe et al. 2010). Thus, stoichiometry for each Muk component could now be obtained by converting the intensity value for a focus into number of molecules.

3.4 Few MukBEF complexes are present in fluorescent foci

For single colour stoichiometry determination, MukB, MukE and MukF mYPet strains described above were used. Most cells had two visible MukBEF foci (summarized in Table 3.2). There was a broad and heterogeneous distribution of the number of MukB, MukE and MukF molecules present in a focus per cell (Fig 3.3A, B, C). However, these graphs represent numbers from a mixed population of cells with 1, 2 or more foci per cell. Interestingly, filtering of results revealed that in cells with multiple foci, one focus tended to have higher stoichiometry than the other foci in the cell. Thus, in cells with two foci, one focus had ~66% of the total number of molecules in foci (for that cell) while the

second focus had 34% of the molecules (Table 3.2). In cells with 3 foci, these values were ~50%, 30% and 20% for focus 1, 2 and 3 respectively.

The number of MukB, MukE and MukF per focus per cell averaged across all cells was 36±3, 36±4 and 19±1 (SEM) respectively. As stated earlier, 66% of cells had two MukBEF foci. In cells with two foci, the focus with higher stoichiometry had 52±7, 53±3 and 31±4 (±SEM) molecules of MukB, MukE and MukF respectively. The second focus had 26±2, 27±2 and 15±2 molecules of MukB, E and F respectively. The total number of molecules per cell for MukB was 438±180. On average each cell had 380±154 MukE and 256±110 MukF molecules. Hence, the proportion of MukBEF complexes in foci when compared to the total number in the whole cell is low. Only 19±10% of MukB molecules was found to be in foci. For MukE and MukF these values were 21±12% and 18±10% respectively (±SD).

Strain	Mean no. of molecules per focus per cell (±SEM)	Mean no. of molecules in foci per cell ±SEM,	Mean no. of molecules per focus: 2 foci cells (focus 1) (±SEM)	Mean no. of molecules per focus: 2 foci cells (focus 2) (±SEM)	Total no. of molecules per cell (±SD)	% of molecules in foci per cell (±SD)
MukB	36±3	82±7	52±7	26±2	438±180	19±10
MukE	36±4	79±3	53±3	27±2	380±154	21±12
MukF	19±1	45±2	31±4	15±2	256±110	18±10

Table 3.2: Summary of MukBEF mYPet slimfield experiments

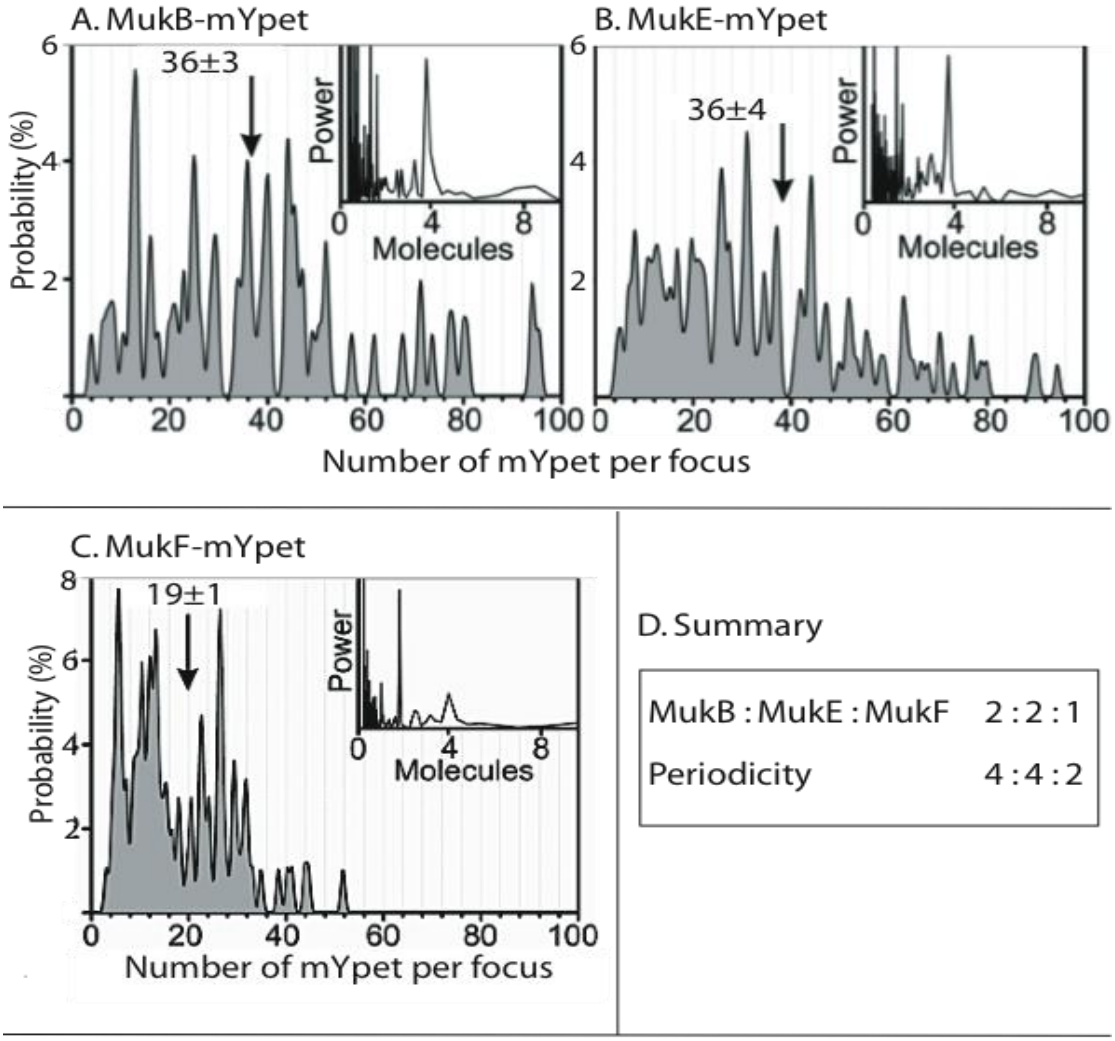

Fig 3.3: MukBEF mYPet has a broad and heterogeneous stoichiometry distribution

A, B, C. Stoichiometry of MukB, MukE or MukF mYPet in a single focus was estimated (using values from step-wise photobleaching traces). Stoichiometry distributions thus obtained were plotted using automated kernel density estimation (with a width of 1 molecule); Mean ± SEM is represented inside the graph. Grid lines (grey lines) are drawn at intervals of 4 molecules. Power spectra of the pairwise difference distribution of detected peaks are in the inset, indicating peaks at 4 (and a weak peak at 2) molecules for MukB and MukE and a peak at 2 for MukF. n – 148-260 foci (60-80 cells)

D. Summary of mean ratio of MukB:MukE:MukF is represented in the box

3.4.1 MukBEF complexes in foci may be ATP bound

The mean values of MukB, MukE and MukF molecules present in a focus suggest a ratio of 2:2:1 for MukB:E:F. The above described stoichiometry distributions were plotted using kernel density estimation, with a width of 1 molecule (corresponding approximately to the measurement noise at the end of a photobleach). It was found that MukB and MukE distributions had stoichiometry peaks broadly consistent with a 4-mer periodicity, while MukF peaks were consistent with a 2-mer periodicity (grey lines in Fig 3.3; drawn at intervals of 4 molecules). Consistent with the above, power spectra for pair-wise difference distribution of detected peaks in the stoichiometry distributions showed peaks at ~4, 4 and 2 for MukB, MukE and MukF respectively. Hence, the above data suggest a ratio of 4:4:2 MukB:E:F, with ~20±4 such complexes in foci per cell. Indeed, a small percentage (less than 10%) of peaks were also consistent with a 2-mer periodicity for MukB and MukE, suggesting the presence of 2:2:1 MukB:E:F complexes as well in a small proportion of foci.

Structural studies have suggested that MukB, MukE and MukF exist in a 2:2:1 ratio upon ATP binding (closed complex) and take up an open 2:4:2 conformation when ATP is hydrolysed or unbound (Fig 3.4A). The 2:2:1 complex is generated due to detachment of one MukEF complex (2:1 MukEF) from the MukEF heterohexameric complex upon ATP binding (Shin et al. 2009; Woo et al. 2009). However, MukF is also thought to form a stable domain swapped dimer via its N terminus (Fennell-Fezzie et al. 2005; Gloyd et al. 2007; Woo et al. 2009; Gloyd et al. 2011). Hence, it possible that one MukBEF complex (2:2:1) could associate with another via the free dimerization interface of MukF, thus generating 4:4:2 MukBEF complex (Fig 3.4A). This model could

explain the periodicity observed in stoichiometry experiments and suggests MukBEF complexes are ATP bound in a focus with a ratio of 4:4:2 MukB:E:F. Indeed, a proportion of foci could have a mixture of 2:2:1 and 4:4:2 complexes as well; the 2:2:1 complexes may represent an intermediate state prior to the formation of the 4:4:2 complex (the more predominant of the two).

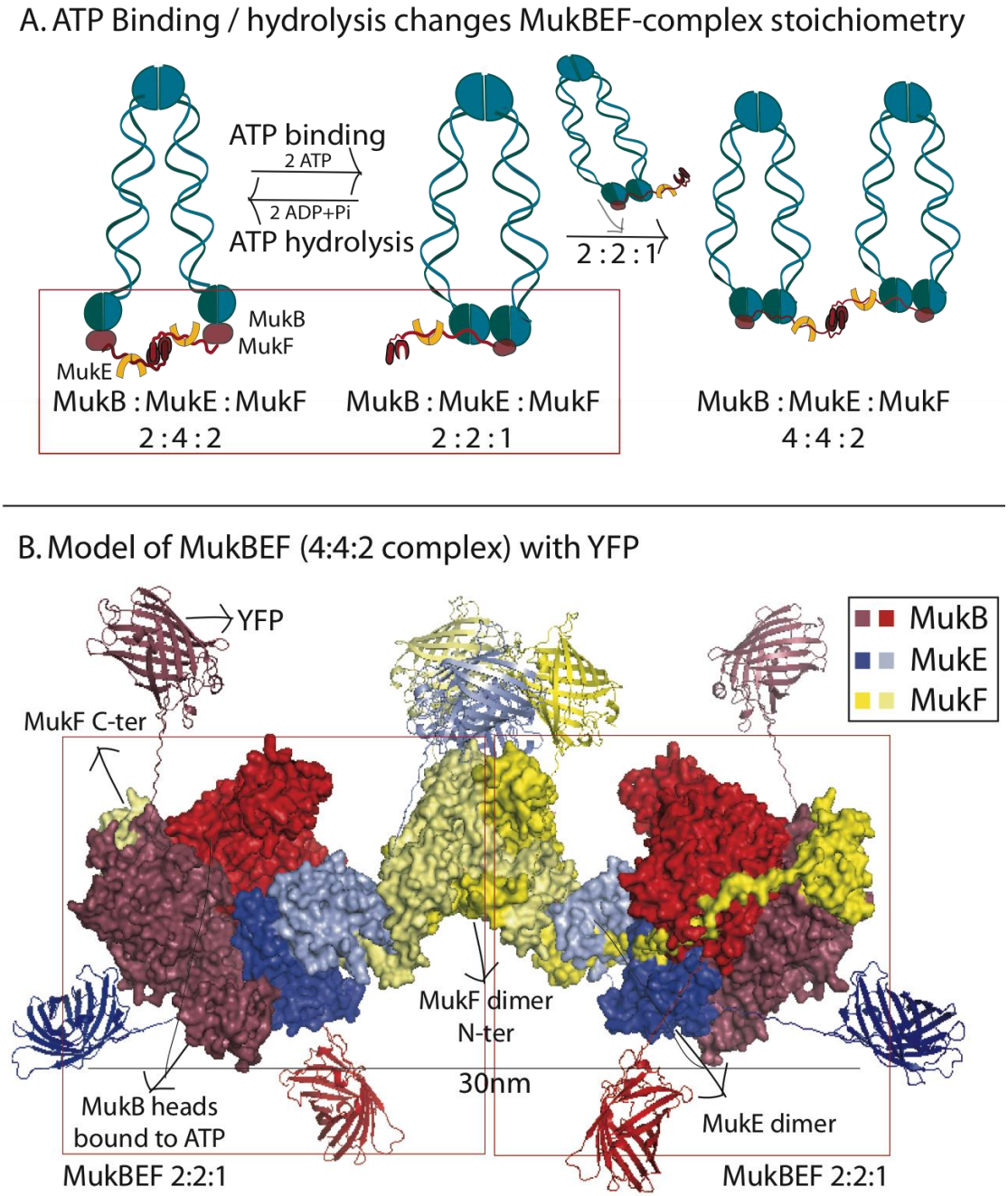

Fig 3.4: MukBEF may be ATP bound in foci with a ratio of 4:4:2

A. Cartoon summarizing structural information about the MukBEF complex (adapted from Woo et al. 2009 – red box). It is thought that MukBEF (without ATP) takes up an open conformation with a 2:4:2 MukB:E:F ratio. ATP binding results in a closed complex with a 2:2:1 MukB:E:F ratio. One possibility is that a second MukBEF (2:2:1) interacts with the closed complex via the N-ter MukF dimerization domain, resulting in a MukBEF 4:4:2 complex, bound to ATP. Structural information is available only for the 2:2:1 complex. The 4:4:2 complex is only a possibility based on stoichiometry results.

B. Structure of possible MukBEF 4:4:2 complex modelled with PyMol. Structural coordinates from Woo et al. 2009. Structure comprises of MukB heads bound to ATP (red), MukE dimer (blue) bound to a single MukF (yellow). The dimerization interface for MukF is marked. 4:4:2 structure is as described in (A). YFP is fused to MukB/ E/ F. Farthest and nearest distance between fluorophores is indicated.

3.5 Size and shape of MukBEF foci

In order to understand the organization of MukBEF complexes inside foci, size and shape of MukBEF foci was analysed (Fig 3.5A) (following Reyes-Lamothe et al. 2010). Focus intensity was fitted using a 2D Gaussian, which was allowed to have different width parallel and perpendicular to the long axis of the cell. Mean full width at half maximum (FWHM or σ) was estimated for all foci, which is indicative of the spread/ size of a focus. Circularity/ shape of the focus was determined by estimating the FWHM σ_x/σ_y ratio (where x-axis is the long axis and y-axis represents width of the cell). While pure mYPet had a mean σ value of 237±12nm, MukBEF foci seemed spread with σ values of 395±20nm, 412±24nm and 402±22nm for MukB, E and F respectively. This suggests that MukBEF foci were not constrained within the point-spread function width (~200-300nm in the microscope). It is interesting to note that single copies of replisome components present in foci has a spread of ~300nm, suggesting a contribution by the movement of foci (Reyes-Lamothe et al. 2010). MukB/E/F also had similar circularity values of 1.57±0.04, 1.75±0.05 and 1.58±0.04 respectively (pure mYPet was ~1). Thus, a MukBEF focus is more extended in the long axis of the cell, with a mean σ_x of 306±6nm. Indeed, σ_y values suggest that the focus did not occupy the entire width of the cell, with a mean value of 188±14nm (cell width is ~250nm). Modelling of the 4:4:2 structure in PyMol (structural coordinates from Woo et al. 2009; YFP was added with a 11aa linker) suggested that a single complex would be ~30nm wide (Fig 3.4B, 3.5B). Previous studies have estimated the length of the coiled-coil to be ~50nm (reviewed in Nasmyth and Haering 2005). Hence, current data suggest that ~10 complexes (possibly 30nm wide and 50-100nm long; Fig 3.5B) would be

present in a focus that may be ~306x188nm. Super-resolution information, revealing the physical packing of complexes would be required to know the maximum number of possible complexes in such a volume.

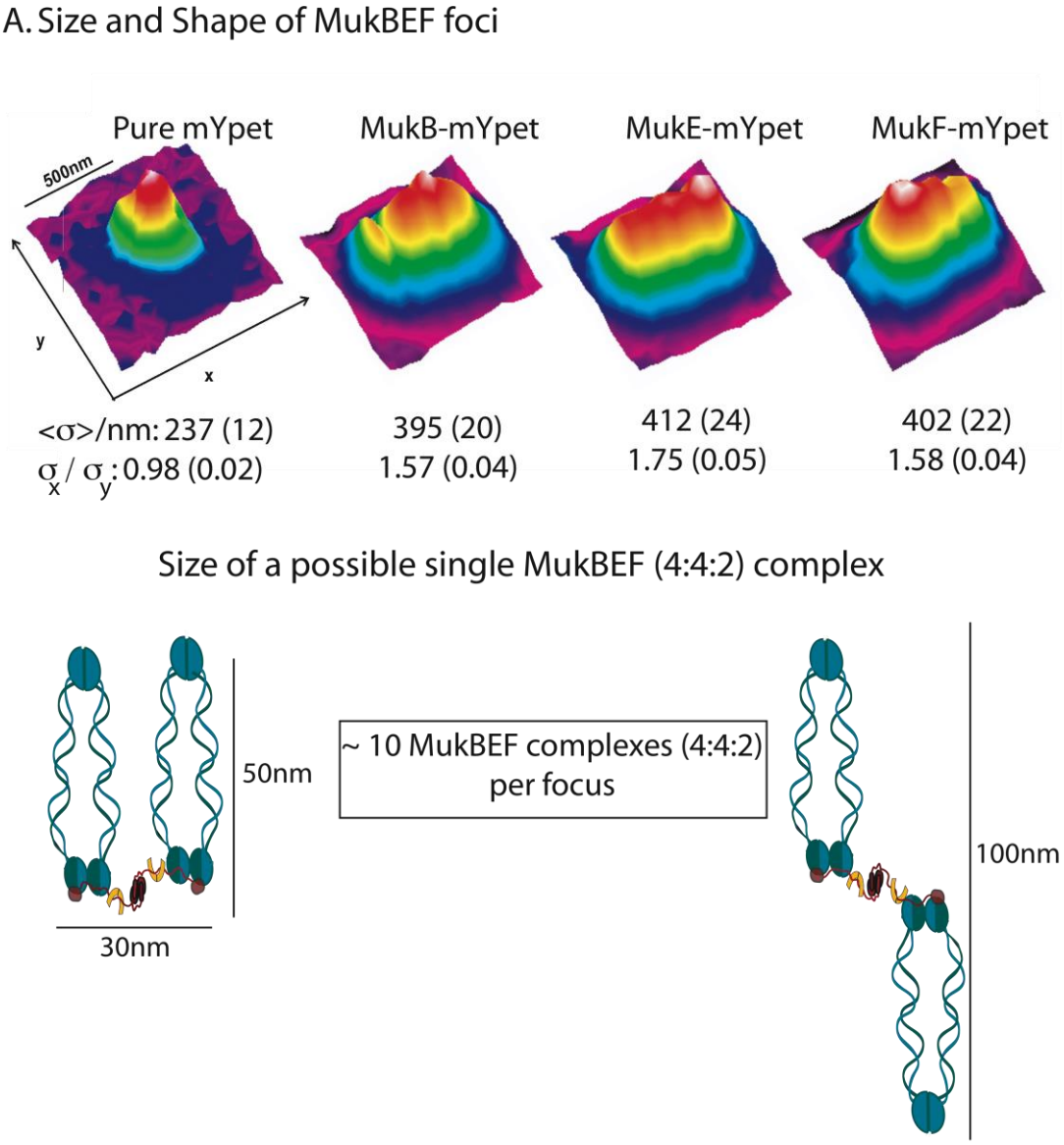

Fig 3.5: MukBEF mYPet foci are spread

A. Size and shape of MukB, MukE and MukF-mYPet foci was calculated (as in Reyes-Lamothe et al., 2010) and compared with purified, surface-immobilized mYPet. Images were first rotated such that the long axis of the cell was parallel to the x-axis (in the figure). Focus intensity was assumed to have a symmetric Gaussian distribution and mean full width at half maximum (FWHM or σ) of this was estimated as an indication of spread of foci; Circularity or shape of the complex was determined by estimating the FWHM σ_x/σ_y ratio of the focus (where the x-axis represents the long axis of the cell and y-axis represents the axis along the width of the cell). Mean (± SD) values are shown. 60-80 cells; 148-260 foci.
Possible size of a MukBEF 4:4:2 complex is also shown. ~10 such complexes need to fit inside a focus.

3.6 Two-colour slimfield experiments suggest MukBEF may be ATP bound in foci

The above observations were made in strains independently expressing MukB, E or F mYPet. Averaging this data could be misleading. In order to test whether MukBEF was indeed ATP bound with a periodicity of 4:4:2 (MukB:E:F) in foci, two colour experiments were carried out. For this, strains expressing MukB-GFP and MukE-mCherry or MukB-GFP and MukF-mCherry were used. Slimfield experiments were done by simultaneously imaging GFP/ mCherry. Thus, now stoichiometry of MukB and MukE or MukB and MukF could be determined in the same focus.

Stoichiometry distributions for MukE/B and MukF/B were plotted as for single colour experiments and had a similar broad and heterogeneous distribution. Indeed, MukB and MukE had an equal proportion of high stoichiometry peaks, which were rarely seen for MukF (Fig 3.6A, 3.7A). KDE peaks were broadly consistent with a 4-mer periodicity for MukB and MukE, while MukF had ~2-mer periodicity. Scatterplots of GFP vs. mCherry for the same colocalized focus in each cell were plotted and these suggested that most foci had equal numbers of MukE and MukB molecules per focus (Fig 3.6B, left panel). In contrast, a majority of foci had half the number of MukF to MukB molecules per focus (Fig 3.7B, left panel). Consistently, kernel density estimation on the ratio of MukE:MukB in foci across all cells had an average ratio of 1±0.3 (±SD), while the average ratio of MukF:MukB is 0.5±0.2 (Fig 3.6B, 3.7B right panel). Thus, these data support a model where the majority of MukBEF complexes are ATP bound in foci with a ratio of 4:4:2 (B:E:F).

Reyes-Lamothe et al. 2010 estimated the percentage of dark, immature mYPet molecules in the experimental setup and found that its contribution to the fluorescence intensity was minimal. Indeed similar maturation times have been reported for GFP-UV4, mCherry and mYPet *in vitro* (15-20minutes) (Iizuka et al. 2011). Hence, % of dark fluorophores in the current experiment may also be small (~1%). However, it is important to determine this in these particular strains.

Fig 3.6: Two-colour stoichiometry of MukB-GFP and MukE-mCherry

A. MukB-GFP and MukE-mCherry were simultaneously imaged and stoichiometry distribution for both proteins in the same focus was estimated and plotted as Fig 3.3. Blue peaks represent GFP, while red represent mCherry.
B. Scatterplot of MukE-mCherry vs. MukB-GFP for the same colocalized focus in each cell was plotted using 2D kernel density estimation. Gradient of the dashed line is 1.0. Kernel density estimation on ratio of MukE:MukB across all cells is plotted on the right. Mean ±SD is indicated in the box.

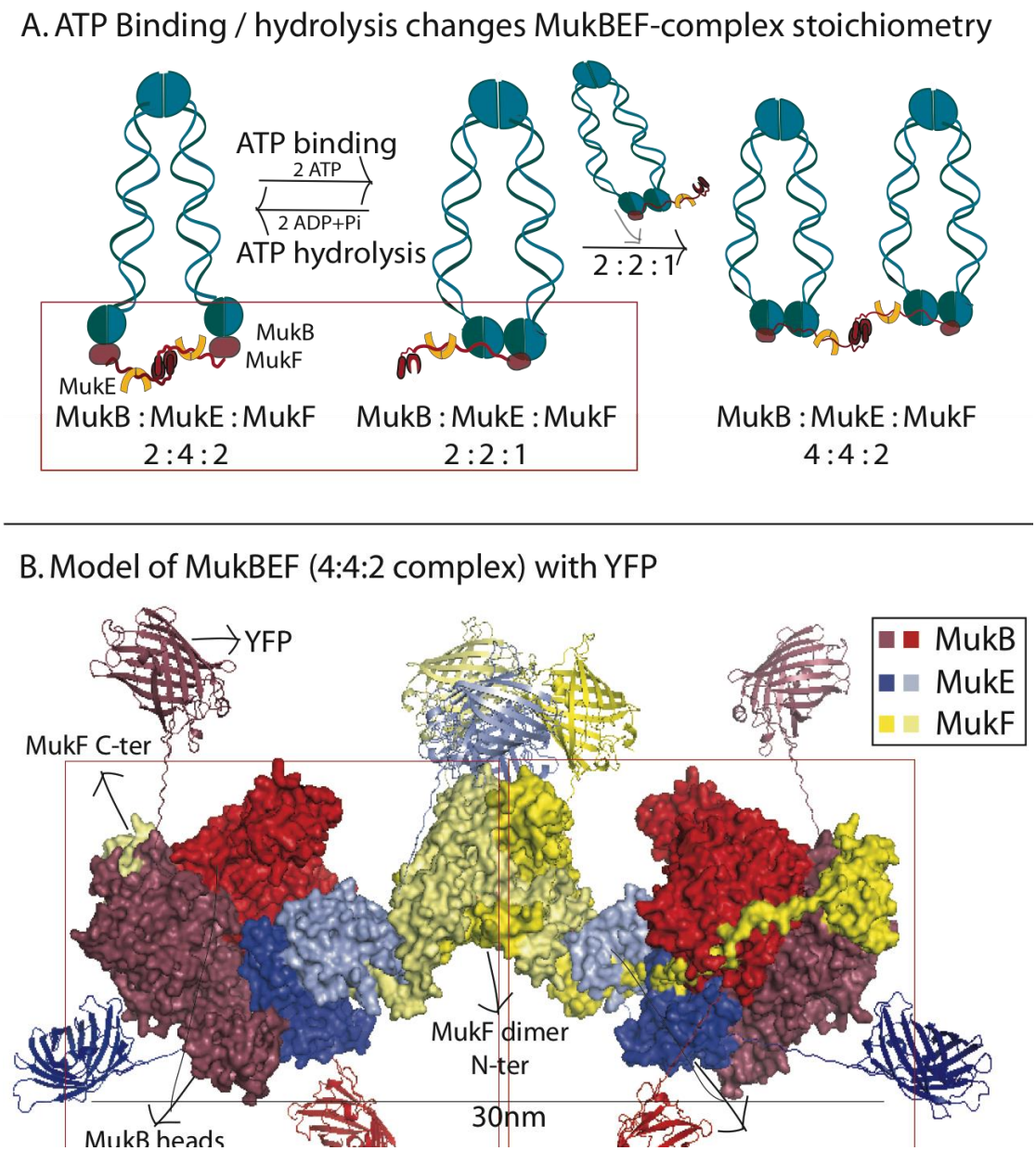

Fig 3.7: Two-colour stoichiometry of MukB-GFP and MukF-mCherry

A. MukB-GFP and MukF-mCherry were simultaneously imaged and stoichiometry distribution for both proteins in the same focus was estimated and plotted as Fig 3.3. Blue peaks represent GFP, while red represent mCherry.

B. Scatterplot of MukF-mCherry vs. MukB-GFP for the same colocalized focus in each cell was plotted using 2D kernel density estimation. Gradient of the dashed line is 0.5. Kernel density estimation on ratio of MukF:MukB across all cells is plotted on the right. Mean ±SD is indicated in the box.

3.7 *In vivo* significance of MukB ATPase activity

Slimfield experiments suggest that MukBEF complexes in foci may be ATP bound with a 4:4:2 stoichiometry. In order to understand the *in vivo* significance of MukB ATPase activity and to confirm whether ATP bound MukBEF complexes formed foci and had a ratio as predicted by structural studies, two ATPase mutants were investigated: The D1406A mutant which is predicted to have no ATP binding ability and the E1407Q mutant which can bind ATP but not hydrolyze it (Arumugam et al. 2003; Weitzer et al. 2003; Hirano and Hirano 2004). Both mutants are present in the Walker B motif and were constructed at the endogenous gene locus with a C-ter GFP fusion (Fig 3.8A).

The mutants had a *muk*$^{-}$ phenotype as previously reported (Shin et al. 2009; Woo et al. 2009). *In vivo,* MukB(D1406A) did not form foci, indicating that ATP binding is essential for focus formation. It is unclear whether the mutant could associate with DNA, but fluorescence signal was present throughout the cell (even in DNA free regions). In contrast, MukB(E1407Q) formed foci (Fig 3.8A) indicating that ATP binding is essential for focus formation, while ATP hydrolysis is required for focus function.

In contrast to wild type cells with mostly ≥2 foci per cell, MukB(E1407Q) (Walker B henceforth) formed a single focus in 59% cells (Fig3.8B). 18% cells had no foci while 11% cells had 2 foci per cell and 10% cells were anucleate (similar to *muk*$^{-}$). While wild type cells had 2.06 MukBEF foci/ cell on average, there were only 0.85 Walker B foci/cell. Walker B MukB and E colocalized in foci with median distance of 85nm between the two (Fig 3.8C) suggesting that Walker B mutants could form complexes *in vivo.*

Fig 3.8: MukB ATP hydrolysis mutant forms foci

A. Alignment of Walker B motif highlighting conservation of D and E residues (left). Two ATPase mutants of MukB were constructed: MukB(D1406A) (prevents ATP binding) and MukB(E1407Q) (prevents ATP hydrolysis – called Walker B henceforth) (Arumugam et al. 2003; Weitzer et al., 2003). While the binding mutant did not form foci, the hydrolysis mutant did (right).
B. No. of wild type MukBEF/ Walker B MukBEF foci per cell was estimated. % cells with 0, 1, 2 or >2 foci as well as % anucleate cells is plotted. Avg. no of Walker B MukBEF foci per cell is indicated in the box. n>500
C. MukB and MukE colocalize in Walker B foci. Distance between Walker B MukB and MukE foci was measured. Median distance (in nm) is indicated inside the box. n>500. Scale bar = 2µm

3.8 Stoichiometry of Walker B MukBEF foci

Structural studies suggest that Walker B MukBEF would have a 2:2:1 ratio (Woo et al. 2009). Indeed, current data for wild type MukBEF foci suggest that the absolute stoichiometry is 4:4:2 MukB:E:F. In order to test the above in Walker B foci, single colour slimfield experiments were carried out in Walker B mutants with MukB, MukE or MukF mYPet fusions. Interestingly, in a proportion of Walker B cells, multiple (2 to 3) transient foci could be seen, that would last only for one frame (3ms) during the slimfield experiment. This event could not be observed previously as images were taken over a 3-5 sec exposure.

Strain (Walker B)	Mean no. of molecules per focus per cell (±SEM)	Mean no. of molecules in all foci per cell ±SEM,	Mean no. of molecules per focus: 1 focus cells (±SEM)	Total no. of molecules per cell (±SD)	% of molecules in foci per cell (±SD)
MukB	55±4	65±6	65±5	333±140	16±9
MukE	54±4	65±5	65±4	393±168	15±9
MukF	20±4	34±13	22±3	204±86	16±9

Table 3.3: Summary of Walker B slimfield experiments

As wild type, Walker B MukBEF had a broad and heterogeneous stoichiometry distribution. The mean number of molecules (±SEM) per focus per cell (averaged across all cells) was 55±4, 54±4 and 20±4 for Walker B MukB, E and F respectively (Table 3.3). 80% of cells had only one focus and the mean number of molecules (±SEM) in these foci was 65±5, 65±4 and 22±3 for MukB, E and F respectively. The total number of molecules (±SD) of Walker B MukBEF was similar to that of wild type (333±140, 393±168 and 204±86 for MukB, E and F respectively) indicating that the mutation does not seem to affect expression levels of the proteins. Thus, 16±9% of Walker B MukB molecules was found in foci. For MukE and MukF these numbers were 15±9%

and 16±9% respectively. Again, these values are similar to wild type cells suggesting that the same number of molecules is recruited into foci. The process of ATP hydrolysis could possibly drive the splitting of foci resulting in multiple foci of lower stoichiometry each, seen in wild type cells.

The mean values of Walker B MukB:MukE:MukF suggest a 2:2:1 ratio of the molecules in a focus. Once more, Walker B MukBEF distributions had a ~4-mer periodicity for MukB and MukE and ~2-mer periodicity for MukF. In summary, the above data suggest that wild type and Walker B MukBEF complexes in foci may be ATP bound with ratio of 4:4:2.

Gel filtration experiments could be carried out to confirm that such complexes are formed *in vitro* as well. Super-resolution imaging (such a PALM) could also be used to study the arrangement of complexes inside foci, obtaining up to ~30nm resolution/ precision.

3.9 Walker B foci are *ter* associated

The above data suggest that ATP binding is essential for focus formation, while ATP hydrolysis is required for the generation of multiple MukBEF foci from a single and MukBEF function. Apart from difference in the number of Walker B and wild type foci, Walker B foci also localized to a region different from wild type. Danilova et al. 2007 found that MukB foci localized around the origin, with 1-2 MukB foci per origin. However, Walker B foci colocalized with the terminus (Fig 3.9A). For wild type MukBEF foci, the median distance of the nearest focus from the origin was ~330nm, while the distance of the nearest focus from the terminus was ~700nm, indicating preferential localization with the origin. In contrast, the distance of the nearest Walker B focus from the origin was ~600nm. Walker B foci colocalized with *ter* with a distance of ~200nm between *ter* and the nearest focus (Fig 3.9B). The ratio of Walker B foci:*ter* was 0.98:1. Thus, there was almost one Walker B focus per *ter*. Indeed, the ratio of Walker B:origin was much lower (0.63:1), opposite to that seen for wild type foci, which have ~1.4 foci/ origin (Table 3.4). Importantly, wild type foci rarely localize with *ter*. Such cases are only observed when *ori* and *ter* colocalize as well (~12%, Danilova et al. 2007). Indeed, while other bacterial SMCs also display localization around the origin, their association with *ter* has not been reported so far.

AB1157 (parental strain)			Two origin strain		Cephalexin	
MukB: *ori1*	Walker B: *ori1*	Walker B: *ter3*	Walker B: *ori1*	Walker B: *oriZ*	Walker B: *ori1*	Walker B: *ter3*
1.4	0.63	0.98	0.61	0.67	0.32	0.93

Table 3.4: Ratio of MukBEF/ Walker B MukBEF foci to *ori1/ ter3*

Were Walker B foci found at the terminus due to active association or due to passive relocation to this region by other processes? One possibility is that Walker B foci associate with the origin as wild type, but are pushed to the terminus due to replication. If this hypothesis were correct, then there would have been a broad distribution of Walker B foci along all regions of the chromosome (while being moved from *ori* to *ter*). However, Walker B strongly colocalized with *ter*. To test the "replication relocation" possibility further, Walker B foci were visualized in cells carrying a chromosome with two origins (*ori1* and *oriZ*) of replication instead of one (Wang et al. 2011), hence replication termination is thought to occur at two independent regions. Thus, if replication were indeed pushing Walker B from *ori* to *ter*, then the number of foci would increase from one to two (one at each termination region). However, most cells had only one focus (Fig 3.9A). The ratio of Walker B:*ori1* and Walker B:*oriZ* was 0.61 and 0.67 respectively (similar to cells with a single *ori*) (Table 3.4).

To test whether the localization of Walker B was dependent on cell division and/ or FtsK activity, cells were treated with cephalexin, a drug that blocks cell division by inhibiting the transpeptidase activity of FtsI (needed for septum constriction) (Pogliano et al. 1997). *dif* recombination is also reduced (Steiner et al. 1999; Kennedy et al. 2008) suggesting FtsK translocase activity may also be affected in the presence of cephalexin.

In cells treated with cephalexin for 2 or 4 generations, colocalization between Walker B foci and *ter* did not change (Fig 3.9A). Ratio of Walker B foci:*ter* was close to 1 (0.93) while the ratio of Walker B foci:*ori* reduced to 0.32 (Table 3.4). Interestingly in Walker B cells treated with cephalexin, *ori* segregation was observed while *ter* segregation was affected. The median distance of the

nearest Walker B focus from *ter* was 200nm (as seen in cells without cephalexin), while the median distance between *ori* and nearest Walker B focus increased to 1µm (Fig 3.9B). Indeed, if multiple *ter* loci are present in one *ter* focus, it is possible that the number of Walker B MukBEF complexes in such a focus would also increase. It would be interesting to test if this is the case.

What governs the association of Walker B MukBEF with *ter*? One possibility is that it is sequence-driven. It is attractive to think that Walker B MukBEF represents the "MukBEF loading complex", which can bind ATP and load on DNA, but cannot migrate to its wild type location due to inability to hydrolyze ATP. The process of ATP hydrolysis would drive the splitting of a "single loading complex" into multiple functional units that have *ori* proximal localization. Thus, the terminus region may be the site where MukBEF loads onto the chromosome.

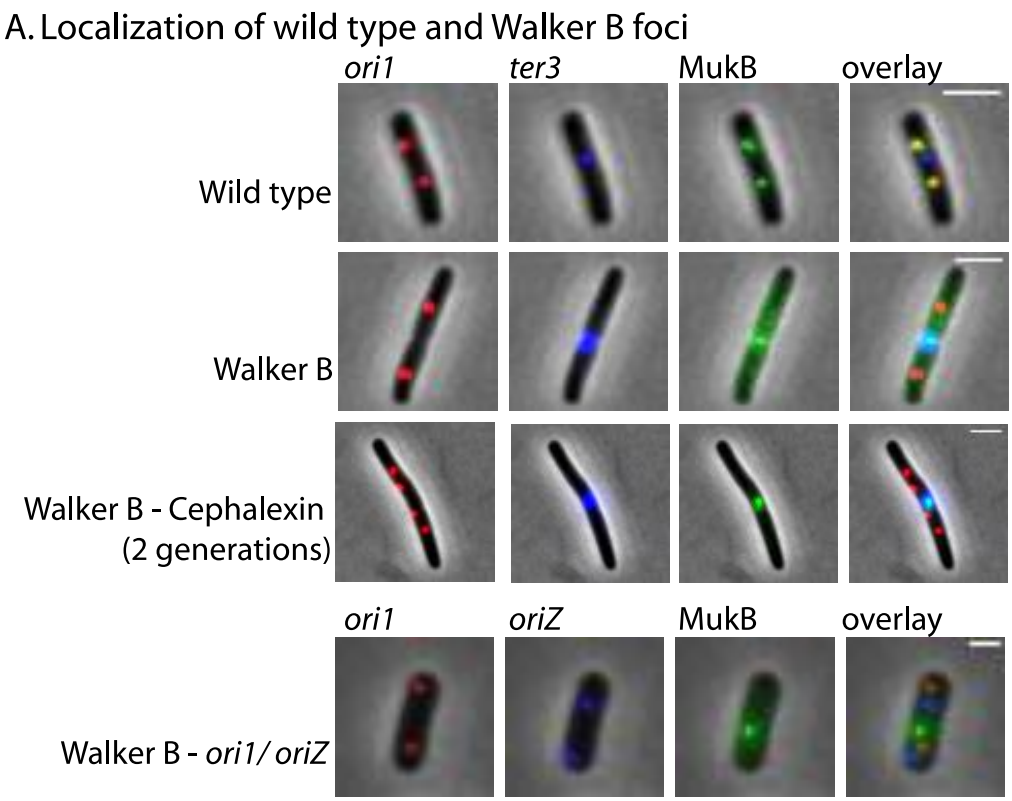

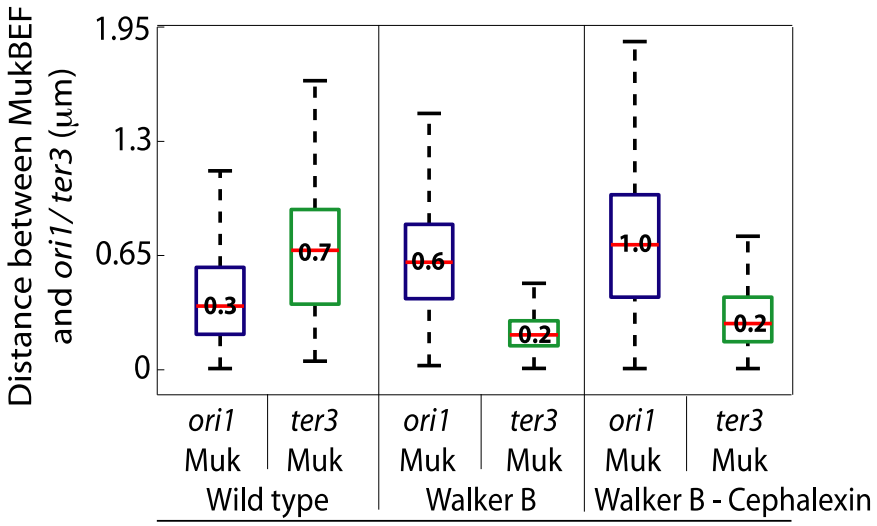

Fig 3.9: Walker B MukBEF foci are *ter* associated

A. While wild type MukBEF foci colocalize with *ori1* (first panel), Walker B foci colocalized with *ter3* (bottom three panels). *ter3* association did not change in cells blocked for cell division/ FtsK translocation (cephalexin treated) or in cells carrying a chromosome with two origins of replication (*ori1/ oriZ).* Scale bar = 2μm

B. Distance of nearest MukBEF focus to *ori1* or *ter3* was measured in wild type and Walker B cells (with or without cephalexin). Median distance is represented inside the box. n>200

3.10 *ter* localization of MukBEF foci during MukE degradation

ter localization of MukBEF foci could also be seen independent of Walker B. Using the MukE degron system, loss of MukB foci over time was observed. As described earlier most cells had no foci or a single weak focus after 2hrs of degradation. Before degradation, median distance of the nearest MukBEF focus from *ori1* was ~330nm while the distance of the nearest focus from *ter* was 700nm. After 20 min of degradation, colocalization with *ori* was lost and a median distance of 200nm separated *ter* and MukBEF (Fig 3.10). This value did not change much over time with distances of 200nm, 260nm and 270nm after 40, 80 and 120 min respectively. 2hrs after degradation, distance of the nearest focus from *ori* was ~900nm. It is possible that degradation of MukE affects ATPase activity of MukB resulting in a “Walker B-like” phenotype. Indeed, *in vitro* studies have suggested that MukEF have a stimulatory effect on MukB ATPase activity (Chen et al. 2008). Furthermore, the linker region of MukF, which interacts with MukE, modulates MukB ATPase activity (Shin et al. 2009); hence loss of MukE could interfere with this activity of MukF. In either case, the loss of MukE could result in an ATPase deficient MukBEF complex, which has similar properties to Walker B MukBEF. Alternatively, it is possible that MukB foci observed upon MukE degradation could represent the “MukBEF loading complex”; complexes that begin to associate with the chromosome but are unable to relocate due to insufficient levels of MukE. It would be key to see whether the reintroduction of MukE in these conditions would permit the movement of MukBEF foci from *ter* to *ori*. Indeed, both of the above-described scenarios need not be independent of each other and *ter* may represent the region for MukBEF loading (in wild type and Walker B).

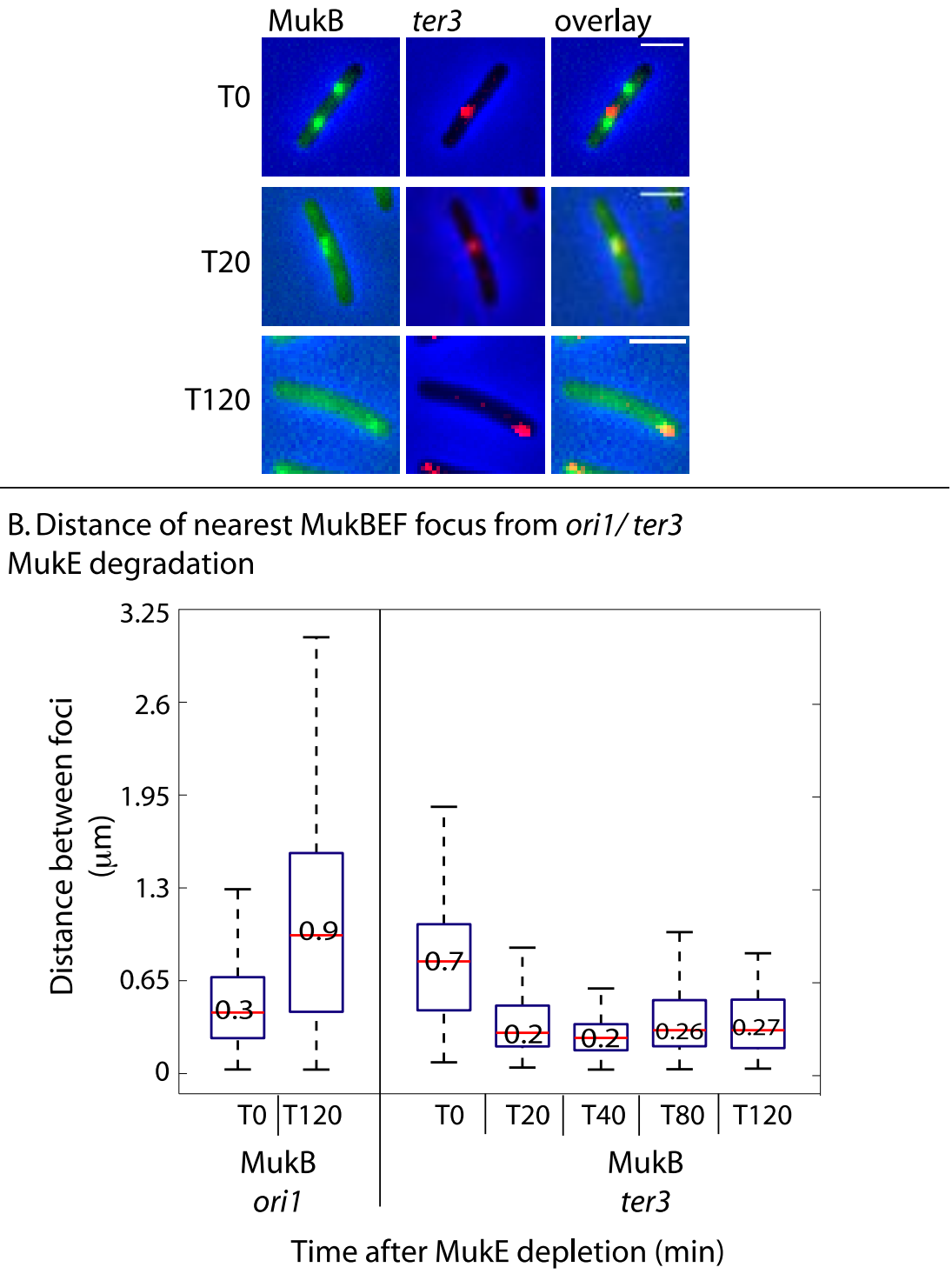

Fig 3.10: MukBEF foci become *ter* associated upon MukE degradation

A. MukBEF foci were followed 20, 40, 80 and 120 min after MukE degradation (using the MukE-degron system; see Chapter2). MukE degradation led to localization of weak foci with the terminus (see T20, T120). Scale bar = 2µm

B. Distance of nearest MukBEF focus from *ori1* or *ter3* was measured before (T0) and after (T20, T40, T80 and T120) MukE degradation. Median distance is represented inside the box. n>200

3.11 Summary

Stoichiometry experiments suggest that active MukBEF may be ATP bound with a ratio of 4:4:2, with ~10±4 such complexes per focus. An ATP binding MukB mutant failed to form foci, while an ATP hydrolysis mutant formed foci (both mutants were non-functional). However, in contrast to wild type, the Walker B mutant tended to form a single, *ter*-associated focus. ~16 Walker B MukBEF complexes were present in a focus with a ratio of 4:4:2 MukB:E:F. Hence, ATP binding is essential for focus formation, while ATP hydrolysis is required for focus dynamics and function. Finally, MukBEF foci also became *ter* associated when MukE was rapidly degraded from the cell. Based on this, one model is that MukBEF complexes load at *ter* in an ATP dependent manner. While MukBEF complexes form independent of ATP binding, hydrolysis may be required for the dynamic relocation of foci to the origin. Finally, wild type complexes are ATP bound in foci. ATP hydrolysis could aid in opening the MukBEF ring to permit entrapment of DNA within it. It is important to understand the mechanism by which Walker B MukBEF associates with *ter*. *ter* association has not been seen in wild type cells possibly due to the transient nature of loading and migration of MukBEF. Time-lapse experiments with the repletion system might capture the possible loading of MukBEF at *ter*. ChIP experiments with Walker B are important test sequence specific association. It is also essential to test proteins that have *ter* specific activity, such as FtsK, TopoIV or MatP, which could recruit Walker B to *ter*. MatP does not seem to play a role in this, as Walker B foci form even in cells deleted for MatP (data not shown).

3.12 Discussion

3.12.1 Towards an understanding of the active MukBEF complex

Much insight gained into the mechanism of action of SMC complexes has been *in vitro* (reviewed in Nasmyth and Haering 2005; Cuylen and Haering 2011; Gruber 2011). It must be remembered though, that, typically, such studies utilize vast excess of protein or do not use the SMC holocomplex. Moreover, the ratios of each component of the complex may be sub-optimal when compared to that in the cell. These studies are also carried out outside the cellular environment and may lack the presence of other factors that may modulate SMC activity in the cell. Furthermore, “bulk experiments” take into account the average behaviour of proteins; their true nature in the cell may be more stochastic. Hence the *in vivo* significance of MukBEF properties such as ATPase activity or DNA binding ability remains to be established. Recent advances in genetics and microscopy have allowed visualization of proteins with single molecule sensitivity in living cells as well as track their dynamic behaviour over short and long timescales (Leake 2010; Li and Xie 2011). Thus, questions about number of active molecules, their conformation/ stoichiometry in multi-protein complexes and their dynamics can now be addressed in the cell’s physiological environment.

3.12.2 Few MukBEF complexes are present in a focus

Using slimfield microscopy, stoichiometry of MukBEF complexes in foci was determined. Current data suggest that only 19-21 (±10)% of MukBEF molecules are present in foci in a cell. Indeed, transient (3ms) interactions of complexes with a static structure like the chromosome can be captured in these

experiments. Such events were rarely recorded (for wild type MukBEF), suggesting that only molecules present in foci were associated with the chromosome stably. It is interesting to note that this is in contrast to *in vitro* studies that required excess protein for detectable compaction of DNA (Strick et al. 2004; Petrushenko et al. 2006a). Indeed, total protein in the bacterial cell is also limited; hence the possibility of having a 100:1 condensin:DNA is unlikely *in vivo.* Whether the action of MukBEF complexes in foci is directed locally (around the origin) or globally is uncertain. Due to change in DAPI staining upon MukE degradation (chapter 2), it is tempting to suggest that the action of few Muk complexes in foci may globally structure the chromosome.

3.12.3 ATPase activity modulates MukBEF focus formation and function

Structural studies have suggested that MukEF (4:2) complex binds one MukB dimer in the absence of ATP (to give a 2:4:2 MukBEF complex). The binding of ATP to MukB displaces one MukEF (2:1) complex resulting in a 2:2:1 MukBEF complex (Woo et al. 2009). Based on the above, stoichiometry data suggest that MukBEF complexes may be ATP bound in foci (ratio of 2:2:1).

In vitro ScpAB inhibit *Bs*SMC ATPase while MukEF stimulate MukB ATPase activity (Hirano and Hirano 2004; Chen et al. 2008). ATPase activity is essential for condensation activity of the complexes (Hirano and Hirano 2004; Chen et al. 2008). It has been proposed that ATP binding engages *Bs*SMC heads and stabilizes its interaction with DNA, while ATP hydrolysis results in its release from DNA. Hence, the binding of ScpAB to SMC may help stabilize it on DNA (Hirano and Hirano 2004; reviewed in Hirano 2006). Similar conclusions have recently been reported in *C. crescentus* as well (Schwartz and Shapiro 2011). *In vitro* MukBEF 2:2:1 complexes form more readily than 2:4:2 complexes

(Petrushenko et al. 2006b). 2:2:1 complexes are also more proficient in DNA bridging (Petrushenko et al. 2010). Hence, it is possible that ATP bound MukBEF may be the active complex *in vitro* and *in vivo.*

Consistent with the above, ATPase activity was essential for MukBEF function *in vivo.* An ATP binding MukB mutant did not form foci, while a hydrolysis mutant (called WB MukB henceforth) formed foci (both mutants were *muk*$^{-}$). Hence, ATP binding seems to be essential for stable association with DNA (and focus formation), while hydrolysis is required for focus function. ATPase activity or complex forming ability of these mutants has not been tested *in vitro* (but is listed in future work). Stoichiometry experiments with Walker B MukBEF show that it also has a 2:2:1 MukB:E:F ratio.

Current data suggest that majority MukBEF molecules have a periodicity of 4:4:2 in foci. Structural and biochemical studies have shown that MukF readily forms a stable domain swapped dimer via its N terminus (Fennel-Fezzie et al. 2005; Woo et al. 2009; Gloyd et al. 2011). Hence, it is possible that two MukBEF (2:2:1) complexes interact with each other via the N-ter of MukF, resulting in a 4:4:2 complex. Although higher order complexes could be formed via MukE-MukE interaction (Gloyd et al. 2011), this may not be a prerequisite for function, as slimfield experiments would have also picked up higher periodicity as well.

3.12.4 Walker B MukBEF may represent the “loading complex”

Although the number of foci formed by wild type and WB MukBEF were different, the same % of molecules was present in foci per cell. Furthermore, while wild type foci localized around *ori*, Walker B foci colocalized with *ter*. This localization was independent of replication, cell division or FtsK activity.

Interestingly, depletion of MukE also led to the association of weak MukBEF foci with *ter*. One possibility is that Walker B represents the “loading complex”, which can bind ATP and stably load onto the chromosome; the process of ATP hydrolysis would drive focus relocation to the origin. This is similar to a recent study with yeast cohesin (Hu et al. 2011). They showed that SMC1/3 Walker B was capable of loading at centromeric regions but could not relocate to pericentric regions (where wild type cohesin is found). FRAP experiments revealed that the mutant was unstable on DNA. Previous studies have also shown that ATP binding was required for cohesin complex formation while hydrolysis was required for stable DNA association (Arumugam et al. 2003; Weitzer et al. 2003). This is in contrast to the current study where Walker B showed little or no recovery when compared to wild type MukBEF (data not shown). Furthermore, work done on *Bs*SMC and *Cc*SMC found that Walker B tended to be more stably associated with DNA (Hirano and Hirano 2004; Schwartz and Shapiro 2011). Despite the difference between cohesin and bacterial SMC, a conserved feature of the two is that ATP binding is required for association with DNA. It is possible that ATP hydrolysis could permit MukBEF ring opening and drive the relocation of MukBEF complexes to other regions of the chromosome. Finally, the rebinding of ATP to MukB could stabilize the complex at its final location (Fig 3.11).

It is interesting to note that the loading site of cohesin is different from its site of action. It has been proposed that the reason why cohesin has not been found at its loading site could be due the transient nature of loading and translocation (Hu et al. 2011); the Walker B mutant allows the capture of such an event. It is tempting to extend a similar argument to MukBEF. It could be possible that wild

type MukBEF loads at the terminus and relocates to other regions of the chromosome. This process may be transient. The Walker B mutant however, is unable to relocate from its site of action due to the inability to hydrolyse ATP; and hence remains in a locked state at the loading site. Unlike passive translocation of cohesin, it is possible that the relocation of MukBEF is more active and involves its association with distant regions of the chromosome. This could also aid in MukBEF mediated chromosome organization/ segregation. Current data suggests that the minimal functional unit of the complex is 4:4:2 MukBEF. One possibility is that, while one MukBEF 2:2:1 complex associates with the terminus, the second is free to associate with another region of the chromosome. This process of "walking" could assist in the relocation of MukBEF complexes.

Another model for MukBEF focus position is based on the ParAB system (as described in Chapter 2). In either case, it is key to determine whether the initial loading of MukBEF on the chromosome is sequence driven.

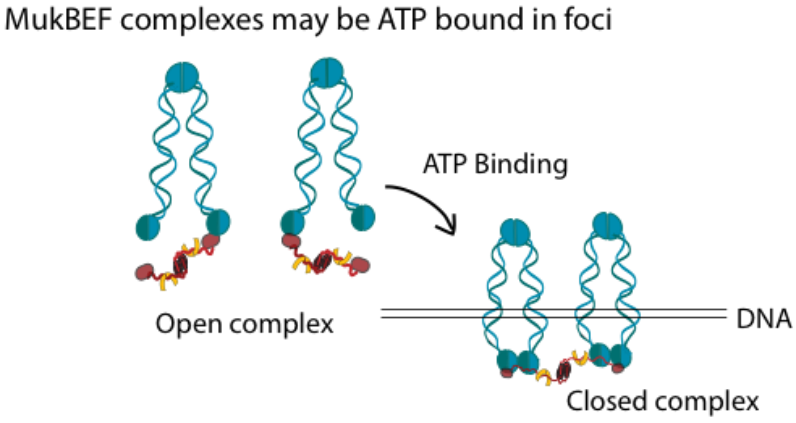

Fig 3.11: Stoichiometry experiments suggest that MukBEF complexes may be ATP bound in foci with a ratio of 4:4:2 (MukB:E:F) (MukB: blue, MukF: red, MukE: yellow). One possibility is that ATP hydrolysis may allow the opening of the MukBEF ring to permit the complex to load onto or come off DNA.

CHAPTER 4

Conclusions

4.1 Conclusions

DNA is packaged into a space within cells that is thousand fold shorter than its length. These highly compacted molecules are also faithfully replicated and segregated into daughter cells. Thus life is maintained and propagated in an extremely limited space at a very fast pace. More than 50 years after the structure of DNA was solved, the method of chromosome organization and segregation remains a mystery. *In vitro* and *in vivo* studies have revealed that the bacterial chromosome is highly organized at the sequence level as well as into topological domains (reviewed in Higgins et al. 2010). Recent studies have shown that the *E. coli* chromosome is also spatially organized with regions close to the origin occupying the centre of the cell and the two replichores positioned on either side of it; DNA sequentially segregates as it is replicated and the above-described organization is recapitulated in the daughter cells (Wang et al. 2006). It is thought that replication plays a key role in spatial organization of the chromosome (Reyes-Lamothe et al. 2008b).

Indeed, genetic studies have shed light on an essential class of proteins involved in chromosome dynamics in all domains of life, the SMC complex (reviewed in Nasmyth and Haering 2005). Despite the immense work done on SMCs, their mechanism of action is still elusive. The field of eukaryotic SMCs has progressed at a fast pace, with the discovery of various dynamic roles the complex plays in the cell. However, eukaryotic model systems have faced limitations of assays and manipulation techniques in the past. While most work done on bacterial SMCs has been *in vitro*, only recent developments in genetic and microscopy techniques have allowed the incisive *in vivo* work with them. Hence, their mode of action in the cell is still unclear.

The aim of this work was to study the role the SMC complex, MukBEF, in *E. coli* chromosome organization and segregation. Current work has highlighted a fundamental role of MukBEF in spatial organization of the chromosome:

a. The degron system was developed to rapidly ablate Muk protein from live cells to observe it effects on spatial chromosome organization.
b. Degradation of MukE resulted in loss of wild type spatial chromosome organization independent of replication. MukBEF could also regenerate wild type position of chromosomal loci independent of replication.
c. MukBEF may also be required to maintain chromosome structure as the degradation of MukE led to a change in nucleoid morphology.
d. These data suggest that MukBEF plays a fundamental role in spatial organization of chromosomes seen in wild type *E. coli* independent of cell cycle.
e. MukBEF foci may represent “centres of activity” of the complex as reorganization of the chromosome was preceded by MukBEF focus formation. While foci displayed *ori* proximal localization finally, their initial position was distant from the origin. Thus, colocalization of MukBEF foci with the origin may not be absolute and the nucleation site of MukBEF may be different from the origin.
f. Wild type MukBEF complexes may be ATP bound in foci with an absolute ratio of 4:4:2 (MukB:E:F). Only few MukBEF complexes (~19% of total protein) are present in foci. These data suggest that formation of higher order complexes may not be a prerequisite for MukBEF function.
g. While ATP binding was required for MukBEF focus formation, an ATP hydrolysis mutant of MukB formed foci, but was *muk*$^{-}$.

h. An ATP hydrolysis mutant formed a single *ter* associated focus with a ratio of 4:4:2 MukB:E:F. The same percentage of MukBEF (as wild type) was recruited into these foci. This may represent the MukBEF loading complex that loads at *ter*. ATP hydrolysis could allow the formation of multiple foci that localize around *ori*.

In vitro studies have suggested that the condensin complex can reshape DNA. Condensin could also cluster on DNA and compact it (reviewed in Graumann and Knust 2009). However, these reactions require excess protein. Indeed, protein levels are limiting in the bacterial cell, and the formation of foci suggests that complexes may instead act in concentrated centres on the chromosome (Danilova et al. 2007; Gruber and Errington 2009; Sullivan et al. 2009). A recent study has suggested that condensin forms rings around DNA molecules and topologically entraps them (Cuylen et al. 2011). Taken together, a possible model is where few active MukBEF complexes organize the chromosome in concentrated centres, by linking distant regions of the chromosome inside ring-like structures. This activity would be required throughout the cell cycle to maintain rigidity/ structure of the chromosome, which would also aid in its faithful segregation. Indeed, it is possible that the binding of ATP to MukB heads stabilizes MukBEF action on DNA hence, the complexes may be ATP bound in foci. Finally, preliminary FRAP data also suggests that MukBEF molecules are dynamic (with a half recovery of 30sec) and this requires ATP hydrolysis. One possibility is that ATP hydrolysis could aid in the unbinding/ opening of the MukBEF ring, thus allowing it to come off DNA. Since some properties of MukBEF bear resemblance to its eukaryotic counterparts, it is tempting to suggest that condensin complexes in other organisms may also be

ATP bound, highlighting the *in vivo* significance of conservation of ATPase activity of SMC proteins. With the development of high-resolution microscopy, estimating stoichiometry of SMC complexes in other organisms would be key to understanding their mechanism of action.

4.2 Future directions

While the tools developed in this study provide a powerful way to investigate the role of MukBEF in chromosome organization and segregation *in vivo,* current data has also raised more questions about the function of these complexes in the cell.

Detailed map of chromosome organization in *muk*$^{-}$ cells

It would be important to test other chromosomal markers during Muk degradation/ repletion along with time-lapse to gain more temporal insight into MukBEF mediated spatial chromosome reorganization. In order to confirm the change in nucleoid morphology upon Muk depletion, other nucleoid markers could be used.

Towards a better understanding of *E. coli* chromosome organization

Several nucleoid-associated proteins play a significant role in chromosome condensation. Indeed, double deletion of HU and Muk is synthetically lethal (Hiraga 2000). However, the reason for this is unclear. MukBEF is also known to interact with TopoIV. The *in vivo* significance of this interaction is unclear. Hence the degron system could be used to test the effect of rapid loss of two or more of these proteins on chromosome organization and segregation.

Where does MukBEF load on the chromosome?

Current data suggests that the loading site for MukBEF could be the terminus. *ter* association has probably not been seen in wild type cells due to the transient nature of loading and migration of MukBEF to *ori*. Time-lapse experiments using the repletion system could allow the observation of such an event. Furthermore, in order to test the possibility of sequence specific loading, ChIP experiments with Walker B MukBEF are key, in combination with visualizing Walker B foci in *E. coli* cells carrying a chromosome deleted for regions of *ter* (Hill et al. 1987).

Understanding the dynamic nature of MukBEF complexes in foci

Previous studies have reported dynamic interaction of condensin with mitotic chromosomes (Gerlich et al. 2006; Oliveira et al. 2007). Preliminary FRAP experiments have suggested that MukBEF complexes in foci are also dynamic. Furthermore, ATP hydrolysis activity seems to be important for this dynamics. However, more experiments and analysis need to be done to confirm the same.

Dissecting the architecture of a MukBEF focus

While *in vivo* stoichiometry experiments suggest that MukBEF complexes may be ATP bound in foci with a stoichiometry of 4:4:2, *in vitro* gel filtration could be performed to test the robustness of these results. Finally, super-resolution imaging (like PALM) with MukBEF complexes carrying fluorescently tagged MukB hinge and head would provide a powerful tool to study the size, shape and arrangement of these complexes in a focus *in vivo*.

CHAPTER 5

Materials and Methods

5.1 Bacterial strains and growth conditions

All cloning was done in *E. coli* strain DH5α. For microscopy, all strains were constructed in K12 derivative, AB1157 (Bachmann 1972). A list of strains/ plasmids used for this work is provided in Table 5.1.

Cells were normally grown at 37°C either in LB or M9 (10XM9 salt solution consisted of 63g Na_2HPO_4, 30g KH_2PO_4, 5g NaCl and 10g NH_4Cl) minimal media supplemented with 100 mg/ml of threonine, leucine, proline, histidine and arginine, 0.5 mg/ml of thiamine, 0.1% 1M $MgSO_4$, 0.1% 100mM $CaCl_2$ and 0.2% of glycerol as carbon source. When needed, ampicillin was used at a final concentration of 100mg/ml, kanamycin at 30mg/ml, 15mg/ml gentamycin, chloramphenicol at 25mg/ml, 10mg/ml tetracycline, 0.4 mM IPTG and 100ng/ml anhydrotetracylcine. *muk*$^{-}$ cells were grown at 22°C for 4 days on plates or for 2 days in liquid medium.

Induction of genes expressed from an arabinose inducible promoter both in the chromosome or from a plasmid (pBAD24) (Guzman et al. 1995) was done by addition of 0.2-0.5% arabinose and inhibited with 0.5-1% glucose.

5.2 DNA transformations

For heat-shock transformation, 50ml of cell culture was grown in LB till OD_{600} of ~0.4. Cultures were centrifuged at 4,000rpm for 10 min at 4^{o}C, washed with 20 ml of TFBI buffer (30 mM potassium acetate pH 5.8, 100 mM RbCl, 10mM $CaCl_2$, 50 mM $MnCl_2$, 15% glycerol), centrifuged once more (at 4°C) and resuspended in 1 ml of TFBII buffer (10 MOPS pH 6.8, 75 mM $CaCl_2$, 10 mM RbCl, 15% Glycerol). For heat-shock, cells were incubated with DNA for 10 min on ice, transferred to 42^{o}C for 2 min and transferred to ice for 10 min. Cells were allowed to recover and selected on plates with appropriate antibiotic.

For electro-competent cells required for λ-Red recombination, an overnight culture of cells carrying pKD46 was sub-cultured in 50 ml LB with ampicilin and 0.2% arabinose at 30°C until they reached an OD_{600} ~0.6. Cells were then washed with 50 μl of cold milli-Q water twice, with 25 ml of milli-Q water once, and resuspended in 0.5 ml milli-Q water. Electroporation was carried out by mixing DNA with 50ml of competent cells in cuvettes with 0.2 cm spacing and a 2.5 kV pulse followed by recovery in 2 YT for at least 1hr.

5.3 Transduction

Preparation of P1 lysate

$CaCl_2$ (final concentration 5mM) was added to 300μl of an overnight culture of desired strain (in LB) and 50-100μl of P1 lysate prepared in the parental strain (AB1157 in most cases) was added to the above. The cells were incubated for 15 min at 37°C, transferred to a tube with 5 ml of LB with $CaCl_2$ (final concentration 5mM) and incubated at 37°C until lysis was observed (~4-6hrs).

Transduction

For transduction, $CaCl_2$ to a final concentration of 5mM was added to 1 ml of an overnight culture and concentrated 10 times (by spinning down at 10krpm for 1min). 10μl of P1 lysate prepared in the donor strain was added to the above and incubated at 37°C for 15min. This was then washed with 1 ml Phage Buffer (100 mM Na_2HPO_4, 22 mM KH_2PO_4, 85 mM NaCl, 1 mM $MgSO_4$, 0.1 mM $CaCl_2$, 0.001% gelatine), resuspended in 1 ml of LB and incubated at 37°C for at least 1hr before plating. In some cases, sodium citrate (final concentration 7.5-10mM) was added to the culture/ plates.

5.4 λ-Red recombination

Oligonucleotides used had a 50 nucleotide complementary sequence to the last 50 base pairs of the gene (not including the stop codon) or 50 base pairs downstream, followed by 20 nucleotides complementary to a 11 aa linker or the end of the kanamycin/ chloramphenicol resistance cassette in the plasmid respectively. Polymerase chain reaction (PCR) was done using pRod60-64 plasmids (Reyes-Lamothe et al. 2008a) as template (these plasmids carried a 11aa linker followed by mYPet or DAS-4tag and an antibiotic resistance cassette). DNA fragment was gel purified and 1μg was electrotransformed into AB1157 cells overexpressing λ-Red proteins from pKD46 (Datsenko and Wanner 2000). Cells were selected on plates with appropriate antibiotic and insertion into the chromosome was checked by PCR.

5.4.1 Construction of chromosomal mYPet fusions

The MukB and MukE strains were constructed in the chromosome at the original location of the genes by the above-described process of λ-Red recombination (Datsenko and Wanner 2000). Primers used to construct *mukB-mYPet* were Forward 5'- AAC TCC CTG AAA CGC TTC CAG GAA CTG ACG AAG CGC CTT CTC AGG CGA GTT CGG CTG GCT CCG CTG C -3' Reverse: 5'- GA AAC GGA GTT TTC GGA AAA AGA AAA GGC GGC ATT GCT GCC GCC TTA ATT CTT ATG AAT ATC CTC CTT AGT TC- 3'

mukE-mYPet Forward: 5' - AAC TCA ACG ATG AAA CCG AAG AGA ATC AGC CAG ATA GCG GAG AGG AAG AAT CGG CTG GCT CCG CTG C -3' Reverse: GTT CCA GTT AAT CAG CGT CAG TGA GCG AAA TTT ACC GCG TTC AAT CAT TAC TTA TGA ATA TCC TCC TTA GTT C- 3'.

For MukF, an N-terminal fusion was constructed using the following primers: 5'-GTT ATA TTC ATG TCA CCG CGC GCA AAC CGC AGA GCA AGG ATA AAG TAT GA T GTA GGC TGG AGC TGC TTC G – 3' Reverse: 5' – TTT CTG GCC CAG GCA ACC AGT TCG GGG ACT GTC TGG GAA AAT TCA CTC AT CGC GCT GCC AGA ACC AGC – 3'

5.4.2 Construction of MukE-degron

Above described λ-Red recombination strategy to construct *mukE-mYPet* was used to construct *mukE* fused to 1X*c-Myc* tag followed by the DAS+4-degron tag (GCA GCG AAT GAC GAA AAT TAT TCC GAA AAC TAT GCA GAC GCG AGC). The plasmid carrying a 6 amino acid linker (A AGG AGC TCG GCT GGC TCC GCT GCT) followed by 1X c-Myc (GAA CAA AAA CTC ATC TCA GAA GAG GAT CTG) and the degron tag was constructed by Rodrigo Reyes-Lamothe and used in (Reyes-Lamothe et al. 2010). The plasmid also carried a kanamycin resistance cassette, flanked by *frt* sites. Primers used to construct *mukE-mYPet* were used to amplify the integration product. λ-Red recombination was carried out in an AB1157 strain deleted for *sspB* and carrying the plasmid pKD46. After fusion of the degron tag to the C-terminus of *mukE*, the fusion was transduced into a strain deleted for *sspB* at the endogenous gene locus, but with an arabinose inducible copy at an ectopic locus on the chromosome. In some cases, a pBAD plasmid carrying *sspB* was transformed into the strain for overexpression of *sspB*. Strains were checked for loss of viability by streaking on plates with 0.2% arabinose.

5.4.3 Construction of MukF-repletion system

Strain carrying the MukF-repletion system has been described previously (Sivanathan et al. 2009). Similarly, the strain was constructed as follows:

An ectopic copy of *mukF::frt* under the *Para* promoter was introduced at the *argE* locus in AB1157. This was then transduced into an AB1157 strain carrying a deletion of *mukF* (replaced by kanamycin) in the operon (described in Yamazoe et al. 1999). Strains were checked for temperature sensitivity by streaking out a single colony on plates containing 0.5% glucose.

5.4.4 Construction of Walker B mutants

Using the primers (Forward 5'- AAC GTA TCG TTT GGT CAG G-3'; Reverse 5'- TT GAG ATT CGA TTT GCG TGC-3') the 3' end of *mukB* fused to GFP::Cm or mYPet::Kn (1175 bp without the fusion and antibiotic cassette) was amplified and cloned into a pGemT vector (Promega cat.no A1360). Site directed mutagenesis was carried out on the resultant plasmid to introduce the D1406A mutation using the primer set: Forward 5'- T GCT GTT CCT CGC TGA AGC AGC GCG –3'; Reverse 5'- CGC GCT GCT TCA GCG AGG AAC AGC A –3'

Or the E1407Q mutation using the primer set: Forward 5'- CTG CTG TTC CTC GAT CAG GCA GCG CGA CTG GAT -3'; Reverse 5'- ATC CAG TCG CGC TGC CTG ATC GAG GAA CAG CAG -3' Insertion of the mutation was checked by sequencing. The fragment was then reintroduced into the chromosome (at the endogenous locus) by the process of λ-Red recombination using the following primers: Forward 5'- AAC GTA TCG TTT GGT CAG G-3'; Reverse 5'- TT GAG ATT CGA TTT GCG TGC-3'. Insertion was checked by assaying temperature sensitivity and by sequencing/ PCR.

5.5 Fluorescence Repressor-Operator binding System (FROS)

The fluorescence repressor-operator system (FROS) developed in the lab (Lau et al. 2003) was used to visualize regions of the chromosome. The system consists of two components: the operator arrays, which are 240 tandem repeats of *lacO or tetO* operator sites inserted at various locations on the chromosome and the fluorescent repressors (LacI or TetR fused to a fluorescent protein) expressed from a plasmid or the chromosome (Wang et al. 2005b; Reyes-Lamothe et al. 2008a). Arrays inserted 15 kb left (*ori1*) of the origin (*oriC*), at position (366) marking *R2* and *L3-R3* at positions (2269) and (872) respectively were used (Fig 2.2E).

5.6 Blocking DNA replication

In order to study non-replicating cells, the depletion/ repletion systems were combined with a *dnaC2* or *dnaA46* mutation. The *dnaC2ts* strain carries a temperature sensitive mutation in DnaC, the helicase loader protein, while *dnaA46* is a temperature sensitive DnaA (replication initiator protein) mutant (Withers and Bernander 1998). These strains can complete replication but not reinitiate new rounds of replication at non-permissive temperature (37°C or 42°C). Thus, at non-permissive temperature, most cells should have a single copy of their chromosome. Cell growth, on the other hand, is not prevented.

5.7 Microscopy

For snapshot experiments, cells were grown in LB (till stationary phase) and subcultured overnight in M9-gly. The following day, cells were subcultured in fresh media and grown till OD 0.05-0.15 before imaging. For induction, 0.2% arabinose was added to 1-2hrs before visualization and for repression 0.5%

glucose was added to over night and subcultures. Cells were concentrated and laid on a 1 % agarose pad on a slide. Nucleoid was visualized using a final concentration of 1 mg/ml 4',6-Diamidino-2-phenylindole (DAPI).

For time-lapse, cells were treated as before but were laid on an M9-Gly 1% agarose pad (with a humidity chamber). Temperature of 30, 37 or 42^{o}C was maintained throughout the experiment. Pictures were taken every 5 or 10 min.

Cells were visualized with a 100x objective on a Nikon Eclipse TE2000-U microscope, equipped with a Photometrics Cool-SNAP HQ CCD camera. Images were taken and processed by Metamorph 6.2. Image analysis was done using ImageJ or MicrobeTracker (Sliusarenko et al. 2011) run in Matlab.

For stoichiometry experiments, cells and slides were prepared as for time-lapse experiments. Imaging was done at room temperature. The slimfield setup has been described previously (Reyes-Lamothe et al. 2010) and consists of a home-built inverted TIRF microscope, using epifluorescence illumination with an excitation wavelength of 532nm (mYPet), 473nm (GFP) or 561nm (mCherry). In case of two-colour imaging, a splitter was placed before the camera and filters compatible with 473nm (for GFP) and 561nm (for mCherry) were used. The calibration for the 532nm experiments was done by injecting pure YPet into a 10μl flow cell with anti-GFP antibodies coating the coverslip and 100nm beads to find the focusing plane (as described in Reyes-Lamothe et al. 2010). Similar calibration was carried out using pure mCherry or GFP. Fluorescence emission was imaged at 50 nm per pixel in frame-transfer mode at 1 Hz by a 128 x 128-pixel, cooled, back-thinned electron-multiplying charge-coupled device camera (iXon DV860-BI, Andor Technology). Images were taken every 3msec till total bleaching (about 300 frames).

For FRAP experiments, cells and slides were prepared as for time-lapse experiments. Imaging was done at room temperature. Imaging was performed using a wide-field spinning disk imaging system (PerkinElmer) and 100X objective. Images were acquired using Volocity imaging software. FRAP was performed by pulse-bleaching using a 488nm laser for 10-15ms and 6-15% laser intensity (diameter of the spot was diffraction limited ~300nm). 2 pre-bleach images were taken, bleach spot was centered on one Muk focus and recovery of bleached region was recorded every 15 sec after bleaching for 3 min. Image capture was done at a 300msec frame rate (4-6% 532nm laser).

5.7.1 MukE degradation experiment in replication blocked cells

Cells were grown in M9-gly at 30°C (to ensure non-overlapping replication cycles) till OD_{600} of 0.05. Cells were shifted to 37°C for 2 hrs. At the end of 2hrs control sample (T0) was collected and 0.5% arabinose was added to the culture at 37°C. Samples were collected 1hr (T60) or 2hrs (T120) after arabinose induction. All samples were spun down immediately at 37°C, spotted on a pre-warmed slide and imaged at 37°C under the microscope. This ensured that no new replication initiation occurred during the process of imaging.

5.7.2 MukF repletion experiment in replication blocked cells

Cells were grown in M9-gly at 30°C overnight; hence the cells should be *muk*$^{-}$. A dilution of the overnight culture was made into M9-gly and grown till OD_{600} of 0.05. Cells were shifted to 37°C (for *dnaC2ts)* or 42°C (for *dnaA46ts)* for 2 hrs. Sample of cells (T0) before adding 0.5% arabinose to the culture was taken. Samples were also taken 20, 40, 60 and 120 min after arabinose addition. All samples were spun down at 37°C or 42°C, spotted on a pre-warmed slide and

imaged at restrictive temperature under the microscope. For time-lapse experiments, the same experimental setup was followed, but no arabinose was added to the culture. Instead, cells were spotted onto a time-lapse slide containing 0.5% arabinose. All imaging was done at 37°C. Images were taken every 5 minutes for 90 minutes.

5.8 Image analysis

ImageJ

In order to estimate the positions of chromosomal loci, the point picker plugin of ImageJ was used. In cells with two copies of each locus, the (x,y) coordinates for the two cell poles and for the two loci were marked. From these, the absolute distances (in nm) of two loci from each cell pole as well as the relative distances, expressed as percentage of cell length was estimated. As a rule, cell pole farthest to the two loci was marked as the first pole (0%) and the opposite pole was marked as the end of the cell (100%). The average position and standard deviation (expressed as % cell length) was plotted for each locus. Sister Chromatid Distance or SCD was expressed as the average distance (% cell length) between the two sister loci in the same cell.

In cells with a single copy of each locus, the position of the locus was marked with respect to nucleoid pole. The nucleoid was divided into three categories: nucleoid middle (40-60% of nucleoid length), nucleoid quarter (60-80% of nucleoid length) and nucleoid edge (80-100% of nucleoid length). As a rule the pole farthest to the locus was marked as the first pole (0%) and the nearest pole as the end of the nucleoid (100%). Hence, no loci were present in the 0-40% half of the nucleoid. Interfocal distance (IFD) was calculated similar to sister chromatid distance (expressed as % nucleoid length).

FRAP

Images were analyzed using ImageJ (bundle developed by MacBiophotonics). In brief, background was subtracted, a region of interested (ROI) was drawn around the bleached/ control spot and a bigger ROI was drawn around the cell to measure total fluorescence and bleaching over time. Normalized intensity vs. time trace was generated using the FRAP profiler plugin:

normalized intensity at time t = $I_t = (Ib_t \div Ib_{max}) \div (Ic_t \div Ic_{max})$

Ibt= intensity of bleached ROI at time t.

Ict= intensity of whole cell at time t.

Stoichiometry determination

Analysis was done as described in Reyes-Lamothe et al. 2010. In brief, image files were read into custom-written analysis software (Lab View 7.1, National Instruments). Each file was frame averaged over ~50 frames (to give clear images of "regions of interest") and positions of these ROIs were detected. In non-frame averaged images, a counting code was used to calculate the intensity for individual ROIs in each image (for 100 frames). Spots detected for at least two consecutive frames were used for further analysis.

MicrobeTracker:

MicrobeTracker is a Matlab-based program written by (Sliusarenko et al. 2011). This package enables the automated/ semi-automated analysis of images for snapshots/ time-lapse. A range of functions (named in brackets) enabled automatic determination of number of foci per cell (SpotfinderZ), total fluorescence signal in each cell normalized to cell area (meaninthist), automated particle tracking in time-lapse (jointthespots), generation of

fluorescence profiles of DAPI stained nucleoids (intprofile) and automatic measurement of distance between two spots in a cell (colocalizespots).

5.9 Western Blot

Cells were grown in LB to an OD_{600} of ~0.5, centrifuged at 4 krpm for 10min at 4°C, resuspended in 90 □l of Cracking Buffer (50 mM Tris-HCl, pH 6.8, 100 mM dithiothreitol, 2% SDS, 0.1% bromphenol blue, and 10% glycerol) and stored at -80°C until further use. Samples were mixed with SDS loading buffer (250 mM TrisHCl pH 6.8, 10% SDS, 30% glycerol, 0.02% bromophenol blue, 0.5 mM DTT) and boiled for 10 minutes at 97°C before loading into an SDS-PAGE gel with a 5% or 10% acrylamide separation gel (for MukB or MukE/MukF respectively). Transfer was performed using the Invitrogen iBlot system with current passage for 7 minutes. Membrane was blocked with 5% milk (in PBS) overnight at 4°C. All washes were performed using PBS+0.1% tween for 5 minutes each (at room temperature). Blot was probed with primary antibody incubation at room temperature for 2hrs (1:3000 to 1:5000 dilution in 0.5% milk+PBST or 5ml Signal Boost solutionI (Thermoscientific cat no. 46640). After several washes in PBST, the blot was incubated with secondary antibody (1:5000 dilution in 0.5% milk+PBST or 5ml Signal Boost solutionII) for 1hr at room temperature. A list of primary and secondary antibodies used is described in Table 5.2. Immunoreactive bands were visualized on blots by using an enhanced chemiluminescence kit (ECL, Thermoscientific cat no. 32109).

Westerns were usually done using samples taken from rich media as minimal media samples produced multiple bands due to non-specific interactions of the antibody. Non-specific interactions could be avoided in LB as fewer genes are

transcribed in rich media (at a higher rate) than minimal media, where transcription of many genes is required.

5.10 Strains/ plasmids used in present study

Strain name	Description	Ref
Depletion/ Repletion		
Ab20	*mukE*-degron:kn, Δ*sspB*, Para *sspB*	This study
Ab20(b)	*mukE*-degron:frt, Δ*sspB*, Para *sspB*	
Ab28	Ab20, *mukB*-GFP:Cm	
Ab64	Ab20(b), lacO@*ori1* (Kn), *dnaC2ts* (Tet)	
Ab68	Ab64, pWX17 (Amp)	
AB76	Ab20(b), tetO@*R3* (Gn)	
AB77	Ab76, lacO@*L2* (Kn)	
Ab79	Ab77, pWX6 (Amp)	
Ab82	Ab77, *dnaC2ts* (Tet)	
AB87	Ab82, pWX6 (Amp)	
AB83	Ab20(b), *mukBmYPet*:kn	
AB86	Ab83, tetO@*ori1* (Gn)	
Ab91	Ab86, pWX9 (Amp)	
Ab168	WX(Δ*mukF*:Kn, Para*mukF*:frt), tetO@*ori1*, PlacI*tetR*:frt, *dnaC2ts* (Tet)	
Ab174(B)	Ab168, *mukB*-GFP (Cm)	
Ab229	Δ*mukF*, Para*mukF,* WX314, *dnaA46*	
Ab233	Δ*mukF*, *mukB*-GFP:Cm	
Stoichiometry		
Ab16	*mukB*-mYPet:Kn	
Ab18	*mukE*-mYPet:Kn	
Ab25	*mukB*-mCherry:frt, *mukE*-mYPet:Kn	
Ab24	*mukB*-mCherry:Kn	
Ab34	*mukE*-mYPet:kn, lacO@*ori1*, PdnaA*lacI*:Cm	
Ab59	Kn:N-mYPet-*mukF*	
Ab60	frt:mYPet-*mukF*	
Ab75	*mukB*-E1407Q-GFP:Cm	
Ab81	Ab60, *mukB*mCherry:Cm	
Ab88	*mukE*-mCherry:frt	
Ab119	RRL48 (*ori1*), Ab75	
Ab124	RRL6-53 (*ori1*, *ter3*), Ab75	
Ab137	Ab88, Ab75	
Ab142	RRL6-53, *mukE*-mYPet:Kn	
Ab145	WX332 (*ori1*, *oriZ*), Ab75	
Ab170	Δ*matP*:frt, Ab75	
Ab191	Kn:N-mCherry-*mukF*	
Ab191	frt:N-mCherry-*mukF*	
Ab198	*mukB*-E1407Q-mYPet:Kn	
Ab213	*mukB*-E1407Q:Kn, Ab60	
Ab220	*mukB*-GFP:Cm, Ab88	
Ab221	*mukB*-GFP:Cm, Ab192	
Ab223	*mukB*-E1407Q:Kn, MukE-mYPet:frt	

Others

RRL126	*ori1tetRdnacTS*	Reyes-Lamothe
RRL80	*mukB*-D1406A-GFP:Cm	Reyes-Lamothe
Kat1	*mukB*-GFP:Cm	Ohsumi et al. 2001
RRL48	tetO@*ori1*, PLacI*terR*-mCeruleon	Reyes-Lamothe
RRL6-53	lacO@*ori1*, teto@*ter3*, PdnaA*lacI*-mCherry, PlacI*tetR*-mCerulean	Reyes-Lamothe
RRL184	Δ*sspB*:frt, Para *sspB*:frt	Reyes-Lamothe
WX332	*ori1*, *oriZ*	Wang et al. 2011
OX28	Ab20(b), lacO@*ori1* (Kn)	Christian Lesterin
OX36	Ab20(b), lacO@*LacZ* (Kn)	Christian Lesterin
WX156	Δ*matP*:frt	Xindan Wang
Plasmid	**Description**	**Ref**
AB38	pGEM-T, *mukB3'*-GFP-Cm(E1407Q)	This study
AB41	pBAD24, *sspB*	
AB46	puc18, Kn, N-mCherry	
AB52	pGEM-T, *mukB3*'-mYPet-Kn(E1407Q)	
AB53	pGEM-T, *mukB3'*-Kn(E1407Q)	
pWX6	pBR322 *ori*, pftski-*lacI*-cfp, *tetR*-yfp	Wang et al. 2005
pWX17	pBR322 *ori*,p ftski-*lacI*-cfp	Wang et al. 2005
pWX9	pBR322 *ori*, pftski-*tetR*-cfp	Wang et al. 2005
pRod36	pGEM-T, *mukB3'*-GFP-Cm	Reyes-Lamothe
pAX851	puc18, *Psmta-smta-mukF-mukE-mukB*:Cm	Yamazoe et al. 1999

Arrays were used from Wang et al., 2005b; Lau et al., 2003. MukB GFP was used from Ohsumi et al., 2001. *muk* deletion strains were used from Yamazoe et al., 1999.

Table 5.2: Western Blot

Strain/ Experiment	Primary Antibody	Secondary Antibody
MukE-degron (chromosomal/ plasmid)	Anti-myc (Sigma)	Anti-mouse HRP (Sigma)
MukB-mYPet WalkerB MukB-mYPet	Anti-MukB (Yamazoe et al., 1999)	Anti-rabbit HRP (GE healthcare)
MukF-Mypet MukE-mYPet	Anti-GFP (invitrogen)	Anti-rabbit HRP (GE healthcare)

Bibliography

Adachi, S., Fukushima, T., and Hiraga, S. 2008. Dynamic events of sister chromosomes in the cell cycle of Escherichia coli. In *Genes Cells*, pp. 181-197.

Anderson, D.E., Losada, A., Erickson, H.P., and Hirano, T. 2002. Condensin and cohesin display different arm conformations with characteristic hinge angles. *J Cell Biol* **156**(3): 419-424.

Arumugam, P., Gruber, S., Tanaka, K., Haering, C.H., Mechtler, K., and Nasmyth, K. 2003. ATP hydrolysis is required for cohesin's association with chromosomes. In *Curr Biol*, pp. 1941-1953.

Arumugam, P., Nishino, T., Haering, C.H., Gruber, S., and Nasmyth, K. 2006. Cohesin's ATPase activity is stimulated by the C-terminal Winged-Helix domain of its kleisin subunit. In *Curr Biol*, pp. 1998-2008.

Aussel, L., Barre, F.X., Aroyo, M., Stasiak, A., Stasiak, A.Z., and Sherratt, D. 2002. FtsK Is a DNA motor protein that activates chromosome dimer resolution by switching the catalytic state of the XerC and XerD recombinases. In *Cell*, pp. 195-205.

Bachmann, B.J. 1972. Pedigrees of some mutant strains of Escherichia coli K-12. *Bacteriol Rev* **36**(4): 525-557.

Bates, D. and Kleckner, N. 2005. Chromosome and replisome dynamics in E. coli: loss of sister cohesion triggers global chromosome movement and mediates chromosome segregation. In *Cell*, pp. 899-911.

Ben-Yehuda, S., Rudner, D.Z., and Losick, R. 2003. RacA, a bacterial protein that anchors chromosomes to the cell poles. In *Science*, pp. 532-536.

Bernhardt, T.G. and de Boer, P.A. 2005. SlmA, a nucleoid-associated, FtsZ binding protein required for blocking septal ring assembly over Chromosomes in E. coli. *Mol Cell* **18**(5): 555-564.

Bigot, S., Saleh, O.A., Lesterlin, C., Pages, C., El Karoui, M., Dennis, C., Grigoriev, M., Allemand, J.F., Barre, F.X., and Cornet, F. 2005. KOPS: DNA motifs that control E. coli chromosome segregation by orienting the FtsK translocase. *EMBO J* **24**(21): 3770-3780.

Blattner, F.R., Plunkett, G., 3rd, Bloch, C.A., Perna, N.T., Burland, V., Riley, M., Collado-Vides, J., Glasner, J.D., Rode, C.K., Mayhew, G.F., Gregor, J., Davis, N.W., Kirkpatrick, H.A., Goeden, M.A., Rose, D.J., Mau, B., and Shao, Y. 1997. The

complete genome sequence of Escherichia coli K-12. *Science* **277**(5331): 1453-1462.

Bouthier de la Tour, C., Toueille, M., Jolivet, E., Nguyen, H.-H., Servant, P., Vannier, F., and Sommer, S. 2009. The Deinococcus radiodurans SMC protein is dispensable for cell viability yet plays a role in DNA folding. *Extremophiles* **13**(5): 827-837.

Boye, E., Lobner-Olesen, A., and Skarstad, K. 2000. Limiting DNA replication to once and only once. *Embo Rep* **1**(6): 479-483.

Breier, A.M. and Cozzarelli, N.R. 2004. Linear ordering and dynamic segregation of the bacterial chromosome. In *Proc Natl Acad Sci USA*, pp. 9175-9176.

Breier, A.M., Weier, H.U., and Cozzarelli, N.R. 2005. Independence of replisomes in Escherichia coli chromosomal replication. *Proc Natl Acad Sci U S A* **102**(11): 3942-3947.

Brezellec, P., Hoebeke, M., Hiet, M.S., Pasek, S., and Ferat, J.L. 2006. DomainSieve: a protein domain-based screen that led to the identification of dam-associated genes with potential link to DNA maintenance. *Bioinformatics* **22**(16): 1935-1941.

Carter, S.D. and Sjogren, C. 2011. The SMC complexes, DNA and chromosome topology: right or knot? *Crit Rev Biochem Mol Biol*.

Castaing, B., Zelwer, C., Laval, J., and Boiteux, S. 1995. HU protein of Escherichia coli binds specifically to DNA that contains single-strand breaks or gaps. *J Biol Chem* **270**(17): 10291-10296.

Cavalier-Smith, T. 2010. Origin of the cell nucleus, mitosis and sex: roles of intracellular coevolution. In *Biol Direct*, pp. 7.

Chen, N., Zinchenko, A.A., Yoshikawa, Y., Araki, S., Adachi, S., Yamazoe, M., Hiraga, S., and Yoshikawa, K. 2008. ATP-induced shrinkage of DNA with MukB protein and the MukBEF complex of Escherichia coli. In *J Bacteriol*, pp. 3731-3737.

Ciosk, R., Shirayama, M., Shevchenko, A., Tanaka, T., Toth, A., Shevchenko, A., and Nasmyth, K. 2000. Cohesin's binding to chromosomes depends on a separate complex consisting of Scc2 and Scc4 proteins. In *Mol Cell*, pp. 243-254.

Cobbe, N. and Heck, M.M.S. 2004. The evolution of SMC proteins: phylogenetic analysis and structural implications. In *Mol Biol Evol*, pp. 332-347.

Cui, T., Moro-oka, N., Ohsumi, K., Kodama, K., Ohshima, T., Ogasawara, N., Mori, H., Wanner, B., Niki, H., and Horiuchi, T. 2007. Escherichia coli with a linear genome. In *EMBO Rep*, pp. 181-187.

Cui, Y., Petrushenko, Z.M., and Rybenkov, V.V. 2008. MukB acts as a macromolecular clamp in DNA condensation. In *Nature structural & molecular biology*, pp. 411-418.

Cuylen, S. and Haering, C.H. 2011. Deciphering condensin action during chromosome segregation. In *Trends in cell biology*.

Cuylen, S., Metz, J., and Haering, C.H. 2011. Condensin structures chromosomal DNA through topological links. In *Nature structural & molecular biology*.

D'Ambrosio, C., Kelly, G., Shirahige, K., and Uhlmann, F. 2008a. Condensin-dependent rDNA decatenation introduces a temporal pattern to chromosome segregation. In *Curr Biol*, pp. 1084-1089.

D'Ambrosio, C., Schmidt, C.K., Katou, Y., Kelly, G., Itoh, T., Shirahige, K., and Uhlmann, F. 2008b. Identification of cis-acting sites for condensin loading onto budding yeast chromosomes. In *Genes Dev*, pp. 2215-2227.

Danilova, O., Reyes-Lamothe, R., Pinskaya, M., Sherratt, D., and Possoz, C. 2007. MukB colocalizes with the oriC region and is required for organization of the two Escherichia coli chromosome arms into separate cell halves. In *Mol Microbiol*, pp. 1485-1492.

Datsenko, K.A. and Wanner, B.L. 2000. One-step inactivation of chromosomal genes in Escherichia coli K-12 using PCR products. *Proc Natl Acad Sci U S A* **97**(12): 6640-6645.

de Boer, P.A. 2010. Advances in understanding E. coli cell fission. *Curr Opin Microbiol* **13**(6): 730-737.

den Blaauwen, T., Lindqvist, A., Löwe, J., and Nanninga, N. 2001. Distribution of the Escherichia coli structural maintenance of chromosomes (SMC)-like protein MukB in the cell. In *Mol Microbiol*, pp. 1179-1188.

Deng, S., Stein, R.A., and Higgins, N.P. 2005. Organization of supercoil domains and their reorganization by transcription. In *Mol Microbiol*, pp. 1511-1521.

Dillon, S.C. and Dorman, C.J. 2010. Bacterial nucleoid-associated proteins, nucleoid structure and gene expression. In *Nat Rev Microbiol*, pp. 185-195.

Donachie, W. 1968. Relationship between cell size and time of initiation of DNA replication. *Nature* **219**(5158): 1077-&.

Dubarry, N., Pasta, F., and Lane, D. 2006. ParABS systems of the four replicons of Burkholderia cenocepacia: new chromosome centromeres confer partition specificity. In *J Bacteriol*, pp. 1489-1496.

Dworkin, J. and Losick, R. 2002. Does RNA polymerase help drive chromosome segregation in bacteria? In *Proc Natl Acad Sci USA*, pp. 14089-14094.

Ebersbach, G., Ringgaard, S., Moller-Jensen, J., Wang, Q., Sherratt, D.J., and Gerdes, K. 2006. Regular cellular distribution of plasmids by oscillating and filament-forming ParA ATPase of plasmid pB171. *Mol Microbiol* **61**(6): 1428-1442.

Espeli, O., Lee, C., and Marians, K.J. 2003a. A physical and functional interaction between Escherichia coli FtsK and topoisomerase IV. In *J Biol Chem*, pp. 44639-44644.

Espeli, O., Levine, C., Hassing, H., and Marians, K.J. 2003b. Temporal regulation of topoisomerase IV activity in E. coli. In *Mol Cell*, pp. 189-201.

Fekete, R.A. and Chattoraj, D.K. 2005. A cis-acting sequence involved in chromosome segregation in Escherichia coli. In *Mol Microbiol*, pp. 175-183.

Fennell-Fezzie, R., Gradia, S.D., Akey, D., and Berger, J.M. 2005. The MukF subunit of Escherichia coli condensin: architecture and functional relationship to kleisins. In *EMBO J*, pp. 1921-1930.

Fiebig, A., Keren, K., and Theriot, J.A. 2006. Fine-scale time-lapse analysis of the biphasic, dynamic behaviour of the two Vibrio cholerae chromosomes. *Mol Microbiol* **60**(5): 1164-1178.

Fogel, M.A. and Waldor, M.K. 2005. Distinct segregation dynamics of the two Vibrio cholerae chromosomes. In *Mol Microbiol*, pp. 125-136.

-. 2006. A dynamic, mitotic-like mechanism for bacterial chromosome segregation. In *Genes Dev*, pp. 3269-3282.

Foley, P.L., Wilson, D.B., and Shuler, M.L. 2010. Macromolecular crowding can account for RNase-sensitive constraint of bacterial nucleoid structure. In *Biochem Biophys Res Commun*, pp. 42-47.

Gerdes, K., Howard, M., and Szardenings, F. 2010. Pushing and pulling in prokaryotic DNA segregation. In *Cell*, pp. 927-942.

Gerlich, D., Hirota, T., Koch, B., Peters, J.-M., and Ellenberg, J. 2006. Condensin I stabilizes chromosomes mechanically through a dynamic interaction in live cells. In *Curr Biol*, pp. 333-344.

Gitai, Z., Thanbichler, M., and Shapiro, L. 2005. The choreographed dynamics of bacterial chromosomes. In *Trends Microbiol*, pp. 221-228.

Gloyd, M., Ghirlando, R., and Guarné, A. 2011. The Role of MukE in Assembling a Functional MukBEF Complex. In *Journal of molecular biology*.

Grainge, I., Bregu, M., Vazquez, M., Sivanathan, V., Ip, S.C.Y., and Sherratt, D.J. 2007. Unlinking chromosome catenanes in vivo by site-specific recombination. In *EMBO J*, pp. 4228-4238.

Grainger, D.C., Hurd, D., Goldberg, M.D., and Busby, S.J.W. 2006. Association of nucleoid proteins with coding and non-coding segments of the Escherichia coli genome. In *Nucleic Acids Res*, pp. 4642-4652.

Graumann, P.L. and Knust, T. 2009. Dynamics of the bacterial SMC complex and SMC-like proteins involved in DNA repair. In *Chromosome Res*, pp. 265-275.

Griffith, K.L. and Grossman, A.D. 2008. Inducible protein degradation in Bacillus subtilis using heterologous peptide tags and adaptor proteins to target substrates to the protease ClpXP. In *Mol Microbiol*, pp. 1012-1025.

Gruber, S. 2011. MukBEF on the march: taking over chromosome organization in bacteria? In *Mol Microbiol*.

Gruber, S., Arumugam, P., Katou, Y., Kuglitsch, D., Helmhart, W., Shirahige, K., and Nasmyth, K. 2006. Evidence that loading of cohesin onto chromosomes involves opening of its SMC hinge. In *Cell*, pp. 523-537.

Gruber, S. and Errington, J. 2009. Recruitment of condensin to replication origin regions by ParB/SpoOJ promotes chromosome segregation in B. subtilis. In *Cell*, pp. 685-696.

Gruber, S., Haering, C.H., and Nasmyth, K. 2003. Chromosomal cohesin forms a ring. In *Cell*, pp. 765-777.

Guacci, V., Koshland, D., and Strunnikov, A. 1997. A direct link between sister chromatid cohesion and chromosome condensation revealed through the analysis of MCD1 in S. cerevisiae. *Cell* **91**(1): 47-57.

Guo, F. and Adhya, S. 2007. Spiral structure of Escherichia coli HUalphabeta provides foundation for DNA supercoiling. In *Proc Natl Acad Sci USA*, pp. 4309-4314.

Guzman, L.M., Belin, D., Carson, M.J., and Beckwith, J. 1995. Tight regulation, modulation, and high-level expression by vectors containing the arabinose PBAD promoter. *J Bacteriol* **177**(14): 4121-4130.

Haering, C.H., Farcas, A.-M., Arumugam, P., Metson, J., and Nasmyth, K. 2008. The cohesin ring concatenates sister DNA molecules. In *Nature*, pp. 297-301.

Haering, C.H., Löwe, J., Hochwagen, A., and Nasmyth, K. 2002. Molecular architecture of SMC proteins and the yeast cohesin complex. In *Mol Cell*, pp. 773-788.

Haering, C.H., Schoffnegger, D., Nishino, T., Helmhart, W., Nasmyth, K., and Löwe, J. 2004. Structure and stability of cohesin's Smc1-kleisin interaction. In *Mol Cell*, pp. 951-964.

Hardy, C.D. and Cozzarelli, N.R. 2005. A genetic selection for supercoiling mutants of Escherichia coli reveals proteins implicated in chromosome structure. In *Mol Microbiol*, pp. 1636-1652.

Hayama, R. and Marians, K.J. 2010. Physical and functional interaction between the condensin MukB and the decatenase topoisomerase IV in Escherichia coli. *Proc Natl Acad Sci U S A* **107**(44): 18826-18831.

Hendrickson, H. and Lawrence, J.G. 2006. Selection for chromosome architecture in bacteria. *J Mol Evol* **62**(5): 615-629.

Higgins, N.P. 2007. Mutational bias suggests that replication termination occurs near the dif site, not at Ter sites: what's the Dif? In *Mol Microbiol*, pp. 1-4.

Higgins, N.P., Booker, B.M., Manna, D., Dame, R.T., and Dorman, C.J. 2010. Molecular Structure and Dynamics of Bacterial Nucleoids Bacterial Chromatin. pp. 117-148. Springer Netherlands.

Higgins, N.P., Yang, X., Fu, Q., and Roth, J.R. 1996. Surveying a supercoil domain by using the gamma delta resolution system in Salmonella typhimurium. *J Bacteriol* **178**(10): 2825-2835.

Hill, T.M., Henson, J.M., and Kuempel, P.L. 1987. The terminus region of the Escherichia coli chromosome contains two separate loci that exhibit polar inhibition of replication. *Proc Natl Acad Sci U S A* **84**(7): 1754-1758.

Hiraga, S. 2000. Dynamic localization of bacterial and plasmid chromosomes. *Annu Rev Genet* **34**: 21-59.

Hiraga, S., Niki, H., Imamura, R., Ogura, T., Yamanaka, K., Feng, J., Ezaki, B., and Jaffé, A. 1991. Mutants defective in chromosome partitioning in E. coli. In *Res Microbiol*, pp. 189-194.

Hiraga, S., Niki, H., Ogura, T., Ichinose, C., Mori, H., Ezaki, B., and Jaffé, A. 1989. Chromosome partitioning in Escherichia coli: novel mutants producing anucleate cells. In *J Bacteriol*, pp. 1496-1505.

Hirano, M., Anderson, D.E., Erickson, H.P., and Hirano, T. 2001. Bimodal activation of SMC ATPase by intra- and inter-molecular interactions. In *EMBO J*, pp. 3238-3250.

Hirano, M. and Hirano, T. 2002. Hinge-mediated dimerization of SMC protein is essential for its dynamic interaction with DNA. In *EMBO J*, pp. 5733-5744.

-. 2004. Positive and negative regulation of SMC-DNA interactions by ATP and accessory proteins. In *EMBO J*, pp. 2664-2673.

-. 2006. Opening closed arms: long-distance activation of SMC ATPase by hinge-DNA interactions. In *Mol Cell*, pp. 175-186.

Hirano, T. 2006. At the heart of the chromosome: SMC proteins in action. In *Nat Rev Mol Cell Biol*, pp. 311-322.

-. 2010. How to separate entangled sisters: interplay between condensin and decatenase. In *Proc Natl Acad Sci USA*, pp. 18749-18750.

Hirano, T., Kobayashi, R., and Hirano, M. 1997. Condensins, chromosome condensation protein complexes containing XCAP-C, XCAP-E and a Xenopus homolog of the Drosophila Barren protein. *Cell* **89**(4): 511-521.

Hirano, T. and Mitchison, T.J. 1994. A heterodimeric coiled-coil protein required for mitotic chromosome condensation in vitro. In *Cell*, pp. 449-458.

Holmes, V.F. and Cozzarelli, N.R. 2000. Closing the ring: links between SMC proteins and chromosome partitioning, condensation, and supercoiling. In *Proc Natl Acad Sci USA*, pp. 1322-1324.

Hopfner, K.P., Karcher, A., Shin, D.S., Craig, L., Arthur, L.M., Carney, J.P., and Tainer, J.A. 2000. Structural biology of Rad50 ATPase: ATP-driven conformational control in DNA double-strand break repair and the ABC-ATPase superfamily. *Cell* **101**(7): 789-800.

Hornig, N.C.D. and Uhlmann, F. 2004. Preferential cleavage of chromatin-bound cohesin after targeted phosphorylation by Polo-like kinase. In *EMBO J*, pp. 3144-3153.

Hu, B., Itoh, T., Mishra, A., Katoh, Y., Chan, K.-L., Upcher, W., Godlee, C., Roig, M.B., Shirahige, K., and Nasmyth, K. 2011. ATP hydrolysis is required for relocating cohesin from sites occupied by its Scc2/4 loading complex. In *Curr Biol*, pp. 12-24.

Hudson, D.F., Marshall, K.M., and Earnshaw, W.C. 2009. Condensin: Architect of mitotic chromosomes. In *Chromosome Res*, pp. 131-144.

Hudson, D.F., Ohta, S., Freisinger, T., Macisaac, F., Sennels, L., Alves, F., Lai, F., Kerr, A., Rappsilber, J., and Earnshaw, W.C. 2008. Molecular and genetic analysis of condensin function in vertebrate cells. *Mol Biol Cell* **19**(7): 3070-3079.

Hudson, D.F., Vagnarelli, P., Gassmann, R., and Earnshaw, W.C. 2003. Condensin is required for nonhistone protein assembly and structural integrity of vertebrate mitotic chromosomes. In *Dev Cell*, pp. 323-336.

Iizuka, R., Yamagishi-Shirasaki, M., and Funatsu, T. 2011. Kinetic study of de novo chromophore maturation of fluorescent proteins. In *Anal Biochem*, pp. 173-178.

Jacob, F. and Brenner, S. 1963. [On the regulation of DNA synthesis in bacteria: the hypothesis of the replicon]. *C R Hebd Seances Acad Sci* **256**: 298-300.

Jaffe, A., Vinella, D., and D'Ari, R. 1997. The Escherichia coli histone-like protein HU affects DNA initiation, chromosome partitioning via MukB, and cell division via MinCDE. *J Bacteriol* **179**(11): 3494-3499.

Jensen, R.B. and Shapiro, L. 1999. The Caulobacter crescentus smc gene is required for cell cycle progression and chromosome segregation. In *Proc Natl Acad Sci USA*, pp. 10661-10666.

Joshi, M.C., Bourniquel, A., Fisher, J., Ho, B.T., Magnan, D., Kleckner, N., and Bates, D. 2011. Escherichia coli sister chromosome separation includes an abrupt global transition with concomitant release of late-splitting intersister snaps. In *Proc Natl Acad Sci USA*, pp. 2765-2770.

Jun, S. and Mulder, B. 2006. Entropy-driven spatial organization of highly confined polymers: lessons for the bacterial chromosome. In *Proc Natl Acad Sci USA*, pp. 12388-12393.

Jun, S. and Wright, A. 2010. Entropy as the driver of chromosome segregation. In *Nat Rev Microbiol*, pp. 600-607.

Kaguni, J.M. 2006. DnaA: controlling the initiation of bacterial DNA replication and more. *Annu Rev Microbiol* **60**: 351-375.

Kapust, R.B. and Waugh, D.S. 2000. Controlled intracellular processing of fusion proteins by TEV protease. *Protein Expr Purif* **19**(2): 312-318.

Karczmarek, A., Martinez-Arteaga, R., Alexeeva, S., Hansen, F.G., Vicente, M., Nanninga, N., and den Blaauwen, T. 2007. DNA and origin region segregation are not affected by the transition from rod to sphere after inhibition of Escherichia coli MreB by A22. *Mol Microbiol* **65**(1): 51-63.

Katayama, T., Ozaki, S., Keyamura, K., and Fujimitsu, K. 2010. Regulation of the replication cycle: conserved and diverse regulatory systems for DnaA and oriC. *Nat Rev Microbiol* **8**(3): 163-170.

Kavenoff, R. and Bowen, B.C. 1976. Electron microscopy of membrane-free folded chromosomes from Escherichia coli. *Chromosoma* **59**(2): 89-101.

Kennedy, S.P., Chevalier, F., and Barre, F.X. 2008. Delayed activation of Xer recombination at dif by FtsK during septum assembly in Escherichia coli. *Mol Microbiol* **68**(4): 1018-1028.

Kimura, K. and Hirano, T. 1997. ATP-dependent positive supercoiling of DNA by 13S condensin: a biochemical implication for chromosome condensation. *Cell* **90**(4): 625-634.

Kimura, K., Rybenkov, V.V., Crisona, N.J., Hirano, T., and Cozzarelli, N.R. 1999. 13S condensin actively reconfigures DNA by introducing global positive writhe: implications for chromosome condensation. In *Cell*, pp. 239-248.

Kouzminova, E.A., Rotman, E., Macomber, L., Zhang, J., and Kuzminov, A. 2004. RecA-dependent mutants in Escherichia coli reveal strategies to avoid chromosomal fragmentation. In *Proc Natl Acad Sci USA*, pp. 16262-16267.

Ku, B., Lim, J.-H., Shin, H.-C., Shin, S.-Y., and Oh, B.-H. 2010. Crystal structure of the MukB hinge domain with coiled-coil stretches and its functional implications. In *Proteins*, pp. 1483-1490.

Lammens, A., Schele, A., and Hopfner, K.-P. 2004. Structural biochemistry of ATP-driven dimerization and DNA-stimulated activation of SMC ATPases. In *Curr Biol*, pp. 1778-1782.

Lammens, K., Bemeleit, D.J., Möckel, C., Clausing, E., Schele, A., Hartung, S., Schiller, C.B., Lucas, M., Angermüller, C., Söding, J., Strässer, K., and Hopfner, K.-P. 2011. The Mre11:Rad50 structure shows an ATP-dependent molecular clamp in DNA double-strand break repair. In *Cell*, pp. 54-66.

Lau, I.F., Filipe, S.R., Søballe, B., Økstad, O.-A., Barre, F.-X., and Sherratt, D.J. 2003. Spatial and temporal organization of replicating Escherichia coli chromosomes. In *Mol Microbiol*, pp. 731-743.

Leake, M.C. 2010. Shining the spotlight on functional molecular complexes: The new science of single-molecule cell biology. In *Commun Integr Biol*, pp. 415-418.

Lemon, K.P. and Grossman, A.D. 2001. The extrusion-capture model for chromosome partitioning in bacteria. In *Genes Dev*, pp. 2031-2041.

Lengronne, A., Katou, Y., Mori, S., Yokobayashi, S., Kelly, G.P., Itoh, T., Watanabe, Y., Shirahige, K., and Uhlmann, F. 2004. Cohesin relocation from sites of chromosomal loading to places of convergent transcription. In *Nature*, pp. 573-578.

Lesterlin, C., Barre, F.-X., and Cornet, F. 2004. Genetic recombination and the cell cycle: what we have learned from chromosome dimers. In *Mol Microbiol*, pp. 1151-1160.

Lesterlin, C., Mercier, R., Boccard, F., Barre, F.-X., and Cornet, F. 2005. Roles for replichores and macrodomains in segregation of the Escherichia coli chromosome. In *EMBO Rep*, pp. 557-562.

Lewis, P.J. and Errington, J. 1997. Direct evidence for active segregation of oriC regions of the Bacillus subtilis chromosome and co-localization with the SpoOJ partitioning protein. In *Mol Microbiol*, pp. 945-954.

Li, G.-W. and Xie, X.S. 2011. Central dogma at the single-molecule level in living cells. In *Nature*, pp. 308-315.

Li, Y., Schoeffler, A.J., Berger, J.M., and Oakley, M.G. 2010a. The crystal structure of the hinge domain of the Escherichia coli structural maintenance of chromosomes protein MukB. In *J Mol Biol*, pp. 11-19.

Li, Y., Stewart, N.K., Berger, A.J., Vos, S., Schoeffler, A.J., Berger, J.M., Chait, B.T., and Oakley, M.G. 2010b. Escherichia coli condensin MukB stimulates topoisomerase IV activity by a direct physical interaction. In *Proc Natl Acad Sci USA*, pp. 18832-18837.

Lim, H.S., Kim, J.S., Park, Y.B., Gwon, G.H., and Cho, Y. 2011. Crystal structure of the Mre11-Rad50-ATPgammaS complex: understanding the interplay between Mre11 and Rad50. In *Genes Dev*, pp. 1091-1104.

Lim, J.-H. and Oh, B.-H. 2009. Structural and functional similarities between two bacterial chromosome compacting machineries. In *Biochem Biophys Res Commun*, pp. 415-419.

Lindow, J.C., Britton, R.A., and Grossman, A.D. 2002. Structural maintenance of chromosomes protein of Bacillus subtilis affects supercoiling in vivo. In *J Bacteriol*, pp. 5317-5322.

Liu, X., Wang, X., Reyes-Lamothe, R., and Sherratt, D. 2010a. Replication-directed sister chromosome alignment in Escherichia coli. In *Mol Microbiol*, pp. 1090-1097.

Liu, Y., Chen, H., Kenney, L.J., and Yan, J. 2010b. A divalent switch drives H-NS/DNA-binding conformations between stiffening and bridging modes. In *Genes Dev*, pp. 339-344.

Lobry, J.R. and Louarn, J.M. 2003. Polarisation of prokaryotic chromosomes. *Curr Opin Microbiol* **6**(2): 101-108.

Löwe, J., Cordell, S.C., and van den Ent, F. 2001. Crystal structure of the SMC head domain: an ABC ATPase with 900 residues antiparallel coiled-coil inserted. In *J Mol Biol*, pp. 25-35.

Maeshima, K. and Eltsov, M. 2008. Packaging the genome: the structure of mitotic chromosomes. In *J Biochem*, pp. 145-153.

Maeshima, K. and Laemmli, U.K. 2003. A two-step scaffolding model for mitotic chromosome assembly. In *Dev Cell*, pp. 467-480.

Mascarenhas, J., Volkov, A.V., Rinn, C., Schiener, J., Guckenberger, R., and Graumann, P.L. 2005. Dynamic assembly, localization and proteolysis of the Bacillus subtilis SMC complex. In *BMC Cell Biol*, pp. 28.

Matoba, K., Yamazoe, M., Mayanagi, K., Morikawa, K., and Hiraga, S. 2005. Comparison of MukB homodimer versus MukBEF complex molecular architectures by electron microscopy reveals a higher-order multimerization. In *Biochem Biophys Res Commun*, pp. 694-702.

Mc Intyre, J., Muller, E.G.D., Weitzer, S., Snydsman, B.E., Davis, T.N., and Uhlmann, F. 2007. In vivo analysis of cohesin architecture using FRET in the budding yeast Saccharomyces cerevisiae. In *EMBO J*, pp. 3783-3793.

McGinness, K.E., Baker, T.A., and Sauer, R.T. 2006. Engineering controllable protein degradation. In *Mol Cell*, pp. 701-707.

McLeod, S.M., Aiyar, S.E., Gourse, R.L., and Johnson, R.C. 2002. The C-terminal domains of the RNA polymerase alpha subunits: contact site with Fis and localization during co-activation with CRP at the Escherichia coli proP P2 promoter. *J Mol Biol* **316**(3): 517-529.

Melby, T.E., Ciampaglio, C.N., Briscoe, G., and Erickson, H.P. 1998. The symmetrical structure of structural maintenance of chromosomes (SMC) and MukB proteins: long, antiparallel coiled coils, folded at a flexible hinge. In *J Cell Biol*, pp. 1595-1604.

Mercier, R., Petit, M.-A., Schbath, S., Robin, S., El Karoui, M., Boccard, F., and Espéli, O. 2008. The MatP/matS site-specific system organizes the terminus region of the E. coli chromosome into a macrodomain. In *Cell*, pp. 475-485.

Michaelis, C., Ciosk, R., and Nasmyth, K. 1997. Cohesins: chromosomal proteins that prevent premature separation of sister chromatids. *Cell* **91**(1): 35-45.

Minnen, A., Attaiech, L., Thon, M., Gruber, S., and Veening, J.W. 2011. SMC is recruited to oriC by ParB and promotes chromosome segregation in Streptococcus pneumoniae. *Mol Microbiol* **81**(3): 676-688.

Moore, S.D. and Sauer, R.T. 2007. The tmRNA system for translational surveillance and ribosome rescue. In *Annu Rev Biochem*, pp. 101-124.

Nasmyth, K. and Haering, C.H. 2005. The structure and function of SMC and kleisin complexes. In *Annu Rev Biochem*, pp. 595-648.

-. 2009. Cohesin: its roles and mechanisms. In *Annu Rev Genet*, pp. 525-558.

Nielsen, H.J., Li, Y., Youngren, B., Hansen, F.G., and Austin, S. 2006. Progressive segregation of the Escherichia coli chromosome. In *Mol Microbiol*, pp. 383-393.

Nielsen, H.J., Youngren, B., Hansen, F.G., and Austin, S. 2007. Dynamics of Escherichia coli chromosome segregation during multifork replication. *J Bacteriol* **189**(23): 8660-8666.

Niki, H. and Hiraga, S. 1998. Polar localization of the replication origin and terminus in Escherichia coli nucleoids during chromosome partitioning. In *Genes Dev*, pp. 1036-1045.

Niki, H., Imamura, R., Kitaoka, M., Yamanaka, K., Ogura, T., and Hiraga, S. 1992. E.coli MukB protein involved in chromosome partition forms a homodimer with a rod-and-hinge structure having DNA binding and ATP/GTP binding activities. In *EMBO J*, pp. 5101-5109.

Niki, H., Yamaichi, Y., and Hiraga, S. 2000. Dynamic organization of chromosomal DNA in Escherichia coli. In *Genes Dev*, pp. 212-223.

Ocampo-Hafalla, M.T. and Uhlmann, F. 2011. Cohesin loading and sliding. In *J Cell Sci*, pp. 685-691.

Ohsumi, K., Yamazoe, M., and Hiraga, S. 2001. Different localization of SeqA-bound nascent DNA clusters and MukF-MukE-MukB complex in Escherichia coli cells. In *Mol Microbiol*, pp. 835-845.

Oliveira, R.A., Coelho, P.A., and Sunkel, C.E. 2005. The condensin I subunit Barren/CAP-H is essential for the structural integrity of centromeric heterochromatin during mitosis. In *Mol Cell Biol*, pp. 8971-8984.

Oliveira, R.A., Heidmann, S., and Sunkel, C.E. 2007. Condensin I binds chromatin early in prophase and displays a highly dynamic association with Drosophila mitotic chromosomes. In *Chromosoma*, pp. 259-274.

Onn, I. and Koshland, D. 2011. In vitro assembly of physiological cohesin/DNA complexes. In *Proc Natl Acad Sci USA*, pp. 12198-12205.

Orelle, C., Dalmas, O., Gros, P., Di Pietro, A., and Jault, J.M. 2003. The conserved glutamate residue adjacent to the Walker-B motif is the catalytic base for ATP hydrolysis in the ATP-binding cassette transporter BmrA. *J Biol Chem* **278**(47): 47002-47008.

Pauli, A., van Bemmel, J.G., Oliveira, R.A., Itoh, T., Shirahige, K., van Steensel, B., and Nasmyth, K. 2010. A direct role for cohesin in gene regulation and ecdysone response in Drosophila salivary glands. *Curr Biol* **20**(20): 1787-1798.

Petrushenko, Z.M., Cui, Y., She, W., and Rybenkov, V.V. 2010. Mechanics of DNA bridging by bacterial condensin MukBEF in vitro and in singulo. In *EMBO J*, pp. 1126-1135.

Petrushenko, Z.M., Lai, C.-H., Rai, R., and Rybenkov, V.V. 2006a. DNA reshaping by MukB. Right-handed knotting, left-handed supercoiling. In *J Biol Chem*, pp. 4606-4615.

Petrushenko, Z.M., Lai, C.-H., and Rybenkov, V.V. 2006b. Antagonistic interactions of kleisins and DNA with bacterial Condensin MukB. In *J Biol Chem*, pp. 34208-34217.

Petrushenko, Z.M., She, W., and Rybenkov, V.V. 2011. A new family of bacterial condensins. In *Mol Microbiol*.

Plank, M., Wadhams, G.H., and Leake, M.C. 2009. Millisecond timescale slimfield imaging and automated quantification of single fluorescent protein molecules for use in probing complex biological processes. In *Integr Biol (Camb)*, pp. 602-612.

Pogliano, J., Pogliano, K., Weiss, D.S., Losick, R., and Beckwith, J. 1997. Inactivation of FtsI inhibits constriction of the FtsZ cytokinetic ring and delays the assembly of FtsZ rings at potential division sites. *Proc Natl Acad Sci U S A* **94**(2): 559-564.

Postow, L., Hardy, C.D., Arsuaga, J., and Cozzarelli, N.R. 2004. Topological domain structure of the Escherichia coli chromosome. In *Genes Dev*, pp. 1766-1779.

Renshaw, M.J., Ward, J.J., Kanemaki, M., Natsume, K., Nedelec, F.J., and Tanaka, T.U. 2010. Condensins promote chromosome recoiling during early anaphase to complete sister chromatid separation. *Dev Cell* **19**(2): 232-244.

Reyes-Lamothe, R., Possoz, C., Danilova, O., and Sherratt, D.J. 2008a. Independent positioning and action of Escherichia coli replisomes in live cells. In *Cell*, pp. 90-102.

Reyes-Lamothe, R., Sherratt, D.J., and Leake, M.C. 2010. Stoichiometry and Architecture of Active DNA Replication Machinery in Escherichia coli. In *Science*, pp. 498-501.

Reyes-Lamothe, R., Wang, X., and Sherratt, D. 2008b. Escherichia coli and its chromosome. In *Trends Microbiol*, pp. 238-245.

Rocha, E.P., Fralick, J., Vediyappan, G., Danchin, A., and Norris, V. 2003. A strand-specific model for chromosome segregation in bacteria. *Mol Microbiol* **49**(4): 895-903.

Rybenkov, V.V. 2009. Towards the architecture of the chromosomal architects. In *Nat Struct Mol Biol*, pp. 104-105.

Salje, J. and Lowe, J. 2008. Bacterial actin: architecture of the ParMRC plasmid DNA partitioning complex. *EMBO J* **27**(16): 2230-2238.

Sawitzke, J.A. and Austin, S. 2000. Suppression of chromosome segregation defects of Escherichia coli muk mutants by mutations in topoisomerase I. In *Proc Natl Acad Sci USA*, pp. 1671-1676.

Scheirer, K.E. and Higgins, N.P. 2001. Transcription induces a supercoil domain barrier in bacteriophage Mu. *Biochimie* **83**(2): 155-159.

Schmidt, C.K., Brookes, N., and Uhlmann, F. 2009. Conserved features of cohesin binding along fission yeast chromosomes. In *Genome Biol*, pp. R52.

Schwartz, M.A. and Shapiro, L. 2011. An SMC ATPase mutant disrupts chromosome segregation in Caulobacter. *Mol Microbiol*.

Shin, H.-C., Lim, J.-H., Woo, J.-S., and Oh, B.-H. 2009. Focal localization of MukBEF condensin on the chromosome requires the flexible linker region of MukF. In *FEBS J*, pp. 5101-5110.

Sinden, R.R. and Pettijohn, D.E. 1981. Chromosomes in living Escherichia coli cells are segregated into domains of supercoiling. *Proc Natl Acad Sci U S A* **78**(1): 224-228.

Sivanathan, V., Emerson, J.E., Pages, C., Cornet, F., Sherratt, D.J., and Arciszewska, L.K. 2009. KOPS-guided DNA translocation by FtsK safeguards Escherichia coli chromosome segregation. In *Mol Microbiol*, pp. 1031-1042.

Sjogren, C. and Nasmyth, K. 2001. Sister chromatid cohesion is required for postreplicative double-strand break repair in Saccharomyces cerevisiae. *Curr Biol* **11**(12): 991-995.

Sliusarenko, O., Heinritz, J., Emonet, T., and Jacobs-Wagner, C. 2011. High-throughput, subpixel precision analysis of bacterial morphogenesis and intracellular spatio-temporal dynamics. *Mol Microbiol* **80**(3): 612-627.

Steiner, W., Liu, G., Donachie, W.D., and Kuempel, P. 1999. The cytoplasmic domain of FtsK protein is required for resolution of chromosome dimers. *Mol Microbiol* **31**(2): 579-583.

Stonington, O.G. and Pettijohn, D.E. 1971. The folded genome of Escherichia coli isolated in a protein-DNA-RNA complex. *Proc Natl Acad Sci U S A* **68**(1): 6-9.

Stray, J.E., Crisona, N.J., Belotserkovskii, B.P., Lindsley, J.E., and Cozzarelli, N.R. 2005. The Saccharomyces cerevisiae Smc2/4 condensin compacts DNA into (+) chiral structures without net supercoiling. In *J Biol Chem*, pp. 34723-34734.

Stray, J.E. and Lindsley, J.E. 2003. Biochemical analysis of the yeast condensin Smc2/4 complex: an ATPase that promotes knotting of circular DNA. In *J Biol Chem*, pp. 26238-26248.

Strick, T.R., Kawaguchi, T., and Hirano, T. 2004. Real-time detection of single-molecule DNA compaction by condensin I. In *Curr Biol*, pp. 874-880.

Sullivan, N.L., Marquis, K.A., and Rudner, D.Z. 2009. Recruitment of SMC by ParB-parS organizes the origin region and promotes efficient chromosome segregation. In *Cell*, pp. 697-707.

Tadesse, S., Mascarenhas, J., Kösters, B., Hasilik, A., and Graumann, P.L. 2005. Genetic interaction of the SMC complex with topoisomerase IV in Bacillus subtilis. In *Microbiology (Reading, Engl)*, pp. 3729-3737.

Teleman, A.A., Graumann, P.L., Lin, D.C., Grossman, A.D., and Losick, R. 1998. Chromosome arrangement within a bacterium. In *Curr Biol*, pp. 1102-1109.

Thanbichler, M. and Shapiro, L. 2006. Chromosome organization and segregation in bacteria. In *J Struct Biol*, pp. 292-303.

Toro, E., Hong, S.H., McAdams, H.H., and Shapiro, L. 2008. Caulobacter requires a dedicated mechanism to initiate chromosome segregation. *Proc Natl Acad Sci U S A* **105**(40): 15435-15440.

Toro, E. and Shapiro, L. 2010. Bacterial chromosome organization and segregation. In *Cold Spring Harb Perspect Biol*, pp. a000349.

Toth, A., Ciosk, R., Uhlmann, F., Galova, M., Schleiffer, A., and Nasmyth, K. 1999. Yeast cohesin complex requires a conserved protein, Eco1p(Ctf7), to establish cohesion between sister chromatids during DNA replication. *Genes Dev* **13**(3): 320-333.

Uhlmann, F., Lottspeich, F., and Nasmyth, K. 1999. Sister-chromatid separation at anaphase onset is promoted by cleavage of the cohesin subunit Scc1. *Nature* **400**(6739): 37-42.

Valens, M., Penaud, S., Rossignol, M., Cornet, F., and Boccard, F. 2004. Macrodomain organization of the Escherichia coli chromosome. *EMBO J* **23**(21): 4330-4341.

Vecchiarelli, A.G., Han, Y.-W., Tan, X., Mizuuchi, M., Ghirlando, R., Biertümpfel, C., Funnell, B.E., and Mizuuchi, K. 2010. ATP control of dynamic P1 ParA-DNA interactions: a key role for the nucleoid in plasmid partition. In *Mol Microbiol*, pp. 78-91.

Viollier, P.H., Thanbichler, M., McGrath, P.T., West, L., Meewan, M., McAdams, H.H., and Shapiro, L. 2004. Rapid and sequential movement of individual chromosomal loci to specific subcellular locations during bacterial DNA replication. In *Proc Natl Acad Sci USA*, pp. 9257-9262.

Volkov, A., Mascarenhas, J., Andrei-Selmer, C., Ulrich, H.D., and Graumann, P.L. 2003. A prokaryotic condensin/cohesin-like complex can actively compact chromosomes from a single position on the nucleoid and binds to DNA as a ring-like structure. In *Mol Cell Biol*, pp. 5638-5650.

Waldminghaus, T. and Skarstad, K. 2009. The Escherichia coli SeqA protein. *Plasmid* **61**(3): 141-150.

Wang, B.D., Eyre, D., Basrai, M., Lichten, M., and Strunnikov, A. 2005a. Condensin binding at distinct and specific chromosomal sites in the Saccharomyces cerevisiae genome. *Mol Cell Biol* **25**(16): 7216-7225.

Wang, J.D. and Levin, P.A. 2009. Metabolism, cell growth and the bacterial cell cycle. *Nat Rev Microbiol* **7**(11): 822-827.

Wang, X., Lesterlin, C., Reyes-Lamothe, R., Ball, G., and Sherratt, D.J. 2011. Replication and segregation of an Escherichia coli chromosome with two replication origins. In *Proc Natl Acad Sci USA*, pp. E243-250.

Wang, X., Liu, X., Possoz, C., and Sherratt, D.J. 2006. The two Escherichia coli chromosome arms locate to separate cell halves. *Genes Dev* **20**(13): 1727-1731.

Wang, X., Possoz, C., and Sherratt, D.J. 2005b. Dancing around the divisome: asymmetric chromosome segregation in Escherichia coli. In *Genes Dev*, pp. 2367-2377.

Wang, X., Reyes-Lamothe, R., and Sherratt, D.J. 2008. Modulation of Escherichia coli sister chromosome cohesion by topoisomerase IV. In *Genes Dev*, pp. 2426-2433.

Wang, X. and Sherratt, D.J. 2010. Independent segregation of the two arms of the Escherichia coli ori region requires neither RNA synthesis nor MreB dynamics. In *J Bacteriol*, pp. 6143-6153.

Webb, C.D., Graumann, P.L., Kahana, J.A., Teleman, A.A., Silver, P.A., and Losick, R. 1998. Use of time-lapse microscopy to visualize rapid movement of the replication origin region of the chromosome during the cell cycle in Bacillus subtilis. *Mol Microbiol* **28**(5): 883-892.

Webb, C.D., Teleman, A., Gordon, S., Straight, A., Belmont, A., Lin, D.C., Grossman, A.D., Wright, A., and Losick, R. 1997. Bipolar localization of the replication origin regions of chromosomes in vegetative and sporulating cells of B. subtilis. In *Cell*, pp. 667-674.

Weitao, T., Dasgupta, S., and Nordström, K. 2000. Role of the mukB gene in chromosome and plasmid partition in Escherichia coli. In *Mol Microbiol*, pp. 392-400.

Weitao, T., Nordström, K., and Dasgupta, S. 1999. Mutual suppression of mukB and seqA phenotypes might arise from their opposing influences on the Escherichia coli nucleoid structure. In *Mol Microbiol*, pp. 157-168.

Weitzer, S., Lehane, C., and Uhlmann, F. 2003. A model for ATP hydrolysis-dependent binding of cohesin to DNA. In *Curr Biol*, pp. 1930-1940.

Wiggins, P.A., Cheveralls, K.C., Martin, J.S., Lintner, R., and Kondev, J. 2010. Strong intranucleoid interactions organize the Escherichia coli chromosome into a nucleoid filament. In *Proc Natl Acad Sci USA*, pp. 4991-4995.

Withers, H.L. and Bernander, R. 1998. Characterization of dnaC2 and dnaC28 mutants by flow cytometry. *J Bacteriol* **180**(7): 1624-1631.

Woldringh, C.L. and Nanninga, N. 2006. Structural and physical aspects of bacterial chromosome segregation. In *J Struct Biol*, pp. 273-283.

Woo, J.-S., Lim, J.-H., Shin, H.-C., Suh, M.-K., Ku, B., Lee, K.-H., Joo, K., Robinson, H., Lee, J., Park, S.-Y., Ha, N.-C., and Oh, B.-H. 2009. Structural studies of a bacterial condensin complex reveal ATP-dependent disruption of intersubunit interactions. In *Cell*, pp. 85-96.

Wu, L.J. and Errington, J. 1994. Bacillus subtilis SpoIIIE protein required for DNA segregation during asymmetric cell division. *Science* **264**(5158): 572-575.

Yamaichi, Y. and Niki, H. 2004. migS, a cis-acting site that affects bipolar positioning of oriC on the Escherichia coli chromosome. In *EMBO J*, pp. 221-233.

Yamanaka, K., Ogura, T., Niki, H., and Hiraga, S. 1995. Characterization of the smtA gene encoding an S-adenosylmethionine-dependent methyltransferase of Escherichia coli. *FEMS Microbiol Lett* **133**(1-2): 59-63.

-. 1996. Identification of two new genes, mukE and mukF, involved in chromosome partitioning in Escherichia coli. *Mol Gen Genet* **250**(3): 241-251.

Yoshimura, S.H., Hizume, K., Murakami, A., Sutani, T., Takeyasu, K., and Yanagida, M. 2002. Condensin architecture and interaction with DNA: regulatory non-SMC subunits bind to the head of SMC heterodimer. *Curr Biol* **12**(6): 508-513.

Yu, W., Herbert, S., Graumann, P.L., and Gotz, F. 2010. Contribution of SMC (structural maintenance of chromosomes) and SpoIIIE to chromosome segregation in Staphylococci. *J Bacteriol* **192**(15): 4067-4073.